Characterisation and formulation of natural cyclodecapeptides with anti-Candida activity

by

Yasamin Masoudi
BScHons (Biochemistry)

March 2021

Thesis presented for the degree
Masters of Science (Biochemistry)
in the
Faculty of Science
at the
University of Stellenbosch

Supervisor: Prof. Marina Rautenbach
Department of Biochemistry
University of Stellenbosch

Declaration

By submitting this thesis electronically, I ***Yasamin Masoudi*** declare that the entirety of the work contained therein is my own, original work, that I am the sole author thereof (save to the content explicitly stated otherwise), that reproduction and publication thereof by Stellenbosch University will not infringe any third-party rights and that I have not previously in its entirety or in part submitted it for obtaining any qualification.

Yasamin Masoudi
Name

15 December 2020
Date

Summary

The increase in the number of fungal infections since the 1980s is a major concern globally. Fungal infections affect various medical and agricultural sectors. A limited number of available antifungal drugs in addition to the development of the antifungal drug resistance, urge the need for the development of new antifungal drugs. *Candida albicans* and *Candida glabrata* are the two most common causes of topical and systemic *Candida* infections, and specifically prone to drug resistance. Therefore, the next generation of antifungal drugs has to be compounds with a low probability to elicit resistance. The tyrocidines (Trcs) and analogues are cyclic decapeptides with a broad antimicrobial spectrum and proven anti-*Candida* activity. The development of resistance is less likely due to their rapid mode of action and multiple targets. The Trcs and analogues have a great tendency to oligomerise and the antimicrobial activity of the Trcs may be dependent on their ability to form active oligomers. In this study, we aimed to manipulate the Trc oligomerisation by combining it with cellulose derivatives as formulants. The goal was to increase the anti-*Candida* activity as well as the stability of theses peptides in solution. Furthermore, if a concomitant decrease in the toxicity against human erythrocytes would also be beneficial. The oligomerisation profile of Trcs is driven by four main factors, namely, concentration, maturation time, peptide structure and the viscosity of the cellulose derivatives used in the formulation. The oligomerisation of Trcs is a dynamic arrangement and rearrangement of the peptide in the Trc mixture throughout the maturation period. For the more viscous cellulose-type formulants, this rearrangement resulted in the release of the more dimeric oligomers and increased the anti-*Candida* activity of the Trc mixture, However, for pure peptides such as TrcA and TpcC, both formulation and the maturation time did not alter the anti-*Candida* activity. This could be that TrcA oligomers are highly stable and maturation time does not result in releasing of more active moieties. Tic is inherently less active, and it may not have the optimal structure to interact with the *Candida* target. It was observed that a high concentration of cellulose derivatives significantly increased the anti-*Candida* activity of the Tic mixture, as well as stabilising the tic peptides in solutions, as detected with fluorescence. Unfortunately, none of the cellulose formulations of try mix decreased the haemolytic activity against human erythrocytes. However, anti-*Candida* activity was maintained and/or improved, as the solution stability of the peptides in the Trc mixture was improved.

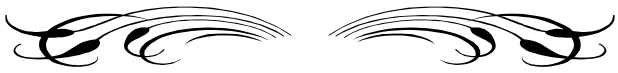

Who does not know, and does not know that he does not know,
remains mired forever in double ignorance

Nasir al-Din al-Tusi
Persian chemist

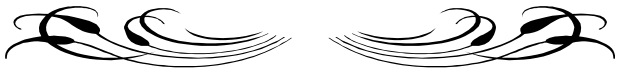

Acknowledgements

I would like to express my thanks and gratitude to the following persons and institutions:

- Prof Marina Rautenbach, the most caring person, for allowing me the opportunity to follow my dreams. Under her mentorship and unconditional support, throughout my MSc, I was not only trained as a scientist but also learnt to never give up
- My colleagues in the BIOPEP Peptide group for their assistance and support in the laboratory and for making the laboratory a pleasant working environment
- Dr Marietjie Stander and her colleagues at the Central Analytical Facilities (CAF), Stellenbosch University for their expertise and technical assistance during mass spectrometry analysis
- Stellenbosch University Faculty of Science and BIOPEP Peptide Fund for their financial support in achieving my MSc degree
- My parents, for their unconditional love and support even though we are many miles apart
- My husband, Steven, who is always beside me and supports me through the different chapters of my life.

Table of Contents

DECLARATION ..... **ii**

SUMMARY ..... **iii**

ACKNOWLEDGEMENTS ..... **v**

TABLE OF CONTENTS ..... **vi**

ABBREVIATIONS AND ACRONYMS ..... **viii**

PREFACE ..... **x**

OUTPUTS OF MSC STUDY ..... **xii**

CHAPTER 1: COMBATING *CANDIDA* INFECTIONS WITH ANTIMICROBIAL PEPTIDES **1-1**

1.1 INTRODUCTION 1-1

1.2 CANDIDA INFECTIONS 1-2

1.3 ANTI-*CANDIDA* DRUGS AND RESISTANCE 1-3

1.4 ANTIMICROBIAL PEPTIDES AS CANDIDATE ANTIFUNGAL DRUGS 1-9

1.4.1 Antifungal peptides *1-10*

1.5 THE TYROCIDINES AS POTENTIAL AFPS 1-13

1.5.5 Trc oligomerisation, toxicity, and structure-activity relationships *1-17*

1.5.6 Formulation of anti-fungal drugs *1-18*

1.6 REFERENCES 1-23

CHAPTER 2: PRODUCTION, PURIFICATION, AND CHEMICAL CHARACTERISATION OF THE CYCLODECAPEPTIDES FROM TYROTHRICIN **2-1**

2.1 INTRODUCTION 2-1

2.2 MATERIALS 2-5

2.3 METHODS 2-6

2.3.1 Production of the cyclodecapeptides *2-6*

2.3.2 Semi-preparative HPLC purification of selected cyclodecapeptides *2-6*

2.3.3 Characterisation of peptide extracts and purified peptides by ES-MS and UPLC-MS analysis *2-7*

2.4 RESULTS AND DISCUSSION 2-9

2.4.1 Analysis of amino acid supplemented crude extracts *2-9*

2.4.2 Purification of cyclodecapeptides from culture extracts *2-14*

2.4.3 Effect of time on aggregation and purification *2-21*

2.4.4 Semi-preparative RP-HPLC purification of single cyclodecapeptide analogues *2-23*

2.5 CONCLUSION 2-31

2.6 REFERENCES 2-32

CHAPTER 3: THE INFLUENCE OF FORMULANTS ON ANTI-*CANDIDA* ACTIVITY OF THE TYROCIDINE COMPLEX 3-1

3.1. INTRODUCTION 3-1

3.2. MATERIALS 3-2

3.3. METHODS 3-3

3.3.1 Culturing of C. albicans and C. glabrata 3-3

3.3.2 Preparation of formulations of Trc mix and purified peptides 3-3

3.3.3 Metabolic inhibition anti-Candida assay 3-5

3.3.4 Data analysis of metabolic inhibition assay 3-5

3.3.5 Haemolytic toxicity 3-6

3.4. RESULTS AND DISCUSSION 3-6

3.4.1 Assessing formulations of Trc mix targeting C. albicans 3-6

3.4.2 Optimising the formulation of Trc mix 3-10

3.4.3 The effect of cellulose derivatives on Trc mix anti-C. glabrata activity 3-13

3.3.4 The effect of cellulose derivatives on Trc mix haemolytic activity 3-13

3.3.5 Anti-Candida of purified TrcA and TpcC and their formulations 3-14

3.5. CONCLUSION 3-17

3.6. REFERENCES 3-18

3.7. SUPPLEMENTARY DATA 3-21

CHAPTER 4: FLUORESCENCE STUDIES ON THE TYROCIDINE FORMULATION WITH CELLULOSE DERIVATIVES 4-1

4.1 INTRODUCTION *4-1*

4.2 MATERIALS *4-4*

4.3 METHODS *4-5*

4.3.1 Fluorescence spectroscopy 4-5

4.4 RESULTS AND DISCUSSION *4-6*

4.4.1 Fluorescence spectrometry of Trc mix and its formulations 4-6

4.4.2 Effect of time and concentration on the formation of oligomers 4-14

4.5 CONCLUSIONS *4-20*

4.6 REFERENCES *4-23*

4.7 SUPPLEMENTARY DATA *4-24*

CHAPTER 5 CONCLUSIONS AND FUTURE STUDIES 5-1

5.1. INTRODUCTION 5-1

5.2. CONCLUSIONS 5-1

5.2.1. Production and purification of single Trcs analogues 5-1

5.2.2. The biological activity of the Trcs 5-2

5.2.3. Investigation of the stability of Trcs utilising fluorescence 5-4

5.3. FUTURE STUDIES 5-6

5.4. LAST WORD 5-6

5.5. REFERENCES 5-7

Abbreviations and Acronyms

$[M+H]^+$	singly charged monomeric molecular ion
$[M+2H]^{2+}$	doubly charged monomeric molecular ion
$[2M+2H]^{2+}$	doubly charged dimeric molecular ion
ACN	acetonitrile
AMP	antimicrobial peptide
AFP	antifungal peptide
B. parabrevis	*Brevibacillus parabrevis*
C. albicans	*Candida albicans*
C. glabrata	*Candida glabrata*
DEE	diethyl ether
DNA	deoxyribonucleic acid
E. coli	*Escherichia coli*
Ems	emission
ESMS	electrospray ionisation mass spectrometry
ESI	electrospray ionisation
ETOH	ethanol
Ex	excitation
GS	gramicidin S
Grm/s	linear gramicidin/s
HPLC	high performance liquid chromatography
HIV	human immunodeficiency virus
IM-MS	ion mobility mass spectrometry
IC_{50}	peptide concentration leading to 50 % microbial growth inhibition
L. monocytogenes	*Listeria monocytogenes*
MIC	minimum inhibitory concentration of peptide targeting *Candida* cells
M_r	relative molar mass
m/z	mass over charge ratio
m/m	mass/mass
Orn	ornithine
O	ornithine
PBS	phosphate buffered saline

PhcA	phenycidine A
RNA	ribonucleic acid
RP-HPLC	reverse phase high performance liquid chromatography
R_t	retention time of analyte in column chromatography
SD	standard deviation
SEM	standard error of the mean
S/N	signal to noise ratio
TFA	trifluoroacetic acid
TGS	tryptone glucose and salts culture medium
TOF	time of flight
TSB	tryptone soy broth
TpcA	tryptocidine A
TpcB	tryptocidine B
TpcB1	tryptocidine B_1
TpcC	tryptocidine C
TpcC1	tryptocidine C_1
Tpc(s)	tryptocidines(s)
TrcA	tyrocidine A
TrcA1	tyrocidine A_1
TrcB/B’	tyrocidine B/B’
TrcB1	tyrocidine B_1
TrcC	tyrocidine C
TrcC1	tyrocidine C_1
Trc(s)	tyrocidine(s)
Trc mix	tyrocidine mixture (tyrocidines purified from commercial tyrothricin)
UPLC-MS	ultra-performance liquid chromatography linked to mass spectroscopy

Standard 3-letter and 1-letter abbreviations were used for the natural amino acids, with uppercase 1-letter abbreviations for L-amino acid residues and lower case 1-letter abbreviations for D-amino acid residues in peptide sequences.

Preface

The significant increase in antimicrobial resistance is a global emergency as antimicrobial resistance can be life-threatening and can affect different life sectors such as the medical, industrial and agriculture sectors. *Candida albicans* (*C. albicans*) is a life-threatening yeast in immunocompromised individuals that can form biofilms on biotic surfaces, with reported resistance to its first-line treatment such as amphotericin B and fluconazole. Therefore, the development of new antifungals with anti-*Candida* activity is essential. Antimicrobial peptides (AMPs) are alternatives for classic antimicrobial agents as they clinically have little side effects, they have rapid activity on their targets, they tend to have the membranolytic mode of action as well as other intracellular targets which make resistance less likely to occur. Apart from planktonic activities, many AMPs have, antibiofilm activity. In this study, we aim to enhance the anti-*Candida* activity of a group of cyclic decapeptides, the tyrocidines, via a formulation with cellulose derivatives, since the previous research by our group indicated that tyrocidines have highly potent activity against *C. albicans*. These peptides remain potent after absorption to surfaces which makes them the possible solution for creating antimicrobial surfaces in the medical sector. Although tyrocidines are haemolytic, it has been previously shown that tyrocidines' toxicity can be lowered in formulations with saccharide derivatives, while the presence of the celluloses does not show a significant change on the activity of the peptide. In this project, the formulation of tyrocidine mixture and purified tyrocidines and tryptocidines was studied in terms of stability and anti-*Candida* activity. The aims and objectives of this study are summarised below.

Aims and objectives

Aim 1: Produce, purify, and analyse the tyrocidines and analogues.

In order to reach the first aim, the following objectives were met in this study:

- Culturing the producer organism *Brevibacillus parabrevis ACCT 8185* (Chapter 2).
- Culturing the high peptide producing cultures in non-supplemented and amino acidsupplemented media to produce the various tyrocidine analogues (Chapter 2).
- Extraction of the tyrocidines and analogues and removal of the linear gramicidins (Chapter 2).

- Purification of tyrocidines and analogues with HPLC and producing pure Trc analogues (Chapter 2).
- Analysing the success of the purification with electrospray mass spectrometry and ultra-performance liquid chromatography (Chapter 2).

Aim 2: Formulation and characterisation of the tyrocidine mixture and the purified tyrocidines and analogues.

In order to reach the second aim, the following objectives were met in this study:

- Formulation of the tyrocidine mixture, tyrocidines and analogues with derivates of soluble cellulose such as hydroxypropyl cellulose and hydroxypropyl methyl cellulose and chitosan (Chapters 3-5)
- Assessing the anti-*Candida* activity of tyrocidines and their cellulose-type formulations (Chapters 3)
- Assessing the haemolytic activity of tyrocidines and their best cellulose-type formulations (Chapter 3)
- Assessing the structure and aggregated form of the peptide in a solution using spectrofluorometry (Chapters 4).

An introduction and background to the study is given in Chapter 1 and concluding remarks and a discussion on future studies are presented in Chapter 5. The experimental chapters in this thesis were written as independent units in article format. This may have led to some repetition, but it was attempted to keep repetition to a minimum.

Outputs of MSc study

Oral Presentations

Masoudi Y. (2019), Characterisation and formulation of natural cyclodecapeptides with anti-Candida activity, Biochemistry Forum, University of Stellenbosch, Oral presentation,MSc Progress Talk

Masoudi Y. (2021), Biochemistry Forum, University of Stellenbosch, Characterisation, and formulation of natural cyclodecapeptides with anti-Candida activity, Biochemistry Forum, University of Stellenbosch, Oral presentation, Oral defence of MSc thesis

Peer-reviewed articles

Rautenbach M, Kumar V. Vosloo, J. Masoudi Y., Wyk R; Stander M. (2021) Oligomerisation of tryptocidine C, a Trp-rich cyclodecapeptide from the antimicrobial tyrothricin complex, *Biochimie,* 181, 123-133

Expected outputs

Masoudi Y, Van Rensburg W, Barnard Jenkins B, Rautenbach M (2021) Characterisation and formulation of natural cyclodecapeptides with anti-*Candida* activity. Draft article from Chapters 3 and 4 for submission to *Journal of Fungi*

Chapter 1

Combating *Candida* infections with antimicrobial peptides

1.1 Introduction

Fungi are a diverse group of eukaryotic organisms. To date, around five million fungi have been discovered worldwide, with more than 600 pathogenic species [1, 2, 3]. Fungal infections are a major concern globally. The number of fungal infections is on the rise since the 1980s due to the antifungal drug resistance and the expanding population of immunocompromised individuals [4]. However, the medical sector is not the only sector affected by fungal infections, various fungal plant pathogens cause major production losses in agricultural, food and beverage industries every year [5, 6].

Infections caused by pathogenic fungi can be moderate or severe. The moderate infections are usually superficial infections which can affect skins and nails of the individuals [7]. Severe infections can involve different body organs such as kidney, liver, and brain [7]. They are usually life-threatening, especially in immunocompromised individuals with a mortality rate of over 50% [7, 8]. The number of fungal infections has increased rapidly in the past two decades as the number of immunocompromised individuals such as cancer and HIV/AIDS patients, people receiving medical implants and elderly people have also increased [9].

Candida and *Aspergillus* species are two of the most common causes of fungal infections. With *C. albicans* being the main pathogen responsible for the mucosal disease, and *Aspergillus fumigatus* being mainly responsible for the allergic fungal disease which can be extremely dangerous in asthma patients [10]. *C. albicans* infections can involve different organs or it can result in a bloodstream infection [11] while *A. fumigatus* primarily involves the lungs by producing airborne spores [10]. *A. fumigatus* is largely responsible for the increased incidence of invasive aspergillosis. Non-invasive *Aspergillus* infection normally occurs after repeated exposure to this pathogen [3].

In this chapter, the focus will be on pathogenic fungi, specifically, *Candida* species as we focused the antifungal studies (Chapter 3) of *C. albicans* as target fungal organism.

1.2 *Candida* infections

Candida species are the most common cause of human fungal infections. They cause a wide range of infections from non-life-threatening illnesses to invasive infection that may involve any organ [11]. *Candida albicans* and *Candida glabrata* are the two major fungal pathogens causing more than 50% of *Candida* infections [12, 13]. Antifungal drug resistance against a wide range of antifungal drugs has been reported, especially in *Candida* species. It is widely reported that *C. albicans* and *C. glabrata* have shown less susceptibility to azole and echinocandins families [14, 15, 16, 17, 18, 19].

Candida species are present in healthy individual's mucosal oral cavities, gastrointestinal tract, and vagina. However, the overgrowth of *Candida* species can lead to various clinical manifestations from mucocutaneous overgrowth to bloodstream infections [20]. Out of 350 heterogeneous *Candida* species, more than 17 different *Candida* species are responsible for human and animal infections. However, the majority of invasive infections are caused by *C. albicans*, *C. glabrata*, *C. parapsilosis*, *C. tropicalis* and *C. krusei* [21, 22.]

C. albicans is present in the microbiota of 40% to 60% healthy individuals [23]. It is often found in the gastrointestinal tract, reproductive tract, oral cavities, and skin. Although

C. albicans is often harmless, it can overgrow when there is a change in its host immune system or the environment [20, 24, 25, 26, 27]. *C. albicans'* overgrowth can be pathogenic in healthy individuals causing mainly oral and vaginal infection [23]. However, it is life-threatening in immunocompromised individuals such as HIV and cancer patients or during the surgical interventions [28, 29]. *C. albicans* has a great tendency to form biofilms. The biofilms usually lead to invasive infection with the mortality rate of (36% to 60% depending on the patient immune system) [30, 31, 32, 33]. Biofilms mainly form on catheters, pacemakers, and implants. Currently, regardless of all the advancement in the medical system, *C. albicans* biofilms on more than 50% of the catheters cost $6.25 billion in the United States of America only [34, 35].

During the course of infection, *C. albicans* can change its cell shape, alter its cell-wall component and secret different types of virulence factors [36]. Furthermore, it can inactivate defensins, antimicrobial peptides of the innate immune system, and inhibit other immune cell functions to weaken the host immune system [36]. *C. albicans* is metabolically highly adaptable to environmental changes such as pH, temperature,

CO_2 level and presence of serum. It can use different nutrition resources and express different metabolic pathways. This phenotype flexibility gives it the ability to survive the host defence mechanisms [37, 38].

Although *C. albicans* is the most common cause of *Candida* infections, non-*Candida albicans* infections are increasing, especially in immunocompromised individuals leading by *C. glabrata* [39]. Based on a study done in the United States of America during 1989-1999, the number of patients infected by *C. glabrata* has significantly increased while the number of patients infected by *C. albicans* decreased, therefore it is possible that in near future, the incidence of *C. glabrata* may exceed that of *C. albicans* [40, 41]. Furthermore, *C. glabrata* has the highest mortality rate which is above 60% [42, 43]. *C. glabrata* holds few unique features which are unlike other *Candida* species. As an example, *C. glabrata* is unable of forming pseudohyphae, or it does not cause a high neutrophil response from the patience immune system [44].

1.3 Anti-*Candida* drugs and resistance

Discovery of antifungal drugs is highly challenging as it is very difficult to find a drug that is toxic to fungi but not to human and/or animal eukaryotic cells [45]. There are currently only four main classes of antifungal drugs, namely, nucleosides (pyrimidines), azoles, polyenes and echinocandins [45]. Table 1.1 summarises the prominent properties of these antifungal agents. Polyenes and azoles target ergosterol in the membrane while echinocandins inhibit β1,3 D-glucan in the cell wall and nucleoside-type drugs inhibit RNA/DNA coding (refer to Table 1.1 and Figure 1.1)

Table 1.1 Summary of the most well-known examples of current clinical antifungal drugs with reported incidences of resistance by *C. albicans* and/or *C. glabrata*.

	Example	Mechanism of action	Reported resistance by *C. albicans/C. glabrata*	Example Structure	Side effects
Polyene	Amphotericin B Nystatin Natamycin	Interaction with ergosterol* resultingin loss of cytoplasma [46, 47] or disruption the integrity of the membrane [48]	Yes [45]	Amphotericin B 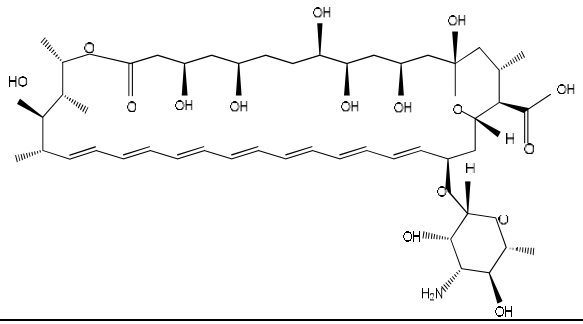	Amphotericin B cause nephrotoxicity [45]
Azole	Ketoconazole (imidazole) Fluconazole (triazoles)	Inhibition of biosynthesis of ergosterol [49]	Yes [50]	Fluconazole 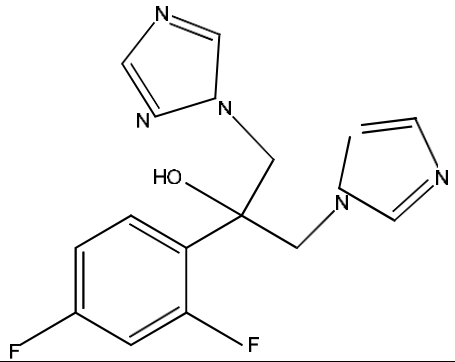	Good safety profile when used systematically with very few side effects [51]

Echinocandin	Caspofungin Micafungin Anidulafungin	Inhibition of biosynthesis of β1,3 D-glucan**[25, 52]	Limited [52]	Caspofungin 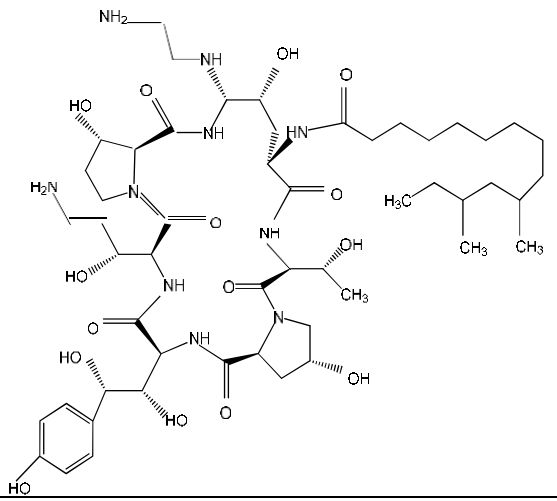	Can only be used intravenously with few side effects [53]
Nucleoside	Flucytosine	Inhibition of RNA/DNA coding [54]	Yes [55]	Flucytosine 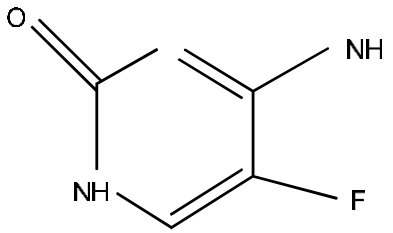	Mild side effect including diarrhoea and dizziness [45]

* ergosterol is a lipid that is crucial for the maintenance of fungal membrane structure [56]
** β (1,3) D-glucan is the main polysaccharide present in the cell wall

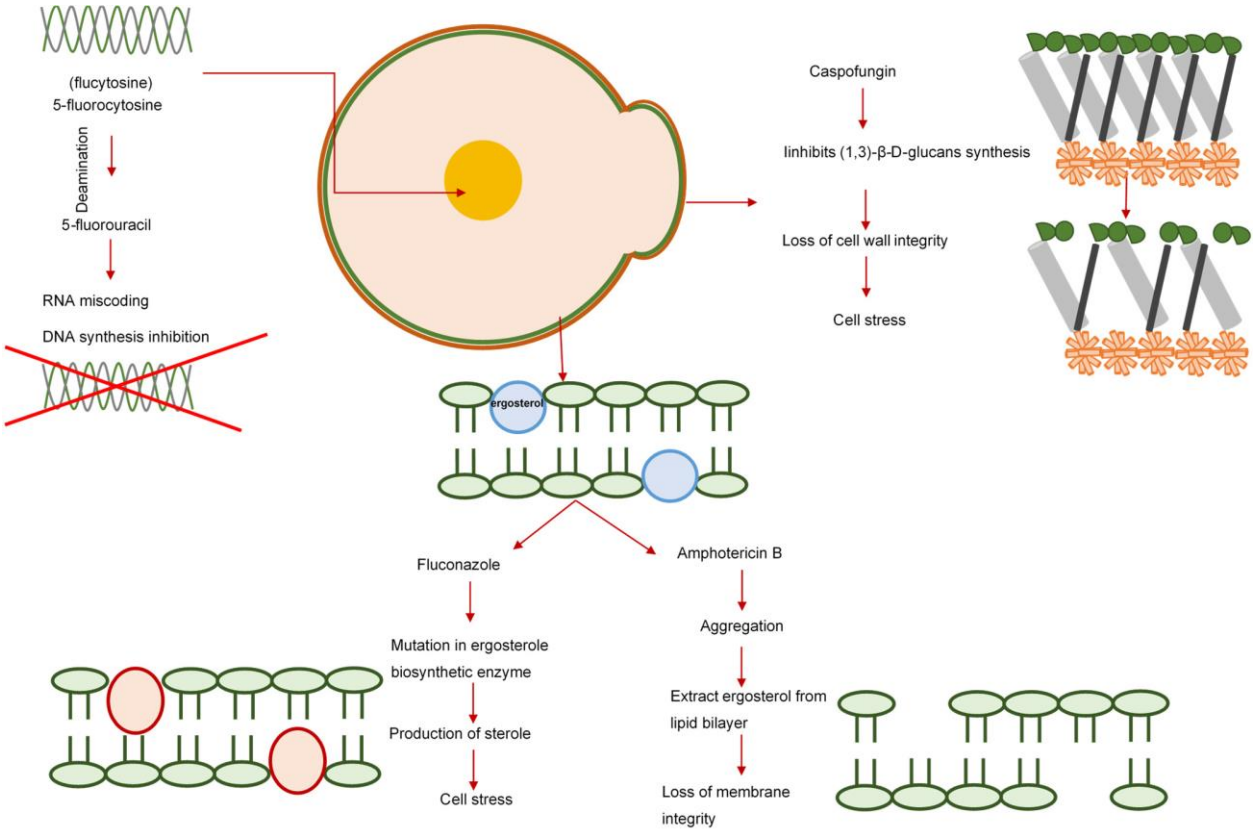

Figure 1.1 Summary of the mode of action of the main clinical antifungal drugs from each of the four drug classes against *C. albicans.*

Candida resistance development

Antifungal drugs are generally used at high dosages as treatment failure against fungal infections can lead to death [56]. Overuse of antifungal drugs and a limited number of existing antifungals have caused a rise in antifungal drug resistance [56]. There are two main categories of resistance namely inherent/primary and acquired resistance [56]. Inherent resistance describes a phenomenon whereby all known isolates of a species possess an innate resistance to an antifungal compound. *C. glabrata* is a well-known example of a species which is inherently resistant to all the drugs in the azole family. The reduced susceptibility of *C. glabrata* to azole family is independent of the presence of acquired resistance determinants [44, 57]. Acquired resistance occurs in susceptible strains and it happens during the therapy. It happens through evolutionary mechanisms that can lower the susceptibility of the organism against a given drug. The predominant example of this group is the azole resistance in *C. albicans* [50]. Acquired resistance is controlled by internal and external factors including environmental pressures, genetic plasticity, and existence of hypermutator strain[58]. The major antifungal drug resistance mechanisms include reduction of

drug uptake or biofilm formation. Lower drug uptake can occur via modification of the drug target, and/or an upregulation of drug efflux transporters (pumps) which results in the reduction in the cellular level of the drug [3]. Worryingly, the resistance level across *Candida* isolates is increasing rapidly. There is a significant rise in the numbers of the reported resistant isolates of *Candida* species [59]. The mechanisms of resistance development have been summarised in Table 1.2.

The azole family is the first-line treatment of *Candida* species infections due to its low toxicity and oral administration. However, increasing numbers of reported azole resistance is a serious concern [60]. Azole resistance is usually a stress response. Change in the expression of any of the stress-related regulators results in the resistance of the *C. albicans* species to the azole family [61]. *Candida glabrata* is inherently less susceptible to the azole family, specifically fluconazole [62]. The mechanism of resistance to polyene is close to the mechanism of resistance to azole as both of these compounds target the ergosterol in the cell membrane [63]. Cross-resistance between azole and polyene drug categories is common [63]. Besides the inherent resistance, *C. glabrata* develop acquired resistance to the azole and polyenes families through different mechanisms of actions [59]. Resistance to flucytosine is relatively fast and common. This is why flucytosine is usually used with other treatments such as amphotericin B [64]. Unlike azole resistance, the number of reported *C. albicans* resistance to echinocandins is relatively low but far from rare. Furthermore, prior exposure to the echinocandins is significantly linked with resistance [59]. Since the beginning of widespread echinocandin use, a significant increase in echinocandins resistance developed by *C. glabrata* has been reported. High genetic plasticity of *C. glabrata* allows for easier genomic rearrangement and adoption of the organism to stressful conditions. Therefore, the resistance pattern of *C. glabrata* should be monitored more carefully [44, 65].

In addition to the explained mechanisms of drug resistance developed by *Candida* species, the formation of biofilms is a major concern in the development of drug resistance. A biofilm is a community of cells adhering to each other or on surfaces, possessing properties that are different from those of free-floating (planktonic) cells. The major difference between biofilms and planktonic cells is the greater resistance of biofilms to drugs [34]. *Candida* species have a great tendency of biofilm formation [67]. *Candida* biofilms are organised three-dimensional structures consisting of cells in an exopolymeric matrix of proteins, nucleic acids, and carbohydrates [68].

Table 1.2 Summary of mechanisms of resistance developed by *C. albicans* and *C. glabrata* towards available clinical antifungal drugs.

Mechanisms of resistance developed by *C. albicans*

nucleoside	A. Point mutation in FYC1 and FYC2, encoding cytosine deaminase, inhibits the drug uptake resulting in less accumulation of the drug in the cell B. Point mutation in FUR1, encoding uracil phosphoribosyltransferase, results in inactivation of uracyl phosphoribosyl transferase leading to an alteration in the metabolism of 5-fluorocytosine [59]
azoles	A. Mutation in Erg11 gene interferes with the inhibition of ergosterol biosynthesis B. Mutation in the upregulation of multidrug transporters uptake results in less accumulation of the drug in the cell [66]
polyene	A. Resistance to amphotericin B occurs through mutations in ERG3 which lowers the concentration of ergosterol in the cell membrane B. Frameshift mutation in ERG2 gens and Point alteration in ERG3 and ERG5 genes decrease ergosterol content in the cell [63]
Echinocandins	Mutation in hotspot regions of FKS2 genes reduce the binding affinity of echinocandins [58, 59]

Mechanisms of resistance developed by *C. glabrata*

nucleoside	A. Point mutation in FYC1 and FYC2, encoding cytosine deaminase, inhibits the drug uptake resulting in less accumulation of the drug in the cell B. Point mutation FUR1, encoding uracil phosphoribosyltransferase, results in inactivation of uracyl phosphoribosyl transferase leading to an alteration in the metabolism of 5-fluorocytosine C. Deletion in FPS1 and FPS2 genes reduced accumulation of the drug [65]
azoles	A. Absence of calcium signalling (essential for azole treatment) results in the inherent resistance [63] B. point mutation in PDR1 transcription factor resulting in the upregulation of drug efflux pump [59]
polyenes	A. Resistance to amphotericin B is developed through point mutations in ERG2 and ERG6 genes which lowers the concentration of ergosterol in the cell membrane B. Point alteration in ERG2 and ERG6decrease ergosterol content in cells [59]
Echinocandins	A. Mutation in hotspot regions of FKS1 genes reduce the binding affinity of Echinocandins B. Mutation in FKS1 decrease glucan synthase processivity for the drug [58, 59]

The greater tendency of the development of resistance by *Candida* biofilms is due to different factors such as alterations in efflux pump expression, changes in the cell membrane and wall composition and the presence of persister cells. Furthermore, the glucan matrix surrounding the biofilm physically prevents antifungal compounds from reaching cells [69]. Fungi are extremely adaptive against cellular stress which usually leads to elevated minimum inhibitory concentration of antifungal compounds. The exposure of the cells to antifungal compounds causes cell stress. As a response to drug-induced stress, stress regulator factors such as Hsp90 and calcineurin would be expressed. The expression of the cellular regulators led to the formation of biofilms or acquired resistance [70]. The drug resistance developed by *Candida* species is directly related to previous exposure especially in the presence of azole and echinocandins [61, 56]. The lack of proper treatment for *Candida* infections and the emergence of resistance intensifies the need for the development of new anti-*Candida* drugs.

1.4 Antimicrobial peptides as candidate antifungal drugs

Antimicrobial peptides (AMPs) are the novel generation of antimicrobial agents. Due to their rapid eradication of the target organism and different mode of actions, resistance is less likely to occur against them [71, 72]. Within the large family of AMPs, there are peptides with the ability for antifungal activity, including tyrocidines (Trcs) and analogues, which are the focus AMP in this project [73, 74, 75].

AMPs are relatively small gene-encoded molecules, comprising 12 to 50 amino acids, which can be found in all prokaryotic and eukaryotic organisms [76]. AMPs are usually the first line of defensive mechanisms in their hosts [77, 78]. Examples of antimicrobial peptides include nisin isolated from bacteria [79], plectasin from fungi [80], cecropins from insect [81, 82] and defensins from plants and humans [83, 84].

Although AMPs share many similarities, they have distinct structural differences. According to a review by Epand and Vogel [85], AMPs are categorised into four categories based on their structures. These categories include α-helical AMPs, β-sheet AMPs, AMPs with unusual amino acids and AMPs consisting of the thio-ether ring. AMPs with alpha-helical structures are mostly cationic and amphipathic such as magainin [86, 87, 88]. However, there are AMPs with α-helical structure that are either anionic such as alamethicin [89] or hydrophobic such as gramicidin A [90]. AMPs that have β-sheet structures are mostly cyclic with disulphide bonds such as certain defensins [91] or N-C cyclisation such as gramicidin S and tyrocidines [92, 93]. Tritrpticin, which is rich in tryptophan, is a typical example

of AMPs with unusual amino acids sequences [94]. The last group belongs to lantibiotics which are bacteriocin with a cyclic structure and a thio-ether ring such as nisin [95].

AMPs are potential alternatives to classical antimicrobial agents as resistance is less likely to occur against them due to their rapid and multiple modes of action [96]. AMP mode of action can be generally classified into two main groups, namely membrane disruptive and membrane non-disruptive [73]. Different theories explain how membrane disruptive AMPs can bind to their target and eradicate them. One such a theory is the Barrel-Stave model [97, 98] which states that peptides undergo horizontal orientation in a way that the hydrophobic part of the peptide can face towards the hydrophobic part of the membrane and hydrophilic part face towards the inside. This orientation leads to the formation of pores that can result in leakage of the cell components [97, 98]. Another theory that explains the mechanism of action of membrane-disruptive mode of actions is called the toroidal pore model [99] which explains that AMPs can bind to the membrane and force the lipid to fold inwards and form channels which can lead to the cell leakage [98, 100, 101]. The carpet model [102] is the third theory which believes in the association of AMPs with the membrane and destruction of the electrostatics of thecytoplasmic membrane which leads to the collapse of the membrane into a micelle and consequently the cell death [98]. Examples of the non-membrane disruptive mode of action include interference with RNA or DNA synthesis, enzyme functions and, the process of cell division [103, 104, 105,106, 107, 108]. AMPs' mode of action is highly dependent on the target's cell membrane organisation and the peptide structure. For instance, the bacterial membrane is a good target for cationic peptide as they mostly contain phospholipids and a negatively charged membrane while eukaryotic cells are normally neutral in charge which leads to alow affinity of peptide [109].

1.4.1 Antifungal peptides

Antimicrobial peptides with antifungal activity (AFPs) have emerged as good candidates for novel antifungal drugs due to their efficacy and lower chance of resistance development. Although AFPs cause fewer side effects compared to classic antifungal agents, the majority of AFPs have cytotoxic properties [110]. Unlike, AMPs with antibacterial properties, little is known about AFPs which makes their classification challenging. In this review, AFPs are categorised into two categories based on the mode of action and origin. In each of the categories, a few examples with anti-*Candida* activity will be mentioned. Antifungal peptides

can be isolated from natural, semisynthetic, or synthetic sources [111]. For the purpose of this review, a few examples of each category with anti-*Candida* activity are given in Table 1.3.

Antifungal peptides with primarily antifungal activity

The majority of AFPs have a broad spectrum of activity with few peptides having primarily or exclusively antifungal activity [112] such as echinocandins, nikkomycins and aureobasidins, defensins and histatins. Echinocandins are a family of cyclic lipopeptides inhibiting glucan synthesis. Echinocandins non-competitively inhibits the enzyme 1,3-β-glucan synthase resulting in destabilisation of the cell wall [113]. Nikkomycins and aureobasidins inhibit the chitin in the cell wall. Chitin is a cell wall component crucial for the maintenance of the structural integrity of the fungus, which is absent in all vertebrates [114, 115, 116]. These peptides show significant anti-*Candida* activity while they are not toxic to human cells [117]. Plant defensins such as HsAFP1 and DmAMP1 [118], as well as insect defensins [119], are membrane-active AFPs with proven anti-*Candida* activity [118]. Histatins are histidine-rich peptides with membrane activity and/or intracellular target [120, 121], Furthermore, histatins have strong anti-*Candida* activity [122, 123].

Antifungal peptides with a wide spectrum of antimicrobial activity

Most AMPs are also AFPs and have a broad spectrum of activity affecting bacteria, fungi, or viruses. Most of these peptides have a membranolytic activity which is usually toxic to mammalian cells at higher concentration [112]. These peptides are broadly categorised in two groups of linear and cyclic peptides [124]. Linear peptides include cecropins [125], magainins [88], and dermaseptins [126] and are small with an amphipathic α-helical structure. They primarily disrupt the membrane but some of them have unique intracellular targets [127], [106]. Although cyclic and linear peptides mainly target the membrane, most of them have their unique mode of action [124].

Table 1.3 Summary of the origin, structure, and mode of action of exampled AFPs with anti-*Candida* activity

Source	Type of AFP	Example	Structure	Mode of action	Reference(s)
Archaea	CAMP-like	VLL-28	Cationic	Cell wall	128
Bacteria	Cyclic decapeptides	Tyrocidines, Tryptocidines, Phenycidines Gramicidin S Loloatins	Cyclic with β-sheet	Membranolytic, have multiple targets	129 92 130
Fungi	Nikkomycins	Nikkomycin X, Z	Peptide nucleosides	Inhibit chitin biosynthesis	117,131
	Polyoxins	Polyoxin A, B, D	Peptide nucleosides	Inhibit chitin biosynthesis	132,133,117,134
	Echinocandins	Echinocandins, pneumocandins, aucleacins, mulundocandins,	Cyclic hexapeptides with N-linked acyl lipid side chains	Inhibit glucan synthesis	135, 136
	Aureobasidins	Aureobasidin A	Cyclic depsipeptide	Delocalising chitin in cell walls	137,111
	Leucinostatins	Leucinostatins A, B, D, H	Contains five unusual amino acids	Uncouplers of mitochondrial function	134,137
Amphibians	Magainins	Magainin 2	Helical, amphiphilic	Lysis by inhibiting ion gradient in cell	111
	Skin-PYY	Skin-PYY	Hairpin-like structure with type II β-turn	Membrane disruption	138,111
Aquatic sources	Aciculitins	Aciculitins A-C	Cyclic peptides and lipid residues	Cell lysis	139
	Theonegramide	Theonegramide	Glycopeptide with unusual amino acids	Unknown	139
	Laxaphycins	Laxaphycins A, B, D and E	Cyclic peptides	Unknown	139
Mammalian	Defensins	Tachycitin	β-sheet	Chitin binding	139
	α-defensins	HNP-1, HNP-2,HNP-3	β-sheet with cysteines	Cell lysis	134
	β-defensins		β-sheet with cysteines	Cell lysis	134
	Protegrins, Cathelicidins	Tracheal antimicrobial protein (TAP) Protegrins 1, 2 and 3	Cationic, cysteine-rich	Pore formations and lysis	134
Semisynthetic	Cilofungin (LY1019)	-	Lipopeptide	Inhibit glucan synthesis	140
	LY 303366	-	Lipopeptide	Inhibit glucan synthesis	111
Synthetic	PMAP-23/ KU2/ KU3	-	α-helix	Membrane	139

1.5 The tyrocidines as potential AFPs

Tyrocidines (Trcs) and analogues are broad-spectrum AMPs with promising anti-*Candida* activity [75, 76]. Trcs and analogues are extracted from the tyrothricin complex, which is non-ribosomally produced by *Brevibacillus parabrevis* [141, 142]. Tyrothricin is a classic antibiotic that was discovered 10 years after penicillin [141]. The remarkable anti-*Candida* potency of Trcs and the fact that there has been no resistant reported to date make Trcs potential candidates for the treatment of *Candida* infections [75].

Tyrocidines (Trcs) are small cyclodecapeptides, sharing the Val-Orn-Leu-D-Phe-Pro pentapeptide sequence with the well-known peptide, gramicidin S [143, 144]. Figure 1.2. shows the primary structure of gramicidin S (GS), tyrocidine A (TrcA) and tyrocidine C (TrcC).

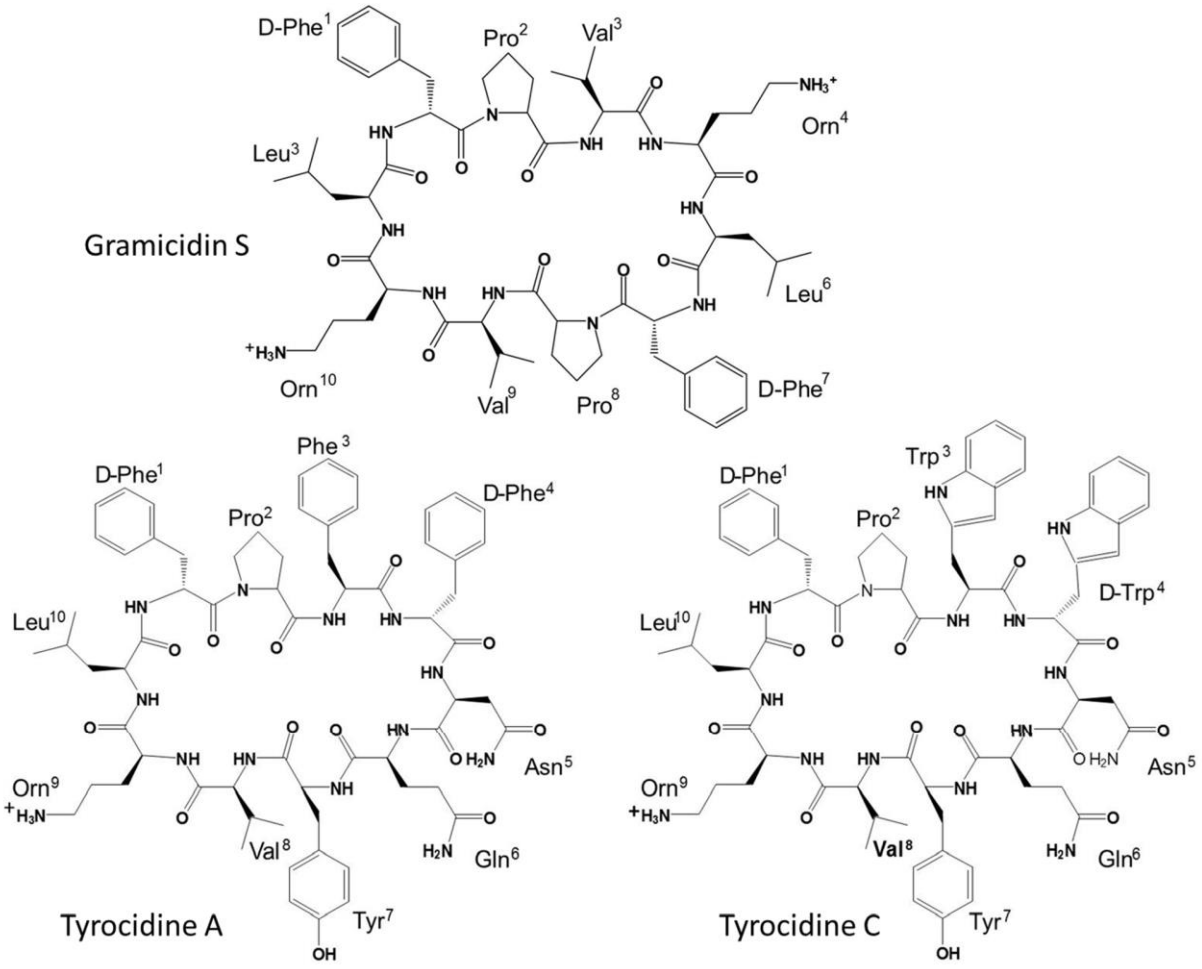

Figure 1.2 Primary structures of analogous cyclodecapeptides TrcA, TrcC and GS. The three peptides share the conserved VOLfP pentapeptide moiety in their cyclic structure. Standard three letter amino acid abbreviations are used in the annotation except Orn representing ornithine. The residue numbering is according to the order of biological synthesis.

The cyclodecapeptides from tyrothricin have a fairly conserved sequence, cyclo (D-Phe[1]-Pro[2]-X[3]-x[4]-Asn[5]-Gln[6]-X[7]-Val[8]-X[9]-Leu[10]) (Figure 1.2). The X[3]/x[4] indicates the variable L- or D-aromatic amino acid residues respectively, with Phe[3]-D-Phe[4] to give the A analogue peptides, such as TrcA, Trp[3]-D-Phe[4] in the B group such as tyrocidine B (TrcB), Phe[3]-D-Trp[4] in the B' group and Trp[3]-D-Trp[4] in the C group such as TrcC (Figure 1.2). The tyrocidines (Trcs) have a Tyr at position 7, while the tryptocidines (Tpcs) have a Trp[7] and the phenycidines (Phcs) a Phe[7]. All these peptides can have either ornithine (Orn) or Lys in position 9 as cationic residue. [144]. Those with Lys[9] is denoted with a subscript 1 after the group for example $TrcA_1$ and $TrcC_1$. The variation at the non-conserved positions accounts for the presence of 24 different analogues of Trcs, which was characterised by Tang *et al*. [144]. However, Leu or Ile can be substituted at position 8 which can give rise to a possible 72 minor analogues [144]. Substitutions of Ile/Leu/Tyr in positions 3 or 4 bring the total to about 450 possible cyclodecapeptide peptides in tyrothricin.

The cyclodecapeptides (Trcs and analogues) constitute 50-60 % and linear gramicidins 10-20% of the peptide mass that are produced as the main components of tyrothricin complex [144] during the late logarithmic growth phase of *Brevibacillus parabrevis* [141, 142]. The benefits for *Brevibacillus parabrevis* that is offered by the production of the tyrothricin complex are not clear, but it is assumed that the antimicrobial activity of tyrothricin towards other organisms provides a competitive advantage for the producer organism. Furthermore, production of tyrothricin complex might play a role in the sporulation [145].

The production of cyclodecapeptides and gramicidins in tyrothricin is non-ribosomal and encoded by the tyrocidine and gramicidin biosynthesis operons [146]. The thio-templated non-ribosomal peptide synthesis is achieved through multi-domain enzyme complexes containing non-ribosomal peptide synthetases (NRPSs) [146, 147]. In the Trc production process, there must be of amino acids available within the growth medium for a sequential addition into the cyclodecapeptide structure by the NRPSs [142, 147]. This process takes place during the late logarithmic growth phase under oxygen limiting conditions [148]. The media of the producer organism must contain nitrogen resources such as urea and carbon [149, 150]. The production of Trcs and its analogues can be manipulated via amino acid supplementation of culture medium. Addition of Trp will shift the production towards the Trp-rich Tpcs while the addition of Phe shifts the production towards the Phe-rich Phcs [151].

TrcA in the tyrothricin complex is one of the first peptides of which the structure was elucidated. It has a secondary structure consisting of an antiparallel β-sheet between

Trp/Phe[3]-Asn[5] and Val[8]- Leu[10] that is linked by a type I (Gln[6]-Tyr[7]) and type II (D-Phe[1]-Pro[2]) β-turn [152] (Figure 1.3). One study indicated that the hydrophobic interaction between someof the side chains of TrcA leads to a curved structure and dimerisation which is responsible for its amphipathic characteristics [153].

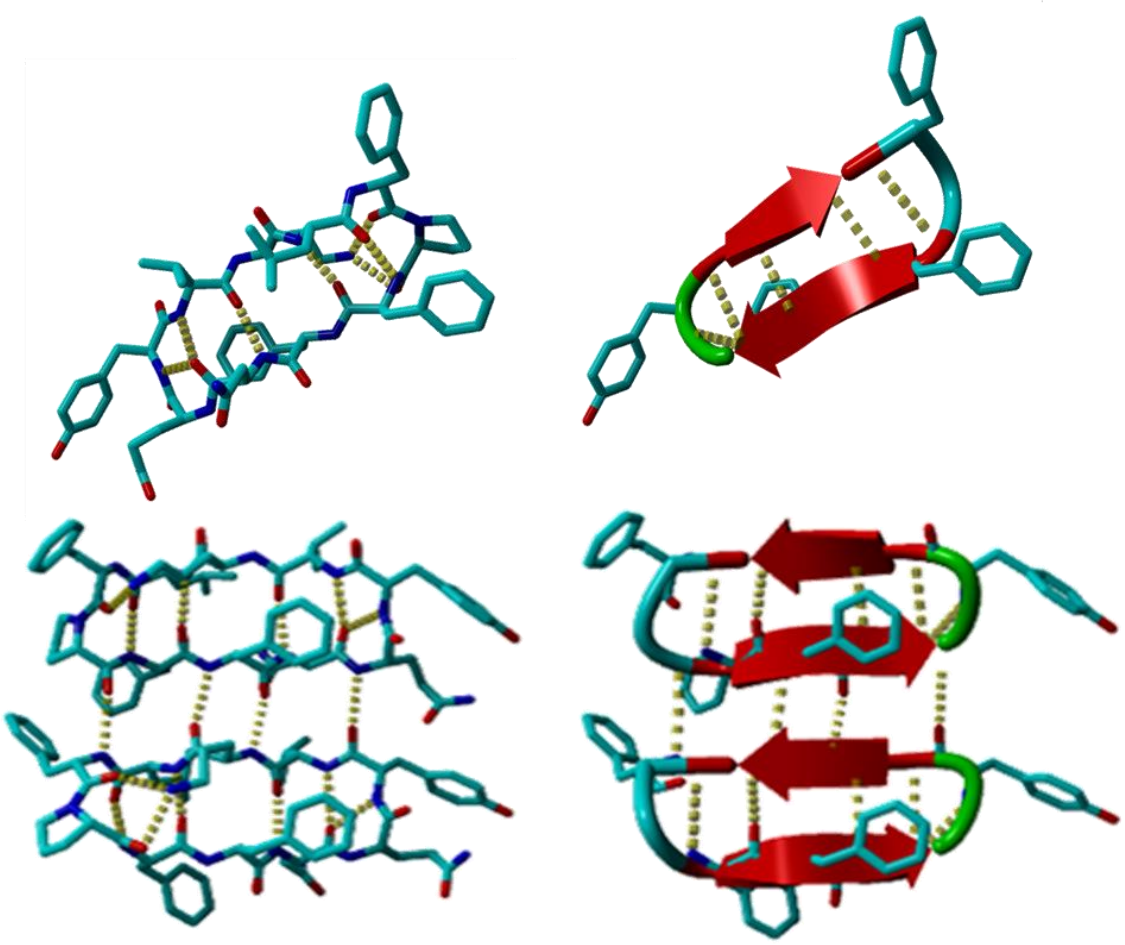

Figure 1.3 The 3D structure of TrcA (top) and an amphipathic dimer of TrcA (bottom). TrcA stick structures are shown on the left and the corresponding ribbon structures with aromatic residues on the right. Carbon is shown in turquoise, nitrogen in blue and oxygen in red. Hydrogens were omitted from the structure. The dotted yellow line indicated hydrogen bonds, the red arrows antiparallel β-sheet, green and turquoise tube β-turns. The images are courtesy of V. Kumar and M. Rautenbach and were modelled utilising Yasara 11.3.2. The original 3D models used to create the 3-D structures were based on models by Munyuki *et al*. [93].

A second study showed that TrcA and TrcC can form various dimeric structures with amphipathic properties [93]. The amphipathic structure of these cyclodecapeptide dimers (Figure 1.3) is important for the association with the negatively charged bacterial/fungal cell membrane which leads to the destabilisation of the membrane and, therefore, death of the cell [93, 152]. Furthermore, it could be that the β-sheet structure of such cyclodecapeptides [154,155, 156] allows them to maintain its stability under different environmental conditions such as a range of temperatures or solvent. The Trcs also maintain its antifungal activity in the

presence of Mg^{2+}, K^{+} and Na^{+} [156]. Ca^{2+} has a negative effect on the antifungal activity of these peptides [157] but increases their anti-*listerial* activity [129].

The activity of the Trcs and analogues is dependent on three main factors including the target organism, mode of action, structure, and resultant oligomerisation. This group of cyclodecapeptides have a broad spectrum of antimicrobial activity against parasites (*Plasmodium falciparum* [159, 160, 161]), Gram-positive bacteria (*Diplococcus pneumoniae, Listeria monocytogenes* [161, 162]) and fungi such as *Candida albicans* [75], *Neurospora crassa* [163] *and filamentous fungi* [158, 164]. However, previous studies on *Escherichia coli,* indicated that Trcs are not very active against Gram-negative bacteria [163]. In addition to the antimicrobial activity, Trcs possess toxicity properties against mammalian cells [165, 166, 167]. Trcs are haemolytic and leukocytolytic [166], however, they are relatively safe when used topically or orally [167].

The Trc antimicrobial and haemolytic activity occur very rapidly. Trcs show their antimicrobial activity within two to four seconds [161, 167]. Moreover, Trcs do not maintain their full antimicrobial activity in the presence of blood serum therefore it is suggested to use the Trcs in the direct contact with the target organism [170]. Although there is still no complete model for tyrocidines mode of action, Trcs' main target has been identified as the microbial membrane, with some studies indicating membrane proteins as targets and unknown intracellular targets [129, 156, 162]. Early studies suggested Trcs have intracellular targets such as DNA in the producer organism resulting in inhibition of some NADH enzymes [170] and the food vacuole or cell cycle regulators in the human malaria parasite [157, 165].

Trc antimicrobial activity has been largely attributed to their membrane lytic mode of actions which is initiated by a series of hydrophobic and ionic interactions as well as hydrogen binding [129]. Trcs oligomers have been proposed to form channels or pores throughout the bacterial membrane resulting in the cell lysis [162, 167]. In a study done by Wenzel *et al*. [143], the mode of action of TrcA and TrcC has been investigated in more detail and compared with that of gramicidin S (GS) which share more than 50% similarity on the sequence identity with Trcs. This study suggested that the difference between the antibacterial activity of Trcs and GS is due to the presence of four aromatic amino acid residues on the Trcs and two Phe in GS. Furthermore, Trcs have the ability to form dimers [93,152] while there has been no evidence to date that GS forms dimers. This study illustrated that Trcs are able to form pores through the membrane, but the exact mechanism of pore-forming ability of Trcs is not clear. Both Trcs and GS target membrane by affecting membrane fluidity. Wenzel *et al*. [143], as

showed that TrcA and TrcC target membrane proteins as well as DNA. In fungi, Trcs also may have both membranolytic activity and intracellular targets [171,172]. Troskie *et al*. [159] showed that the removal of the fungal cell walls significantly influenced the Trc activity. Rautenbach *et al*.[110] showed that these peptides have a rapid membranolytic activity that is influenced by ergosterol, glucosylceramides and the fluidity of the phospholipids in the fungal membrane.

1.5.5 Trc oligomerisation, toxicity, and structure-activity relationships

Trcs have a strong tendency to oligomerise [152, 173]. Interestingly, the antimicrobial activity of Trcs may be dependent on their ability to form oligomers. One of the first studies done by Ruttenberg *et al*. [173] showed that the lack of oligomerisation results in loss of biological activity. However, another early study showed extensive oligomerisation of Trcs results in loss of activity [174]. Therefore, there could be a critical point of oligomerisation which results in the maximum antimicrobial activity of the Trcs [174] and manipulation of Trcs oligomerisation profile can potentially result in a change in their biological activity. It is hypothesised that Trcs dimers are responsible for the antimicrobial activity of Trcs. Based on a model designed by Loll *et al*. [152] Trcs can form arrow-shaped dimers that interact with membranes.

Based on the study done by Troskie and Rautenbach [76], TrcA is the most active analogue of Trcs against *C. albicans* while phenycidine A (PhcA) with a Phe^7 rather than a Tyr^7 was the least active analogue. The aromatic residue differences in the cyclodecapeptide primary structure led to differences in hydrophobicity, while the different M_r led to a difference in *m/z* ratio, as well as overall surface and volume of the peptide [93, 144]. This can cause minor conformational differences of the peptide which could change the oligomerisation, as well as affinity or type of the interaction with the target cell and result in the change in the activity of the peptide [93, 152].

Manipulation of the structure of most AMPs results in a change of their antimicrobial and haemolytic activity. As an example, introduction of positively charged residues to the analogous GS has increased the biological activity while decreasing the haemolytic activity [175, 176, 177]. According to Kohli and Wash [178], the antimicrobial activity of Trcs has been correlated to D-Phe^4 and Gln^6 residues within the Trc amino acid sequence. Substitution of D-Phe^4 that can insert into the hydrophobic bilayer, with basic D-amino acids, Orn, Arg or Lys, led to a more cationic peptide and significantly improved the biological activity and selectivity [178]. Substitution of the D-Phe^4 residue by negatively charged D-Glu or D-Asp led

to a loss of antibacterial activity [177]. The enhanced activity of Trc upon increasing positive charge might be attributed to the better ability of the Trc to interact with the negatively charged phospholipid bilayer. The previous study on synthetic TrcA by Marques *et al*. [179] showed that manipulation of Trc A structure leads to a change in the antibacterial activity of the peptide against *E. coli.* This group attempted to find the relationship between the overall amphipathic character and the biological activity of TrcA. With solid-phase synthetic methodology, they synthesised TrcA and eight different analogues. These analogues were achieved via point substitution that would affect either the polar or nonpolar face of the molecule. The result showed that there was an increase in antibacterial activity when the amphipathicity of TrcA was increased [179]. Furthermore, amino acid substitution can alter the oligomerisation profile that can result in the change of the activity [176, 178]. As observed for GS, cyclic conformation is also important for the antibacterial activity of the tyrocidines [176]. In short, the activity and selectivity of Trcs are dependent on the balance of amphipathicity and positive net charge [172]. Therefore, change in the amphipathicity, hydrophobicity or general structure of the peptide results in a change in the haemolytic or antimicrobial activity of the Trcs.

Although structural modification of Trcs showed enhanced biological activity and lower toxicity, this complicated synthetic process, as well as the high cost, do not favour utilisation of this method for large scale production. Alternatively, drug combinations could lower the amount needed and therefore result in lower toxicity. Troskie *et al*. [75] attenuated the TrcA anti-*Candida* activity via combination with an antifungal drug. In this study, the lower TrcA concentrations needed for activity reduced the toxicity when synergistic mixtures of TrcA+caspofungin and TrcA+amphotericin B was used to obtain potent anti- *Candida* activity. Furthermore, peptide formulation could be more of cost and time effective. If a suitable formulation for the Trcs can be found, specifically a formulation that can increase the peptide stability, oligomerisation, and selectivity, it can yield better preparations for topical and oral administration. It could also be combined with synergistic antifungal drugs for last resort systemic applications.

1.5.6 Formulation of anti-fungal drugs

Formulation or covalent modifications of the peptides are used for various reasons, namely, the Improvement of the peptide's biological activity [179, 180], broadening the antimicrobial activity [181], lowering the toxicity [182], improvement of solubility (especially in an aqueous environment) [183, 184], improvement of stability and increasing the drug shelf life [185]. In some

cases, the formulations or modifications are used to overcome the antimicrobial resistance [186] or it is used as a targeted delivery system for the drug of interest [187]. This delivery system can protect the drug from the hosts' enzymes, especially when the drug is consumed orally [188], or it can lead to the controlled release of the drug [189].

The most successful formulations for many drugs, including peptides entail the use of different types of lipids (including lipid-type detergents) and saccharides. A brief overview of these two types of formulants will be given.

Lipid formulations

Lipid-based drug delivery systems, by encapsulating or solubilising the drug of interest in a lipid formulant, are became more prevalent in drug formulations in the past few decades. Lipid formulations can the done through multiple approaches, such as, solubilising a lipophilic drug in an oily solution [190], or through the formation of mixed micelles and liposomes, or even by using a solid lipid nanoparticle [191]. In a system that consists of more than one compound with differing hydrophobicity, the formulation can occur through the formation of mixed micelles. In detergent-lipid mixed micelles, the detergent molecules enhance the emulsification of the lipid of hydrophobic molecules to ensure better aqueous compatibility [191]. Formulation through the formation of liposomes is done by using phospholipids to form the vesicles and encapsulate the drug [192]. Phospholipids are amphiphilic as the fatty acyl chains form the hydrophobic tail groups and the phosphate form the head group. As the consequence of this property, they can form bilayer structures such as vesicles or liposomes with the hydrophobic tails facing each other and the polar head group on the surface and on the inside of the bilayer structure [192]. The advantage of this system is that both hydrophobic and hydrophilic drugs can be formulated. Lipid nanoparticles are typically spherical nanoparticles with both liposomal and micellular character and can be used to solubilise lipophilic drugs for systemic applications [191].

In lipid formulations, the drug is encapsulated by lipid therefore, when the drug is consumed orally, it will not get degraded by the gastrointestinal tract enzymes. After the absorption of the lipid-drug formulation by the enterocytes, possibly via the chylomicron system, the lipid capsule will slowly degrade to release the drug [193]. For nasal administration, this could lead to slower and more controlled release in the nasal passages, as well as protect the drug from the host and pathogen enzymes [187, 188, 194]. Lipid formulations can also be used for systemic application via direct infusion into the bloodstream [190, 191, 195]. Also, the immune response, as well as the toxicity of most drugs are decreased in lipid formulations [195, 196].

A well-known example of a successful lipid formulation of a peptide is the lipid formulation used for the drug cyclosporin A. Cyclosporin A is a non-ribosomally synthesised peptide with weak antimicrobial activity [197], which is mainly used for arthritis treatment [197]. Due to the side effects of this peptide such as neurotoxicity, cytotoxicity hepatotoxicity, and nephrotoxicity, long term treatment is extremely limited. However, cyclosporin A formulated by a polymeric Micelle (methoxy poly (ethylene glycol)-hexyl substituted poly (lactide)) and surfactants (Cremophor EL) shows significantly lower toxicity and improved stability [197]. An example of a lipid formulation that improved the activity of an AMP is that of gramicidin A, a non-ribosomal AMP that is found in the well-known tyrothricin complex [90, 182]. Gramicidin A formulated by cationic bilayer fragments forming disc-like structures shows a broader biological activity towards both Gram-positive and Gram-negative bacteria [182]. These lipid bilayer discs were prepared by sonication of charged lipids or by using liposome fragments [182].

Another benefit of lipid-formulation is that lipid formulation can protect AMPs from host enzymes. A study showed that lipid-formulation of the AMP, α-helical CM3, protected the peptide from peptidases when it was inhaled [194]. Liposomes encapsulate α-helical CM3 successfully delivered via an inhaler to the lungs of the rats infected by *P. aeruginosa.* This formulation also reduced the toxicity of the peptide, combined with protecting the peptide against proteolytic degradation [194].

Amphotericin B (AmB) is a well-known antifungal drug, with similar membranolytic and haemolytic activity than the Trcs [198, 199, 200]. AmB is one of the most reliable anti-fungal treatments and a last-resort drug [197]. AmB has been successfully formulated with lipids to limit is toxicity and allow systemic application [199] as it is not only haemolytic, but it has other toxicities such as nephrotoxicity [45, 199]. Therefore, to reduce the toxicity, different lipid-formulations have been developed. The lipid formulations of AmB not only results in less toxicity but also protects the drug from enzymatic degradation and the host immune system. The liposomal formulation of AmB (L-AmB), marketed as Ambisone™ is used for a controlled drug release [194, 195, 196]. A slow release of AmB results in the diversion of the drug from the kidney. The other lipid formulation of AmB includes AmB lipid complex (ABLC) marketed as Abelcet ™, and AmB colloidal dispersion (ABCD) marketed as Amphocil™ and Amphotec ™ [195, 196, 201, 202]. Pure lipids are not the only formulant for hydrophobic drugs, such as AmB. As an example, AmB is formulated by a bile-salt (steroid-type detergent) called sodium deoxycholate, marketed as Fungizone™ that increased the AmB solubility in

saline, as well as lowered its toxicity [201]. This detergent formulation of AmB results in the formation of a ribbon-like self-assembly structure that forms a mixed colloidal dispersion [201].

Saccharide-type formulations

Novel saccharide based formulants are predicted to be the next breakthrough in drug discovery due to the high molecular weight and the strong interaction with the drug molecule and low manufacturing costs [197]. The formulation of drugs via saccharides can occur through different approaches such as solubilisation, nanoparticles [203] or Dextran-based gel-coupled drugs [204, 205.]

Cyclodextrins (CDs) are the most well-known saccharide group used in drug formulation. CDs are cyclic oligosaccharides that are produced by enzymatic degradation of starch [206]. These molecules have a doughnut-shaped structure with a hydrophilic outer surface and a relatively hydrophobic inner cavity. The hydrophobic drug molecules can be entrapped by the hydrophobic inner cavity of the CDs [206]. A wide range of molecules especially peptides and proteins can interact with the CDs hydrophobic inner cavity. The main forces of the interaction between the CD's cavity and drug molecules include van der Waal forces, hydrophobic bonding and hydrogen bonding [207]. However, CDs complex formation is a dynamic equilibrium in which one drug molecule continuously associates and dissociates with one CD molecule [207]. Furthermore, CDs can form water-soluble inclusion complexes with poorly soluble compounds [207]. By substitution of different functional moieties such as methyl (CH_3), hydroxypropyl (CH_2-CHOH), and sulpho-butylether ((CH_2)$_4$-SO_3Na) with the CD's hydroxyl groups, different CD derivatives can be obtained [208]. CD-containing formulations have been extensively used for drug delivery and controlled drug release [209],[210, 211] enhancing drug permeation [212], increasing drug solubility and stability [213]. Furthermore, CDs formulation have shown to reduce several drugs toxicity [214]. However, the toxicity of the CDs alone depends on the administration route. As an example, natural CDs and their derivatives are well tolerated when consumed orally and they are listed as an inactive ingredient by the FDA [214]. Formation of self-assembly structures of CD-drug complexes can lead to innovative drug delivery system, as an example; water-soluble or water-insoluble drugs can be loaded on the hydrophobic or hydrophilic parts of CDs, while CDs act as nanocarriers for drug delivery. CDs can be structurally tailored to form different nanostructures such as nanospheres, nanomicelles and nanoparticles [216]. The most common application of CDs as formulant is to increase the solubility of less soluble drugs in

water. To formulate the poorly-water-soluble drugs, the drug must have a lipophilic moiety capable of entering the hydrophobic CD cavity [216].

Chitosan is a naturally occurring saccharide and it is considered as a non-toxic polymer for oral admiration in many countries such as Japan and Italy [217]. Chitosan is found in a varietyof molecular weight [218], size and deacetylation forms [219]. Chitosan has a concentration-based viscosity in which the viscosity increases as the concentration increases [220]. These characteristics make chitosan an easy polymer for further modification and therefore, a suitable saccharide for the drug formulation. Exendin-4 is an example of a peptide, althoughit is not an AMP, that was successfully formulated in chitosan nanoparticles [221]. This peptide promotes insulin synthesis and secretion [222]. It also inhibits the apoptosis of pancreatic β- cells, leading to the reversion of diabetes type II [222]. Formulated exendin-4 as inhalable nanoparticles that was composed of glycol chitosan showed an enhanced therapeutic effect on diabetes type II [219].

Cellulose derivatives are also ideal for drug formulations, as they are cheap and biodegradable and non-toxic [223]. Cellulose is the main structural component of plant cells [223]. It is a polysaccharide consisting of linear chains of 1-4-linked β-D-glucopyranose units [223]. Cellulose molecules can have different polymer chain lengths, but they mainly have a high molecular weight, are insoluble and mostly contain 1-4-linked glycosidic bonds which makes it non-digestible in the gastro-intestinal tract [224]. This stability makes cellulose-type formulants good candidates for drug formulation [225, 226]. Natural celluloses with shorter chain lengths are only weakly water-soluble [225, 226]. However, partial hydrolysis and the etherification of hydroxyl groups give rise to new cellulose derivatives with significantly better water-solubility [225, 226]. Ether-cellulose derivates include methylcellulose, (MC), ethylcellulose (EC), hydroxypropylcellulose (HPC), hydroxyethylcellulose (HEC), and hydroxypropyl methylcellulose (HPMC) [225]. As the interest of this project focused on HPC and HPMC, they will be briefly discussed. HPMCs are non-ionic, hydrophilic, and soluble in water, methanol, ethanol, propanol, and dichloromethane. Their solubility in most organic solvent makes them a perfect candidate for formulation while their water solubility eases the formulation preparation as the freeze-drying technique can be utilised during the preparation [225, 226]. They are often used as formulant for stabilising agent or to increase drug solubility [225]. In a study done by Jung and Yoo [227], the anti-fungal drug. itraconazole, was successfully formulated by HPMC, using solid dispersion techniques. This formulation exhibited increased water solubility while maintaining the activity. In another study done by Terreni *et al.* [228] a synthetic AMP called hLF 1-11, which is a peptide utilise in curing

infectious ocular keratitis was formulated by HPMC in an attempt to increase the drug stability and shelf- life. The result was extremely promising as the activity of the peptide was maintained while the stability increased [228].

In this study, we will be focusing on cellulose type formulations of the Trcs to increase the stability of the peptides in solution, lower the toxicity and maintain or increase the activity against the pathogen. *C. albicans*. We will first report the preparation of the Trcs in Chapter 2 and track the activity and stability in Chapter 3 and 4. The overall conclusion on the success and failures of the cellulose-type formulations will be given in Chapter 5.

1.6 References

1 Bongomin, F., Gago, S., Oladele, R. O, Denning, D. W. (2017) Global and multi-national prevalence of fungal diseases-estimate precision. *J. Fungi (Basel). 3,* 57.

2 Perfect, J. R. (2017) The antifungal pipeline: a reality check. *Nat. Rev. Drug Discov. 16*, 603–616.

3 Brown, G. D., Denning D. W., and Levitz, S. (2012) Tackling human fungal infections. Sci. *336*, 647–647.

4 De pauw, B. E. (2011) What are fungal infections? *Mediterr. J. Hematol. Infect. Dis. 3*, e2011001

5 Enoch, D. A., Ludlam, H. A., and Brown, N. M. (2006) Invasive fungal infections: a review of epidemiology and management options. *Food Microbiol*. *5*, 809–818.

6 Spadaro, D., and Gullino, M. L. (2004) State of the art and future prospects of the biological control of postharvest fruit diseases. *Food Microbiol*. *91*, 185–194.

7 Brown, G. D., Denning, D. W., Gow, N. A. R., Levitz, M. S., Netea, M. G., and Theodore, C. (2012) Hidden killers: human fungal infections. *Sci Transl Med*. *4*, 165.

8 Campoy, S., and Adrio, J. L. (2017) Antifungals. *Biochem. Pharmacol*. *133,* 86–96.

9 Brown, G. D, Denning, D. W, and Levitz, M. S. (2012) Tackling human fungal infections. *Science 336*, 647–647.

10 Latgé, J. P. (1999) *Aspergillus fumigatus* and aspergillosis, *Clin. Microbiol. Rev. 12* 310–350

11 Pappas, P., Rex, J. H., Sobel, J.D., Filler, S. G., Dismukes, W., Walsh, T. J., and Edwards, J. E. (2004) Guidelines for treatment of candidiasis. *Clin. Infect. Dis. 38*, 161–189.

12 Pappas, P., Alexander, B. D., Andes, D. R., Hadley, S., Kauffman, C. A., Freifeld, A., Anaissie, E.J., Brumble, L. M., Herwaldt, L., Ito, J., Kontoyiannis, D. P., Lyon, G. M., Marr, K. A., Morrison, V. A., Park, B. J., Patterson, T. F., Perl, T. M., Oster, R. A., Schuster, M. G., Walker, R., Walsh, T. J., Wannemuehler, K. A., and Chiller, T. M. (2011) Invasive fungal infections among organ transplant recipients: Results of the Transplant-Associated Infection Surveillance Network. *Clin. Infect. Dis. 60*, 1101-1111.

13 Krcmery, V., and Barnes, A. (2002) Non-*albicans Candida* spp. causing fungaemia: pathogenicity and antifungal resistance. *J. Hosp. Infect. 50*, 243-260.

14 Imtiaz, T., Lee, K. K., Munro, C., Maccallum, D., Shankland, G., and Johnson, E. (2012) Echinocandin resistance due to simultaneous FKS mutation and increased cell wall chitin in a *Candida albicans* bloodstream isolate following brief exposure to caspofungin. *Int. J. Med. Microbiol. 61*, 13330–4.

15 Lee, K. K., Maccallum, D. M., Jacobsen, M. D., Walker, L. A., Odds, F. C, and Gow, N. A. (2012) Elevated cell wall chitin in *Candida albicans* confers echinocandin resistance in vivo. *Antimicrob. Agents Chemother*. *56*, 208-17

16 Sanguinetti, M., Posteraro, P., and Posteraro, B. (2010) Echinocandin antifungal drug resistance in *Candida* species: a cause of concern. *Curr. Opin. Infect. Dis*. *12*, 437–43.

17 Alexander, B. D., Johnson, M. D., Pfeiffer, C. D., Jime, C., and Catania, J. (2012) Increasing echinocandin resistance in *Candida glabrata*: clinical failure correlates with FKS mutations and elevated minimum inhibitory concentrations. *Clin. Infect. Dis*. *56*, 1724–32.

18 Sing-Babak, S. D., Babak, T., Diezmann, S., Hill, J.A., Xie, J. L., and Chen, Y. L., (2012) Global analysis of the evolution and mechanism of echinocandin resistance in *Candida glabrata*. *PLoS Pathogens 8*, 1002718.

19 Shields, R. K., Nguyen, M. H., Press, E. G., and Updike, C. L. (2013) Caspofungin MICs correlate with treatment outcomes among patients with *Candida glabrata* invasive *Candidiasis* and prior echinocandin exposure. *Antimicrob. Agents Chemother*. 57, 3528–35.

20 Achkar, J. M., and Fries, B. (2010) *Candida* infections of the genitourinary tract. *Clin Microbiol. Rev. 23*, 253–73.

21 Ruhnke, M. (2006) Epidemiology of *Candida albicans* infections and role of non-*Candida albicans* yeasts. *Curr. Cancer Drug Targets 7*, 495–504.

22 Ruhnke, M., Rickerts, V., and Cornely O. A. (2011) Diagnosis and therapy of *Candida* infections: joint recommendations of the German Speaking Mycological Society and the Paul-Ehrlich-Society for Chemotherapy. *Mycoses 54*, 279–310.

23 Gow, N. A., and Yadav, B. (2017) Microbe profile: *Candida albicans*: A shape-changing, opportunistic pathogenic fungus of humans. *Microbiol*. *163***,** 1145–1147.

24 Ganguly, S., and Mitchell, A. (2011) Mucosal biofilms of *Candida albicans*. *Curr. Opin. Microbiol. 14,* 380–58.

25 Kennedy, M. J., and Volza, P. A. (1985) Ecology of *Candida albicans* gut colonization: inhibition of *Candida* adhesion, colonization, and dissemination from the gastrointestinal tract by bacterial antagonism. *Infect. Immun. 49***,** 654-63.

26 Kumamoto, C. (2002) *Candida* biofilms. *Curr. Opin. Microbiol. 5,* 608–611.

27 Kumamoto, C. (2011) Inflammation and gastrointestinal *Candida* colonization. *Curr Opin. Microbiol. 14,* 386–91.

28 Kullberg, B. J, and Arendrup, M. C. (2015) Invasive *Candidiasis*. *N. Engl. J. Med. 373,* 1445–1456.

29 Ramla, S., Sharma, V., and Patel, M. (2016) Influence of cancer treatment on the *Candida albicans* isolated from the oral cavities of cancer patients. *Support. Care Cancer 24,* 2429–2436.

30 Chandra, J., Kuhn, D. M., Mukherjee, P. K., Hoyer, L. L., and McCormick T. G. M. (2001) Biofilm formation by the fungal pathogen *Candida albicans*: development, architecture, and drug resistance. *J. Bacteriol. 183,* 5385–94.

31 Fox, E. P., and Nobile, C. J. (2012) A sticky situation: untangling the transcriptional network controlling biofilm development in *Candida albicans*. *Transcription 3,* 315–22.

32 Ramage, G., Mowat, E., Jones, B., Williams, C., and Lopez-Ribot, J. (2009) Our Current understanding of fungal biofilms fungal biofilms. *Crit. Rev. Microbiol*. *35,* 340–355.

33 Ramage, G., Saville, S. P., and Thomas, D. P. (2005) *Candida* biofilms: An update. *Eukaryot. Cell. 4,* 633–38.

34 Kolter, R. (2010) Biofilms in lab and nature: A molecular geneticist's voyage to microbial ecology. *Int. Microbiol. 13,* 1–7.

35 Mitchell, K. F., Taff, H. T., Cuevas, M. A., Reinicke, E. L., and Sanchez, H., (2013) Role of matrix β-1,3 glucan in antifungal resistance of non-*albicans Candida* biofilms. *Antimicrob. Agents Chemother. 57,* 1918–20.

36 Netea. M., Joosten. L., Van Der Meer, B., and Van De Veerdonk, F. (2015) Immune defence against *Candida* fungal infections. *Nat. Rev. Immunol*. *15,* 630–642.

37 Noble, S. M., Gianetti, B. A., Witchley, J. N., Francisco, S., Division, D., and Francisco, S. (2017) *Candida albicans* cell-type switching and functional plasticity in the mammalian host. *Nat. Rev. Microb. 15,* 96–108.

38 Brown, A., Brown, G. D., Netea, M. G., Gow, N. A. R. (2014) Metabolism impacts upon *Candida* immunogenicity and pathogenicity at multiple levels. *Trends Microbiol. 22,* 614–622.

39 Pfaller, M. A., Pappas, P. G., and Wingard, J. R. (2006) Invasive fungal pathogens: current epidemiological trends. *Clin. Infect. Dis. 43:* S3–S14.

40 Trick W. E., Fridkin, S. K., Edwards, J. R., Hajjeh, R. A., and Gaynes, R. P. (2002) Secular trend of hospital-acquired C*andidemia* among intensive care unit patients in the United States during 1989–1999. *Clin. Infect. Dis*. *35,* 627–630.

41 Diekema, D. (2012) The changing epidemiology of healthcare-associated *Candidemia* over three decades. *Diagn. Microbiol. Infect. Dis. 73,* 45–48.

42 Ahmad, K. M., Koko, J., and Ishchuk, O. P. (2014) Genome structure and dynamics of the yeast pathogen *Candida glabrata*. *FEMS Yeast Res*. *14,* 529–535.

43 Tortorano, A. M., and Dho, G. (2012) Invasive fungal infections in the intensive care unit: a multicentre, prospective, observational study in Italy (2006-2008). Mycoses *55***,** 73–9.

44 Glockner, A. (2015) *Candida glabrata* – unique features and challenges in the clinical management of invasive infections. *Mycoses 58,* 445–450.

45 Robbins, N., Wright, G. D., and Cowen L. E. (2016) Antifungal drugs: The current armamentarium and development of new agents. *Microbiol Spectr. 4,* 1–20.

46 Gruszecki, W. I., Gagos, M., Herec, M., and Kernen, P. (2003) Organization of antibiotic amphotericin B in model lipid membranes. *Mol. Biol. Cell. 8,* 161–170.

47 Ostrosky-Zeichner, L., Casadevall, A., Galgiani, J. N., Odds, F. C., and Rex, J. H. (2010) An insight into the antifungal pipeline: selected new molecules and beyond. *Nat. Rev. Drug Discov. 9,* 719–727.

48 Anderson, T. M., Clay, M. C., Cioffi, A. G., Diaz, K. A., Hisao, G. S., Tuttle M. D., Nieuwkoop, M., Comellas, G., Maryum, N., Wang, S., Uno, B. E., Wildeman, E. L., Gonen, T., Rienstra, C. M., and Bruk, M. D. (2014) Amphotericin forms an extramembranous and fungicidal sterol sponge. *Nat. Chem. Biol. 10,* 400–406.

49 Shao, P. L., Huang, L. M., and Hsueh, P. R. (2007) Recent advances and challenges in the treatment of invasive fungal infections, *Int. J. Antimicrob. Agents 30,* 487– 495.

50 Rex, J. H., and Rinaldi, M. G. (1995) Resistance of *Candida* species to fluconazole. *Antimicrob. Agents Chemother.* 39, 1–8.

51 Brammer, K. W., and Farrow, P. R. (1990) Pharmacokinetics and tissue penetration of fluconazole in humans. *Rev Infect Dis 12,* S318–26.

52 Keating, G. M., and Figgitt D. P. (2003) Caspofungin. *Drugs 63,* 2235–2263.

53 Cannon, R. D., Lamping, E., Holmes, A. R., Niimi, K., Tanabe, K., Niimi, M., and Monk, B. (2007) Mini-Review *Candida albicans* drug resistance – another way to cope with stress. *Microbiology 153***,** 3211–3217.

54 Onyewu, C. H. J. (2007) Unique applications of novel antifungal drug combinations. *Antiinfect. Agents 6,* 3–15.

55 Chang, Y., Yu, S., and Heitman, J. (2017) New facets of antifungal therapy. *Virulence 8*, 222–236.

56 Perlin, D. S., Shor, E., and Zhao, Y. (2015) Update on antifungal drug resistance. *Curr. Clin. Microbiol. Rep. 1*, 84–95.

57 Pfaller, M. A., and Diekema, D. (2004) Rare and emerging opportunistic fungal pathogens: concern for resistance beyond *Candida albicans* and *Aspergillus fumigatus*. J*. Clin. Microbiol.* 42, 4419–4431.

58 Revie, N. M., Iyer, K. R., Robbins, N., and Cowen, L. E. (2018) Antifungal drug resistance: evolution, mechanisms and impact. *Curr. Opin. Microbiol. 45,* 70–76.

59 Ksiezopolska, E., and Gabald, T. (2018) evolutionary emergence of drug resistance in *Candida* opportunistic pathogens. *Genes (Basel) 9,* 461.

60 Whaley, S. G., Berkow, E. L., Rybak J. M., Nishimoto, A. T., Barker K. S., and Rogers P. D., (2017) Azole antifungal resistance in *candida albicans* and emerging non-*albicans Candida* species. *Front. Microbiol.* 7, 1–12.

61 Lafayette, S. L., Collins, C., Zaas, A. K., Schell, W. A., Betancourt-Quiroz M., Leslie-Gunatilaka A. A., and Perfect, J.R. (2010) PKC signaling regulates drug resistance of the fungal pathogen *Candida albicans* via circuitry comprised of Mkc1, calcineurin, and Hsp90. *PLOS Pathogens 6*, e1001069.

62 Miyazaki, T., Yamauchi, S., Inamine, T., Nagayoshi, Y., Saijo, T. K, I., Seki, M., Kakeya, H., Amamoto, Y., and Yanagihara, K. (2010) Roles of calcineurin and Crz1 in antifungal susceptibility and virulence *of Candida glabrata*. *Antimicrob. Agents Chemother. 54,* 1639–1643.

63 Nolte, F. S., Parkinson, T., Falconer, D. J., Dix, S., Williams, J., Gilmore, C., and Geller, R., (1997) Isolation and characterization of fluconazole and amphotericin B-resistant *Candida albicans* from blood of two patients with leukemia. *Antimicrob Agents Chemother. 44,* 196–199.

64 Day J. N., Chau, T. T., Wolbers P. P., Dung, N. T., Mai, P. N., Nghia, H. D., Phong, N. D., Thai, C. Q., Chuong L. V., Sinh, D. X., Hoang, T. N., Diep, P. T., Campbell, J. I.,

Sieu, T. P., Baker, S. G., and Lalloo, D. G. (2013) Combination antifungal therapy for cryptococcal meningitis. *N. Engl. J. Med. 368,* 1291–1302.

65 Chapeland-Leclerc, F, Hennequin C, Papon N, Noe T, Ribaud P, Lacroix C. (2010) Acquisition of flucytosine, azole, and caspofungin resistance in *Candida glabrata* bloodstream isolates serially obtained from a hematopoietic stem cell transplant recipient. *Antimicrob. Agents Chemother*. *54,* 1360–1362.

66 Marichal, P., Koymans, L., Willemsens, S., Bellens, D., Verhasselt, P., Luyten, W., Borgers, M., Ramaekers, F., and Bossche, H. (1999) Contribution of mutations in the cytochrome P450 14a-demethylase (Erg11p, Cyp51p) to azole resistance in *Candida albicans*. *Microbiology 145***,** 2701–2713.

67 Finkel, J. S., and Mitchel, l. A. P. (2011) Genetic control of *Candida albicans* biofilm development. *Nat. Rev. Microbiol*. *9,* 109–118

68 Kumamoto, C.A. (2002) *Candida biofilms*. *Curr Opin Microbiol. 5***,** 608–11.

69 D'Enfert, C. (2006) Biofilms and their role in the resistance of pathogenic *Candida* to antifungal agents. *Curr Drug Targets. 7,* 465–470.

70 Ramage, G., Rajendran, R., Sherry, L., and Williams, C. (2012) Fungal biofilm resistance. *Int J Microbiol. 2012,* 528521. doi:10.1155/2012/528521

71 Jenssen, H., Hamill, P., and Hancock, R. E. W. (2006) Peptide antimicrobial agents. *Clin. Microbiol. 19,* 491–511.

72 Hale, J. D., and Hancock, R. E. (2007) Alternative mechanisms of action of cationic antimicrobial peptides on bacteria. *Expert Rev. Anti-infect. Ther. 5,* 951–959.

73 Kretschmar, M., Nichterlein, T., Nebe, C. T., and Hof, H. (1996) Fungicidal effect of tyrothricin on *Candida albicans*. *Mycoses. 39*, 45–50.

74 Mach, B., and Slayman, C. W. (1996) Mode of action of tyrocidine on Neurospora. *Biochim. Biophys. Acta 124*, 351–361.

75 Troskie, A. M., Rautenbach, M., Delattin, N., Vosloo, J. A., Dathe, M., Cammue, B, and Thevissen, K. (2014) Synergistic activity of the tyrocidines, antimicrobial cyclodecapeptides from *Bacillus aneurinolyticus*, with amphotericin B and caspofungin against *Candida albicans* biofilms *Antimicrob. Agents Chemother. 58,* 3697–3707.

76 Powers, J. P, and Hancock, R. E. (2003) The relationship between peptide structure and antibacterial activity. *Peptides. 24,* 1681–1691.

77 Hancock, R. E. W, and Scott M. G. (2000) The role of antimicrobial peptides in animal defenses. *Proc. Natl. Acad. Sci. U.S.A. 97,* 8856–8861.

78 Hancock, R. E., and Diamond, G. (2000) The role of cationic antimicrobial peptides in innate host defences. *Trends Microbiol. 8,* 402–410.

79 Hurst, A. (1966) Biosynthesis of the antibiotic nisin by whole *Streptococcus lactis* organisms. *J. Gen. Microbiol. 44,* 209–220.

80 Mygind, P. H., Fischer, R. L., Schnorr, K. M., Hansen, M. T., Sönksen, C. P., Ludvigsen, S., Raventós, D., Buskov, S., Christensen, B., De-Maria, L., Taboureau, O., Yaver, D., Elvig-Jørgensen, S. G., Sørensen, M. V., Christensen, B. E., Kjærulff, S., Frimodt-Moller, N., Lehrer, R. I., Zasloff, M., and Kristensen, H. H. (2005) Plectasin is a peptide antibiotic with therapeutic potential from a saprophytic fungus. *Nature. 437,* 975–980.

81 Hultmark, D., Engström, A., Bennich, H., Kapur, R., and Boman, H. G. Insect immunity: isolation and structure of cecropin D and four minor antibacterial components from Cecropia pupae. (1982) *Eur J Biochem. 127,* 207-17

82 Bulet, P., Hetru, C., Dimarcq, J. L., and Hoffmann, D. (1999) Antimicrobial peptides in insects; structure and function. *Dev. Comp. Immunol. 23,* 329–344.

83 Van der Weerden N. L., and Anderson, M. A. (2013) Plant defensins: Common fold, multiple functions. Fungal Biol. Rev. *26,* 121–131.

84 Johansson, J., Gudmundsson, G. H., Rottenberg, M. E., Berndt, K. D. Agerberth, B., and Rottenberg, E. (1998) Conformation-dependent antibacterial activity of the naturally occurring human peptide LL-37. *J Biol Chem. 6, 3718-24*

85 Epand. R. M., and Vogel, H.J. (1999) Diversity of antimicrobial peptides and their mechanisms of action. *Biochim Biophys Acta Biomembr 1462,* 11–28.

86 Bradshaw, J. P. (2003) Cationic antimicrobial peptides: Issues for potential clinical use. BioDrugs. *17,* 233–240.

87 Hancock, R. E. (2001) Cationic peptides: Effectors in innate immunity and novel antimicrobials. Lancet Infect. Dis. *1,* 156–164.

88 Zasloff, M. (1987) Magainins, a class of antimicrobial peptides from Xenopus skin: isolation, characterization of two active forms, and partial cDNA sequence of a precursor. *Proc. Natl. Acad. Sci. U.S.A 84,* 5449–53.

89 Sansom M. S. (1991) The biophysics of peptide models of ion channels. *Prog. Biophys. Mol. Biol. 55,* 139–235.

90 Ketchem, R., Hu, W., and Cross, T. (1993) High-resolution conformation of gramicidin A in a lipid bilayer by solid-state NMR. *Science 261*, 1457–1460.

91 Cornet, B., Bonmatin, J., Hetru, C., Hoffmann, J. A., Ptak, M. and Vovelle, F. (1995) Refined three-dimensional solution structure of insect defensin A. *Structure. 3*, 435-448

92 Mogi, T., and Kita, K. (2009) Gramicidin S and polymyxins: The revival of cationic cyclic peptide antibiotics. *Cell. Mol. Life Sc. 66,* 3821–3826.

93 Munyuki, G., Jackson, G. E., Venter G. A., Kövér, K. E., Szilágyi, L., Rautenbach, M., Spathelf, B. M., Bhattacharya, B., Van Der Spoel, D. (2013) β-sheet structures and dimer models of the two major tyrocidines, antimicrobial peptides from *Bacillus aneurinolyticus*. *Biochemistry 52,* 7798–7806.

94 Brewer, D., Hunter, H., and Lajoie, G. (1998) NMR studies of the antimicrobial salivary peptides histatin 3 and histatin 5 in aqueous and nonaqueous solutions. *Biochem. J. Cell Biol. 76,* 247–256.

95 TJ, M., and Chen, Y. (1998) Mechanistic action of pediocin and nisin: recent progress and unresolved questions. Appl. *Microbiol. Biotechnol. 50,* 511–519.

96 Boman, H. G. (1991) Antibacterial peptides: Key components needed in immunity. *Cell 65***,** 205–207.

97 He, K., Ludtke, S. J., Huang, H. W., and Worcester, D. L. (1995) Antimicrobial peptide pores in membranes detected by neutron in-plane scattering. *Biochemistry 34,* 15614–15618

98 Wu, M., Maier, E., Benz, R., and Hancock, R. E. W. (1999) Mechanism of interaction of different classes of cationic antimicrobial peptides with planar bilayers and with the cytoplasmic membrane of *Escherichia coli*. *Biochemistry 38,* 7235–7242.

99 Shai, Y. (1999) Mechanism of the binding, insertion, and destabilization of phospholipid bilayer membranes by α-helical antimicrobial and cell non-selective membrane-lytic peptides. *Biochim. Biophys. Acta. Biomembr. 1462, 55–70*

100 Yang, L., Harroun, T. A., Heller, W. T, Weiss T. M, and Huang, H. W. (1998) Neutron off-plane scattering of aligned membranes. I. Method of measurement. *Biophys. J. 75,* 641–645.

101 Matsuzaki, K., Murase, O., Fujii, N., and Miyajima, K. (1996) An antimicrobial peptide, magainin 2, induced rapid flip-flop of phospholipids coupled with pore formation and peptide translocation. *Biochemistry 35,*11361–11368.

102 Shai, Y. and Oren, Z. (2001) From “carpet” mechanism to de-novo designed diastereomeric cell-selective antimicrobial peptides. *Peptides 22,* 1629-1641

103 Park, C. B., Kim, M. S., and Kim, S. C (1996) A novel antimicrobial peptide from *Bufo Bufo gargarizans*. Biochem. *Biophys. Res. Commun. 218,* 408–13.

104 Park C. B, Kim H.S, and Kim S. C. (1998) Mechanism of action of the antimicrobial peptide buforin II: Buforin II kills microorganisms by penetrating the cell membrane and inhibiting cellular functions. *Biochem. Biophys. Res. Commun. 244,* 253–257.

105 Park, C. B., Yi, K. S., Matsuzaki, K., Kim, M. S, and Kim, S.C. (2000) Structure-activity analysis of buforin II, a histone H2A-derived antimicrobial peptide: The proline hinge is responsible for the cell-penetrating ability of buforin II. *Proc. Natl. Acad. Sci. U.S.A. 97*, 8245–8250.

106 Hsu, C. H, Chen, C., Jou M. L., Lee, A. Y. L., Lin, Y. C, Yu, Y. P, Huang, W. T, and Wu, S. H. (2005) Structural and DNA-binding studies on the bovine antimicrobial peptide, indolicidin: Evidence for multiple conformations involved in binding to membranes and DNA. *Nucleic Acids Res. 33,* 4053–64.

107 Tomasinsig, L., and Zanetti, M. (2005) The cathelicidins - structure, function, and evolution. *Curr. Protein Pept. Sci. 6,* 23–34.

108 Boman, H. G, Agerberth, B., and Boman, A. (1993) Mechanisms of action on Escherichia coli of cecropin P1 and PR-39, two antibacterial peptides from pig intestine. *Infect. Immun. 61,* 2978–2984.

109 Bagheri, M. (2015) Cationic Antimicrobial Peptides (AMPs): Thermodynamic characterization of peptide-lipid interactions and biological efficacy of surface- tethered peptides. *Open Chem. 4,* 389–393.

110 Rautenbach, M., Troskie, A. M., and Vosloo, J. A. (2016) Antifungal peptides: To be or not to be membrane active. *Biochimie 130,* 132–145.

111 De Lucca, A. J. (2000) Antifungal peptides: potential candidates for the treatment of fungal infections. *Expert Opin. Investig. Drugs 9,* 273–299.

112 Cole, A., and Ganz, T. (2009) Human antimicrobial peptides: analysis and application. *Biotechniques. 4,* 828–830.

113 Kurtz, M., and Douglas, C. (1997) Lipopeptide inhibitors of fungal glucan synthase. *J Med Vet Mycol. 35,* 79–86.

114 Hori, M., (1997) Studies on the mode of action of polyoxins. VI. Effect of polyoxin B on chitin synthesis in polyoxin-sensitive and resistant strains of Alternaria kikuchiana. *J. Antibiot*. 27, 260–6.

115 Brillinger, G. U. (1979) Metabolic products of microorganisms. 181. Chitin synthase from fungi, a test model for substances with insecticidal properties. *Arch. Microbiol. 121,* 71–4.

116 Chen, W., Zeng, H., and Tan, H. (2000) sequencing, and function of sanF: A gene involved in nikkomycin biosynthesis of Streptomyces ansochromogenes. *Curr. Microbiol. 41*, 312–6.

117 McCarthy, P., Troke, P., and Gull, K. (1985) Mechanism of action of nikkomycin and the peptide transport system of *Candida albicans. J. Gen. Microbiol. 131,* 775–80.

118 Thevissen, K., Kristensen, H. H., Thomma, B., Bruno, P.A.C., and Franscois, I. (2007) Therapeutic potential of antifungal plant and insect defensins. *Drug Discov. Today 12,* 966–71.

119 Fehlbaum, P. (1994) Insect immunity. Septic injury of Drosophila induces the synthesis of a potent antifungal peptide with sequence homology to plant antifungal peptides. *J. Biol. Chem. 269,* 33159–63.

120 Helmerhorst, E. J. (2001) Characterization of histatin 5 with respect to amphipathicity, hydrophobicity, and effects on cell and mitochondrial membrane integrity excludes a Candidacidal mechanism of pore formation. *J. Biol. Chem. 276,* 5643–9.

121 Helmerhorst, E. J., Breeuwer, P., Van't Hof, W., Walgreen-Weterings, E., Oomen, L. C., Veerman, E. C., Amerongen, A. V., and Abee, T. (1999) The cellular target of histatin 5 on *Candida albicans* is the energized mitochondrion. *J. Biol. Chem. 274,* 7286–7291.

122 Raj, P., Soni, S., and Levine, M. (1994) Membrane-induced helical conformation of an active candidacidal fragment of salivary histatins. *J. Biol. Chem. 269,* 9610–9.

123 Pollock, J. J, (1984) Fungistatic and fungicidal activity of human parotid salivary histidine-rich polypeptides on *Candida albicans*. *Infect. Immun. 44*, 702–7.

124 Matejuk, A., Leng, Q., Begum, M. D., Woodle, M. C, Scaria, P., Chou, S. T., and Mixson, A. J. (2010) Peptide-based antifungal therapies against emerging infections. *Drug Future 35,* 197.

125 Steiner, H. (1981) Sequence and specificity of two antibacterial proteins involved in insect immunity. *Nature 292,* 246–8.

126 Mor, A. (1991) Isolation, amino acid sequence, and synthesis of dermaseptin, a novel antimicrobial peptide of amphibian skin. *Biochemistry 30,* 8824–30.

127 Morton, C. (2007) Global phenotype screening and transcript analysis outlines the inhibitory mode (s) of action of two amphibian-derived, alpha-helical, cationic peptides on Saccharomyces cerevisiae. *Antimicrob. Agents Chemother. 51,* 3948–59.

128 Roscetto, E., Contursi, P., Vollaro, A., Fusco, S., Notomista, E., and Catania, M. (2018) Antifungal and anti-biofilm activity of the first cryptic antimicrobial peptide from an archaeal protein against *Candida* spp. *Sci. Rep. 8,* 17570.

129 Leussa, A. N., and Rautenbach, M. (2014) Detailed SAR and PCA of the tyrocidines and analogues towards leucocin A-sensitive and leucocin A-resistant *Listeria monocytogenes*. *Chem. Biol. Drug Dis. 84,* 543–557.

130 Gerard, J. M., Haden, P., Kelly, M. T., and Andersen, R. J. (1999) Loloatins A-D, cyclic decapeptide antibiotics produced in culture by a tropical marine bacterium. *J. Nat. Prod*. *62,* 80-5.

131 Hector R. F., Zimmer, B. L., and Pappagianis, D. (1990) Evaluation of nikkomycins X and Z in murine models of coccidioidomycosis, histoplasmosis, and blastomycosis. *Antimicrob. Agents Chemother.* 34, 587–593.

132 Suzuki, S., Isono, K., Nagatsu, J., Mizutani,T., Kawashima, Y., and Mizuno, T. (1965) A new antibiotic, polyoxin A. *J. Antibiot 18,* 131.

133 Isono, K., Asahi, K., and Suzuki, S. (1969) Polyoxins, antifungal antibiotics. XIII. Structure of polyoxins. *J. Am. Chem. Soc. 91,* 7490–7505.

134 Lucca, A. J., and Walsh, T. J. (1999) Antifungal peptides: Novel therapeutic compounds against emerging pathogens. *Antimicrob. Agents Chemother. 43,* 1–11.

135 Eschenauer, G., Depestel, D. D., and Carver, P. L. (2007) Comparison of echinocandin antifungals*. Ther. Clin. Risk Manag 3,* 71–97.

136 Abe, H., Kawada, M., Sakashita, C., Watanabe, T., and Shibasaki, M. (2018) Structure-activity relationship study of leucinostatin A, a modulator of tumor–stroma interaction. *Tetrahedron 74,* 5129–5137.

137 Endo, M., Takesako, K., Kato, I., and Yamaguchi, H. (1997) Fungicidal action of aureobasidin A, a cyclic depsipeptide antifungal antibiotic, against *Saccharomyces cerevisiae. Antimicrob*. *Agents Chemother. 41*, 672–676.

138 Vouldoukis, I., Shai, Y., Nicolas, P., and Mor, A. (1996) Broad spectrum antibiotic activity of skin-PYY. *FEBS Lett. 380,* 237–240.

139 Bondaryk, M., Staniszewska, M., Zielinska, P., and Urbanczyk-Lipkowska, Z. (2017) Natural antimicrobial peptides as inspiration for design of a new generation antifungal compounds. *J. Fungi (Basel) 3,* 46.

140 Pfaller, M., Gordee, R., Gerarden, T., Yu, M., and Wenzel, R. (1989) Fungicidal activity of cilofungin (LY121019) alone and in combination with anticapsin or other antifungal agents. *Eur. J. Clin. Microbiol. Infect. Dis. 8,* 564–567.

141 Hotchkiss, R. D., and Dubos, R. J. (1941) The isolation of bactericidal substances from cultures of *Bacillus brevis*. *Biol. Chem. 141,* 155–162.

142 Fujikawa, K., Suzuki, T. and Kurahashi, K. (1968) Biosynthesis of tyrocidine by a cell-free enzyme system of *Bacillus brevis ATCC 8185*: I. Preparation of partially purified enzyme system and its properties. *Biochim. Biophys. Acta. 161*, 232–246

143 Wenzel, M., Rautenbach, M., Vosloo, J. A., Siersma, T., Aisenbrey, C. H. M., Zaitseva, E., Laubscher, W. E., van Rensburg, W., Behrends, J. C., Bechinger, B., Hamoen, L. (2018) The multifaceted antibacterial mechanisms of the pioneering peptide antibiotics tyrocidine and gramicidin S. *J. Am. Chem. Soc*. *18,* 9: e00802

144 Tang, X. J. Thibault, P., and Boyd R. K. (1992) Characterisation of the tyrocidine and gramicidin fractions of the tyrothricin complex from *Bacillus brevis* using liquid chromatography and mass spectrometry. *Int. J. Mass Spectrom. Ion Process. 122,* 153–179.

145 Hansen, J., Pschorn, W., and Ristow, H. (1982) Functions of the peptide antibiotics Tyrocidine and Gramicidin: Induction of conformational and structural changes of superhelical DNA. *Eur. J. Biochem. 126,* 279–284.

146 Mootz, H. D., and Marahiel, M. (1997) The tyrocidine biosynthesis operon of *Bacillus brevis*: complete nucleotide sequence and biochemical characterization of functional internal adenylation domains. *J. Bacteriol*. *179,* 6843–6850.

147 Mach, B., Reich, E., and Tatum, E. L. (1963) Separation of the biosynthesis of the antibiotic polypeptide Tyrocidine from protein biosynthesis. *Proc. Natl. Acad. Sci. U.S.A. 50,* 175–181.

148 Dubos, R. J. and Cattaneo, C. (1939) Studies on a bactericidal agent extracted from a soil Bacillus: III. Preparation and activity of a protein-free fraction. J. *Exp. Med. 70,* 249-256

149 Lee, S. G., Roskoski, R., Bauer, K., and Lipmann, F. (1973) Purification of the polyenzymes responsible for Tyrocidine synthesis and their dissociation into subunits. *Biochemistry 12,* 398–405.

150 Stokes, J. L., and Woodward, J. R. (1943) Formation of Tyrothricin in submerged cultures of *Bacillus Brevis*. *J. Bacteriol*. *46***,** 83–88.

151 Vosloo, J. A., Stander, M. A, Leussa, A. N. N., Spathelf, B. M, and Rautenbach, M. (2013) Manipulation of the tyrothricin production profile of *Bacillus aneurinolyticus*. *Microbiology (UK) 159,* 2200–2211.

152 Loll, P. J., Upton, E. C, Nahoum, V., Economou, N. J, and Cocklin, S. The high resolution structure of tyrocidine A reveals an amphipathic dimer. (2014) *Biochim. Biophys. Acta 1838*, 1199-1207

153 Kuo, M., and Gibbons, W. (1979) Total assignments, including four aromatic residues, and sequence confirmation of the decapeptide tyrocidine A using difference double resonance. Qualitative nuclear Overhauser effect criteria for beta turn and antiparallel beta-pleated sheet conformation. *J. Biol. Chem. 254,* 6278–6287.

154 Vosloo, J. A. (2016) Optimised bacterial production and characterisation of natural antimicrobial peptides with potential application in agriculture. Ph.D. Thesis, Department of Biochemistry, University of Stellenbosch. http://hdl.handle.net/10019.1/98411

155 Vosloo, A. J., Beims, J., and Allsopp, M. (2017) Tolerance of honeybee adults and larvae toward tyrothricin peptides derived from *Brevibacillus parabrevis*. *Apidologie 48,* 833–844.

156 Troskie, A. M., de Beer, A., Vosloo, J. A., Jacobs, K., and Rautenbach, M. (2014) Inhibition of agronomically relevant fungal phytopathogens by tyrocidines, cyclic antimicrobial peptides isolated from *Bacillus aneurinolyticus*. *Microbiol. (United Kingdom) 160,* 2089–2101

157 Gibbons, W. A, Beyer, C. F, Dadok, J., Sprecher, R. F., and Wyssbrod, H. R. (1975) Studies of individual amino acid residues of the decapeptide Tyrocidine A by proton double-resonance difference spectroscopy in the correlation mode. *Biochemistry 14,* 420–429.

158 Salgado, J., Grage, S. L., Kondejewski, L. H., Hodges, R. S., McElhaney, R. N., and Ulrich, A. S. (2001) Membrane-bound structure and alignment of the antimicrobial β-sheet peptide gramicidin S derived from angular and distance constraints by solid state 19F-NMR. *J. Biomol. NMR 21,* 191–208.

159 Rautenbach, M., Vlok, N. M., Stander, M., and Hoppe, H. C. (2007) Inhibition of malaria parasite blood stages by tyrocidines, membrane-active cyclic peptide antibiotics from *Bacillus brevis*. *Biochim. Biophys. Acta Biomembr. 1768,* 1488–1497.

160 Jokonya, S., Langlais, M., Leshabane, M., Reader, P. W., Vosloo, J. A., Pfukwa, R., Coertzen, D., Birkholtz, L. M., Rautenbach, M., and Klumperman, B. (2020) Poly (N-vinylpyrrolidone) *antimalaria* conjugates of membrane-disruptive peptides. *Biomacromol. 21*, 5053–5066

161 Leussa, N. N. A. (2014) Characterisation of small cyclic peptides with *antilisterial* and *antimalarial* activity. Ph.D. Thesis, Department of Biochemistry, University of Stellenbosch. http://hdl.handle.net/10019.1/86161

162 Spathelf, B. M., and Rautenbach, M. (2009) Anti-*listerial* activity and structure – activity relationships of the six major tyrocidines, cyclic decapeptides from *Bacillus aneurinolyticus. Bioorg. Med. Chem*. *17,* 5541–5548.

163 Mach, B., and Slayman C. (1966) Mode of action of tyrocidine on Neupospora. *Biochim Biophys Acta Biomembr* Acta *124,* 351–361.

164 Rautenbach, M., Troskie, A. M., Vosloo, J. A., and Dathe, M. D. (2016) Antifungal membranolytic activity of the tyrocidines against filamentous plant fungi. *Biochimie 130,* 122-131

165 Robinson, H. J., and Moltor, H. (1942) Some toxicological and pharmacological properties of gramicidin, tyrocidine and tyrothricin. *J. Pharmacol. Exp. Ther. 74,* 75–82.

166 Mann, F. C, Heilman, D. and Herrell, W. E. (1943) Effect of serum on haemolysis by gramicidin and tyrocidine. *Exp. Biol. Med. (Maywood) 52***,** 31–33.

167 Rammelkamp, C. H. and Weinstein, L. (1941) Haemolytic effect of tyrothricin *Exp. Biol. Med. (Maywood) 48,* 211–214.

168 Henderson, J. (1946) The status of tyrothricin as an antibiotic agent for topical application. *J. Am. Pharm. Assoc. 35,* 141–147.

169 Spathelf, B. M. (2010) Qualitative structure-activity relationships of the major tyrocidines, cyclic decapeptides from *Bacillus aneurinolyticus*. Ph.D. Thesis, Department of Biochemistry, University of Stellenbosch, http://scholar.sun.ac.za/handle/10019.1/4001

170 Aranda, F. J., and De Kruijff, B. (1988) Interrelationships between tyrocidine and gramicidin A' in their interaction with phospholipids in model membranes. *Biochim. Biophys. Acta Biomembr. 937,* 195–203.

171 Bohg, A. Ristow, H. (1987) Tyrocidine-induced modulation of the DNA conformation in *Bacillusbrevis*, *Eur. J. Biochem*, 170 253–258.

172 Bohg, A. Ristow, H. (1986) DNA-supercoiling is affected in vitro by the peptide antibiotics tyrocidine and gramicidin, *Eur. J. Biochem*. *160*, 587–591.

173 Ruttenberg, M. A., King, T. P., and Craig, L. C. (1965) The Use of the Tyrocidines for the study of conformation and aggregation behaviour. *J. Am. Chem. Soc.* 87, 4196–4198.

174 Hwang, P. M., and Vogel, H. J. (1998) Structure-function relationships of antimicrobial peptides. *Biochem. Cell. Biol. 76,* 235–246.

175 Laiken, S. L., Printz, M. P., and Craig, L. C. (1971) Studies on the mode of self-assosiation of tyrocidine B. *Biochem. Biophys. Res. Commun. 43,* 595–600.

176 Kondejewski, L. H., Farmer, S. W., Wishart, D. S., Kay, C. M., Hancock, R. E. W., and Hodges, R. S. (1996) Modulation of structure and antibacterial and haemolytic activity by ring size in cyclic gramicidin S analogues. *Biol. Chem. 271,* 25261.

177 Prenner, E. J., Kay, C. M., Mcelhaney, R. N., and Hodges, R. S. (2002) Conformation and interaction of the cyclic cationic antimicrobial peptides in lipid bilayers. *J. Pept. Res. 60,* 23–36.

178 Kohli, R. M., Walsh, C. T., and Burkart, M. D. (2002) Biomimetic synthesis and optimization of cyclic peptide antibiotics. *Nature 418,* 658–661.

179 Marques, M. A., Citron, D. M., and Wang, C. C. (2007) Development of tyrocidine A analogues with improved antibacterial activity*. Bioorg. Med. Chem. Lett. 15,* 6667–6677.

180 Rotem, I., and Radzishevsky, A. M. (2006) Physicochemical properties that enhance discriminative antibacterial activity of short dermaseptin derivatives. *Antimicrob. Agents Chemother. 50,* 2666–2672.

181 Carvalho, C. A., Olivares-Ortega, C., Soto-Arriaza, M. A., Carmona-Ribeiro, A. M. (2012) Interaction of gramicidin with DPPC/DODAB bilayer fragments. *Biochim. Biophys. Acta Biomembr. 1818,* 3064–3071.

182 Ragioto, D. A. M. T., Carrasco, L. D. M., and Carmona-Ribeiro, A. M. (2014) Novel gramicidin formulations in cationic lipid as broad-spectrum microbicidal agents. *Int. J. Nanomed. 9,* 3183–3192

183 Wang, F., Qin, L., Pace, C. J., Wong, P., Malonis, R., and Gao, J. (2012) Solubilized gramicidin A as potential systemic antibiotics. *Chembiochem 13,* 51–55.

184 Charkoftaki, G., Kytariolos, J., and Macheras, P. (2010) Novel milk-based oral formulations: proof of concept. *Int. J. Pharm. 390,* 150–159

185 El Tayar, N., Mark, A. E., Vallat, P., Brunne, R. M., Testa, B., and van Gunsteren, W. F. (1993) Solvent-dependent conformation and hydrogen-bonding capacity of cyclosporin A: Evidence from partition coefficients and molecular dynamics simulations. *J. Med. Chem. 36,* 3757–3764.

186 Kumar, T. P., and Eswaraiah, M. C (2020) Evaluation of the antifungal and wound-healing properties of a novel peptide-based bioadhesive hydrogel formulation *J. Pharm. Pharmacol. 8,* 249-254

187 Paranjpe, M., and Müller-Goymann, C. C., (2014) Nanoparticle-mediated pulmonary drug delivery: A review. *Int. J. Mol. Sci.* 15, 5852–5873

188 Mei, L., Zhang, Z., Zhao, L., Huang, L., Yang, X. L., Tang, J., and Feng, S. S. (2013) Pharmaceutical nanotechnology for oral delivery of anticancer drugs. *Adv. Drug Deliv. Rev. 65,* 880–890.

189 Park, C. W., Li, X., Vogt, F. G., Hayes, D., Jr., Zwischenberger, J. B., Park, E. S., and Mansour, H. M. Advanced spray-dried design, physicochemical characterization, and aerosol dispersion performance of vancomycin and clarithromycin multifunctional controlled release particles for targeted respiratory delivery as dry powder inhalation aerosols. *Int. J. Pharm. 455,* 374–392

190 Larsen, D. B., Joergensen, S., Olsen, N. V, Hansen, S. H, and Larsen, C. (2002) In vivo release of bupivacaine from subcutaneously administered oily solution: comparison with in vitro release. *J. Control. Release 81,*145–54.

191 Gill, K. K, Kaddoumi, A., Nazza, I. S. (2012) Mixed micelles of PEG2000 -DSPE and vitamin-ETPGS for concurrent delivery of paclitaxeland parthenolide: Enhanced chemo sensitization and antitumorefficacy against non-smallcell lung cancer (NSCLC) cell lines. *Eur. J. Pharm. Sci. 46,* 64–71.

192 Zhao, Y.Z., Dai, D. D., Lu, C. T., Chen, L. J., Lin, M., and Shen, X. T, Epirubicin loaded with propyleneglycol liposomes significantly overcomes multidrug resistance in breast cancer. *Cancer Lett 330,* 74–83.

193 Delie, F., and Blanco-Príeto, M. J., (2005) Polymeric particulates to improve oral bioavailability of peptide drugs. *Molecules 10,* 65–80.

194 Lange, C. F., Hancock, R. E. W., Samuel, J., and Finlay, W. H. (2001) In vitro aerosol delivery and regional airway surface liquid concentration of a liposomal cationic peptide. *J. Pharm. Sci. 90,* 1647–1657.

195 Slain, D. (1999) Lipid-based amphotericin B for the treatment of fungal infections. *Pharmacotherapy 19,* 306–23.

196 Wasan, K. M., and Lopez-Berestein, G. Diversity of lipid-based polyene formulations and their behavior in biological systems. (1997) *Eur. J. Clin. Microbiol. Infect. Dis. 16,* 81–92.

197 Mondon, K., Zeisser-Labouèbe, M., Gurny, R., and Möller, M. (2011) Novel cyclosporin A formulations using MPEG-hexyl-substituted polylactide micelles: A suitability study. *Eur J Pharm Biopharm 77,* 56–65.

198 Teerlink, T., De Kruijff, B., and Demel, R. A. (1980) The action of pimaricin, etruscomycin and amphotericin B on liposomes with varying sterol content. *Biochem Biophys Acta 599,* 484–92.

199 Rautenbach M, Vlok NM, Stander M, Hoppe HC* (2007) Inhibition of malaria parasite blood stages by tyrocidines, membrane-active cyclic peptide antibiotics from Bacillus brevis, *Biochim. Biophys. Acta Biomembranes 1768*, 1488–1497

200 Wiehart UIM, Rautenbach M, Hoppe HC* (2006) Selective lysis of erythrocytes infected with the trophozoite stage of Plasmodium falciparum by polyene macrolide antibiotics, *Biochem. Pharmacol. 71*, 779–790

201 Gallis, H. A, Drew, R. H, and Pickard, W. W. (1990) Amphotericin B: 30 years of clinical experience. *Int. J. Infect. Dis.12,* 308–29.

202 Wasan, K. M., Rosenblum, M. G., and Cheung, L. (1994) Influence of lipoproteins on renal cytotoxicity and antifungal activity of amphotericin B. *Antimicrob. Agents Chemother. 38,* 223–7

203 Chavan, R. B, Rathi, S., Jyothi, V. G. S. S, and Shastri, N. R. (2019) Cellulose based polymers in development of amorphous solid dispersions. *Asian J Pharm Sci. 14,* 248–64.

204 Lee, C., Choi, J. S., Kim, I., Oh, K. T., Lee, E. S., Park, E. S., Lee, K. C., and Youn, Y. S. (2013) Long-actinginhalable chitosan-coated poly (lactic-co-glycolic acid) nanoparticles containing hydrophobically modified exendin-4 for treating type 2 diabetes. *Int. J. Nanomed 8,* 2975–2983.

205 Sobczak, M., Dębek, C., Olędzka, E., and Kozłowski, R. (2013) Polymeric systems of antimicrobial peptides—Strategies and potential applications. *Molecules 18,* 14122–37

206 Basan, H., Gümüşderelioğlu, M., Tevfik, M. (2007) Release characteristics of salmon calcitonin from dextran hydrogels for colon-specific delivery. *Eur J Pharm Biopharm. 65,* 39–46.

207 204) Connors, K. A. (1997) The stability of cyclodextrin complexes in solution. *Chem. Rev. 97,*1325–58.

208 Loftsson, T., Hreinsdóttir, D., and Másson, M. (2005) Evaluation of cyclodextrin solubilization of drugs. *Int J Pharm 302,*18–28.

209 Jambhekar, S. S, and Breen, P. (2016) Cyclodextrins in pharmaceutical formulations I: Structure and physicochemical properties, formation of complexes, and types of complex. *Drug, Dis. Today 21,* 356–62.

210 Gibaud, S., Zirar, S. B., Mutzenhardt, P., Fries, I., and Astier, (2005) A. Melarsoprol–cyclodextrins inclusion complexes. *Int. J. Pharm. 306,* 107–21.

211 Loftsson, T. (2014) Self-assembled cyclodextrin nanoparticles and drug delivery. *J. Incl. Phenom. Macrocycl. Chem. 80,* 1–7

212 Klang, V., Matsko, N., Zimmermann, A. M, Vojnikovic, E., and Valenta, C. (2010) Enhancement of stability and skin permeation by sucrose stearate and cyclodextrins in progesterone nanoemulsions. *Int. J. Pharm. 30*, 152-60.

213 Rodriguez-Aller, M., Guinchard, S., Guillarme, D., Pupier, M., Jeannerat, D., and Rivara-Minten, E. (2015) New prostaglandin analog formulation for glaucoma treatment containing cyclodextrins for improved stability, solubility, and ocular tolerance. *Eur. J. Pharm. Biopharm. 95,* 203–14.

214 Irie, T., and Uekama, K. (1997) Pharmaceutical applications of cyclodextrins. III. Toxicological issues and safety evaluation*. J. Pharm. Sci.* 86, 147–62.

215 Brewster, M. E, and Loftsson, T. (2007) Cyclodextrins as pharmaceutical solubilizers. *Adv. Drug. Del. Rev. 59*, 645–66.

216 Lim Chin, W. W, Parmentier, J., Widzinski, M., Tan, E. H, and Gokhale, R. (2014) A brief literature and patent review of nanosuspensions to a final drug product. *J Pharm Sci 103*, 2980–99.

217 Thanou, M., Verhoef, J. C. and Junginger, H. E. (2021) Oral drug absorption enhancement by chitosan and its derivatives. *Adv. Drug Delivery Rev. 52,* 117–126.

218 Richardson, S. C. Kolbe, H. V. and Duncan, R. (1999) Potential of low molecular mass chitosan as a DNA delivery system: biocompatibility, body distribution and ability to complex and protect DNA. *Int. J. Pharm. 178,* 231–243.

219 2Verheul, R.J., Amidi, M., van Steenbergen, M. J., van Riet E., Jiskoot, W., and Hennink, W. E. (2009) Influence of the degree of acetylation on the enzymatic degradation and in vitro biological properties of trimethylated chitosans. *Biomaterials 30,* 3129–3135.

220 Bazunova, M. V., Chernova, V. V., and Lazdin, R. Y. (2018) A Study of the viscosity characteristics of chitosan solutions in the presence of organic cosolvents. *Russ. J. Phys. Chem. 12*, 1039–1044.

221 Lee, C., Choi, J. S., Kim, I., Oh, K. T., Lee, E. S., Park, E. S., Lee, K. C., and Youn, Y. S. (2013) Long-actinginhalable chitosan-coated poly (lactic-co-glycolic acid) nanoparticles containing hydrophobically modified exendin-4 for treating type 2 diabetes. *Int. J. Nanomed. 8,* 2975–2983.

222 Loftsson, T., and Brewster, M. E. (1996) Pharmaceutical applications of cyclodextrins. 1. Drug solubilization and stabilization. *J. Pharm. Sci. 85,* 1017–25

223 Nair, A. R., Lakshman, Y. D., and Anand, V.S. K. (2020) Overview of extensively employed polymeric carriers in solid dispersion technology. *AAPS Pharm. Sci. Tech. 21,* 309

224 Chavan, R. B., Rathi, S., Jyothi, V., and Shastri, N. R. (2019) Cellulose based polymers in development of amorphous solid dispersions. *Asian. J. Pharm. 14,* 248–64.

225 Chavan, R. B., Rathi, S., Jyothi, V., and Shastri, N. R. (2019) Cellulose based polymers in development of amorphous solid dispersions. *Asian J. Pharm .14,* 248–64.

226 Ford, J. L. (1999) Thermal analysis of hydroxypropylmethylcellulose and methylcellulose: powders, gels and matrix tablets. *Int. J. Pharm. 179,* 209–28.

227 Jung, J. Y. Yoo, S. D., Lee, S. H, Kim, K. H, Yoon, D. S, and Lee, K. H. (1999) Enhanced solubility and dissolution rate of itraconazole by a solid dispersion technique. *Int. J.Pharm. 187,* 209–218.

228 Terreni, E., Burgalassi, S., and Chetoni, P. (2020) Development and characterization of a novel peptide-loaded antimicrobial ocular insert. *Biomolecules 10,* 664.

Chapter 2

Production, purification, and chemical characterisation of the cyclodecapeptides from tyrothricin

2.1 Introduction

Antimicrobial peptides are potential alternatives for the classic antifungal drugs as resistance is less likely to occur against them due to their multiple modes of action [1]. Tyrocidines (Trcs) are one of the first group of antimicrobial peptides discovered by Dubos in 1939 [2, 3]. They show a wide range of antimicrobial activity to different targets including, human malaria parasite, (*Plasmodium falciparum*) [4], Gram-positive bacteria [5], and various pathogenic fungi [6, 7, 8]. For this study, the antifungal activities against *Candida albicans* [8] motivated us to investigate this group of peptides further.

The Trcs are relatively small cyclic peptides with a conserved sequence of 10 amino acids, with a general conserved sequence as cyclo (D-Phe^{1}-Pro^{2}-X^{3}-x^{4}-Asn^{5}-Gln^{6}-X^{7}-Val^{8}-X^{9}-Leu^{10}). The X/x indicates the variable L- or D- amino acid residues respectively, namely Trp or Phe at residue positions 3 and 4, Trp, Phe, or Tyr at position 7, and the cationic residues ornithine (Orn) or Lys at position 9 [9]. Table 2.1 summarises different Trc analogues that are generally found in tyrothricin extracts from cultures of the producer organism *Brevibacillus parabrevis (B. parabrevis)* [10].

This study aimed to enhance the anti-*Candida* activity of Trcs via cellulose derivatives formulation, in addition to, characterisation of formulated Trcs via biophysical studies. To investigate the biophysical characteristics and biological activity of the Trcs, purities of 90% or higher is required, as with a low purity of peptide, other compounds might influence the peptide's biological activity or biophysical characteristics. A multi-step organic solvent extraction method, already established within the BIOPEP Peptide Group was used to separate the cationic cyclo-decapeptides (Trcs) from the non-polar linear gramicidins (Grms) present in sample [11]. To achieve high purity of Trcs, an optimised method of reversed-phase high- performance liquid chromatography (RP-HPLC) was utilised as it is efficient in isolating Trcs analogues based on their physiochemical properties.

Table 2.1 Summary of the cyclodecapeptides generally found in tyrothricin extract from *Br. parabrevis* cultures with their monoisotopic M_r and mass/charge (*m/z*) used for identification [12]

Peptide Identity	Abbreviation	Sequence [a]	Theoretical monoisotopic M_r [b]	Monoisotopic *m/z*	
				$[M+H]^+$	$[M+2H]^{2+}$
Phenycidines					
Phenycidine A[c]	PhcA	Cyclo-(fP**Ff**NQFVOL)	1253.6597	1254.6675	627.8377
Phenycidine A_1[c]	$PhcA_1$	Cyclo-(fP**Ff**NQFVKL)	1267.6753	1268.6832	634.8455
Tyrocidines					
Tyrocidine A	TrcA	Cyclo-(fP**Ff**NQYVOL)	1269.6546	1270.6624	635.351
Tyrocidine A_1	$TrcA_1$	Cyclo-(fP**Ff**NQYVKL)	1283.6703	1284.6781	642.8430
Tyrocidine B	TrcB	Cyclo-(fP**Wf**NQYVOL)	1308.6655	1309.6733	655.3406
Tyrocidine B'	TrcB'	Cyclo-(fP**Fw**NQYVOL)	1308.6655	1309.6733	655.3406
Tyrocidine B_1	$TrcB_1$	Cyclo-(fP**Wf**NQYVKL)	1322.6812	1323.6890	662.3484
Tyrocidine B_1'	$TrcB_1$'	Cyclo-(fP**Fw**NQYVKL)	1322.6812	1323.6890	662.3484
Tyrocidine C	TrcC	Cyclo-(fP**Ww**NQYVOL)	1347.6764	1348.6842	674.8460
Tyrocidine C_1	$TrcC_1$	Cyclo-(fP**Ww**NQYVKL)	1361.6921	1362.6999	681.8539
Tryptocidines					
Tryptocidine A	TpcA	Cyclo-(fP**Ff**NQWVOL)	1292.6706	1293.6784	647.3431
Tryptocidine A_1	$TpcA_1$	Cyclo-(fP**Ff**NQWVKL)	1306.6862	1307.6941	654.3509
Tryptocidine B	TpcB	Cyclo-(fP**Wf**NQWVOL)	1331.6815	1332.6893	666.8486
Tryptocidine B_1	$TpcB_1$	Cyclo-(fP**Wf**NQWVKL)	1345.6971	1346.7050	673.8564
Tryptocidine C	TpcC	Cyclo-(fP**Ww**NQWVOL)	1370.6924	1371.7002	686.3540
Tryptocidine C_1	$TpcC_1$	Cyclo-(fP**Ww**NQWVKL)	1384.7080	1385.7159	696.3618

[a] Standard one letter amino acid abbreviations used in peptide sequences, O representing Ornithine and lower-case letters representing the D-amino acids.
[b] Theoretical monoisotopic relative molar mass (M_r) calculated as the sum of the monoisotopic M_r values of amino acid residues in each peptide. [c] Low amounts detected.

As RP-HPLC involves the separation of molecules based on their hydrophobicity, the stationary phase contains hydrocarbons such as C_4, C_8 and C_{18} [13, 14]. In this study, C_{18} HPLC matrix was utilised as longer chain carbons are more appropriate for the separation of peptides due to their amphipathicity. The mobile phases in RP-HPLC of peptides generally comprises of a polar solvent such as water that is followed by a more non-polar organic solvent such as acetonitrile [13, 14]. Trifluoroacetic acid (TFA, 0.1-0.5% *v/v*) is frequently used as solvent modifier for peptide separation [13]. In the separation amphipathic peptides interact with the C_{18} chain. The organic solvent in the flowing mobile phase utilising a gradient will compete with the C_{18} interactions and the peptides will elute based on their hydrophobicity [14]. Peptides with weaker hydrophobic interaction (more polar peptides) will elute first while peptides with stronger hydrophobic interaction (more hydrophobic peptides) will be retained on the column longer until the hydrophobicity of the mobile phase is sufficient for them to elute. In this study 1%, trifluoroacetic acid was included in the mobile phase as this acid is a counter ionto the peptide, the peptides and the acid can form an ion pair with sufficient hydrophobic properties [13, 14, 15]. It is also proposed that TFA decorates the peptide backbone presenting the Fluor-group leading to a more hydrophobic complex [13]. Resolution during reversed-phase HPLC chromatography is highly dependent on the composition of the mobile phase, small changes such as variation in temperature or the flowrate can affect the separation and resolution [13, 14, 15]. Therefore in this study, chromatography was done at a constant temperature of 35°C, a constant flow rate of 3mL/min and a strict timed gradient program that allowed peptide association, the best resolution possible and column regeneration and equilibration. The purified fractions of the peptide analogues were then analysed using reverse phase ultra-performance liquid chromatography linked to high resolution electrospray mass spectrometry, (UPLC-ESMS) to confirm the identity and integrity of the peptides and determine the purity, present within the sample.

The peptides present within the *B. parabrevis* extract presents a wide range of molecular masses, with peptides differing from one another by only one or two different amino acid residues. The peptides also tend to form dimers and associate with sodium and potassium leading to overlapping molecular masses. Mass spectrometry, in particular, high resolution electrospray mass spectrometry (ESMS) is the ideal method

for the analysis of such complex peptide mixtures and has become extremely popular for the structural investigation for peptides mixture or highly pure peptides, because of the high accuracy of this technique (<5 ppm error on M_r of a compound) [16]. A mass spectrometer consists of three main components: an ionisation source that is responsible for the ionisation of molecules, a mass analyser for maintenance of the electric field and separation of molecules based on their mass over charge (*m/z*) ratio and a detector such as a photomultiplier which is responsible for detection and conversion of ions to an electronic signal, all of which are maintained under an extremely high vacuum [16].

The ionisation source utilised in this study was an electrospray ionisation (ESI) source. ESI is a popular ionisation method specifically for proteins and peptides. ESI is an evaporation-based ionisation mode which involves the production of the fine spray of charged liquid droplets using a high voltage. Thereafter, high vacuum and high temperature (i.e., 275 °C) are applied to the highly charged sample droplets which result in the evaporation of the solvent and release solvent-free ions in the gas phase into the analyser. This method of “soft” ionisation is capable of generating singly charged and multiple charged ions. On average one charge is added for every KDa of the massof the protein sample [17].

If we pass the gas phase ions of complex peptide mixture through a powerful magnetic field in the mass analyser, the different peptides will be deflected differently by the *m/z*, if all molecules present within the mixture carries the same charge, the separation would be only based on their mass [18]. There are various types of mass analysers, but the analyser used for this study is called the quadrable time of flight analyser (Q-TOF). When ions are moving towards the analyser, smaller ions will move faster than bigger ions, the time that each ion will take to move towards the detector is called Time Of Flight (TOF) from this parameter the *m/z* value of each ion can be determined. In quadrable mass analyser, varying radiofrequency allows for selection of a specific *m/z* ratio. The Synapt G2 Q-TOF instrument used in this study is a ‘hybrid’ high resolution mass spectrometer combining quadrupole technologies with a time-of-flight mass analyser [19].

The goal of the reported study in this chapter is the successful purification of major cyclodecapeptides from the biologically produced or commercial tyrothricin complex.

This was accomplished by the production of the tyrothricin complex from the soil bacterium, followed by, isolation and characterisation of Trcs single analogue within the biological or commercial tyrothricin complex. Trc A, B, C, as well as TpcB and C were successfully produced and purified to the purity of >90%, as determined by Ultraperformance Liquid Chromatography (UPLC) linked to Electrospray Mass Spectrometry (ESMS).

2.2 Materials

Tyrocidines were purified from the tyrothricin complex produced by *Br. parabrevis* ATCC 8185 obtained from the American Type Culture Collections (Manassas, VA, USA). The medium used for peptide production was made up from tryptone soy broth (TSB), agar, D-glucose, tryptone, monopotassium phosphate (KH_2PO_4), magnesium sulphate ($MgSO_4$), calcium chloride ($CaCl_2$), ferric sulphate ($FeSO_4$), manganese sulphate ($MnSO_4$), sodium chloride (NaCl), obtained from Merck (Darmstadt, Germany). Potassium chloride (KCl) was supplied by Sigma-Aldrich (St Louis, USA). L-amino acids (L-tryptophan and L-phenylalanine) were purchased from Lurgi (Frankfurt, Germany). The media was filter sterilised using mixed cellulose syringe filters (0.22 µm) purchased from Merck-Millipore (Massachusetts, USA).

The purification of tyrocidines from the tyrothricin complex was achieved using the following organic solvents: Methanol (MeOH) and trifluoroacetic acid (TFA, >98%) supplied by Sigma-Aldrich (St Louis, USA), ethanol (EtOH), diethyl ether (DEE) and acetone were supplied by Merck (Darmstadt, Germany) and acetonitrile (HPLC-grade) was from Romil Ltd (Cambridge, United Kingdom). Activated carbon was purchased from Lurgi (Frankfurt, Germany). Analytical grade water was prepared by filtering water from a reverse osmosis plant through a Milli-Q® water purification system (Milford, USA). Phosphorous pentoxide and commercial tyrothricin extract were obtained from Sigma-Aldrich (St Louis, USA). The Nova-Pak HR C_{18} RP-HPLC semi-preparative column (6 µm particle size, 300 mm x 7.8 mm), C_{18} Nova-Pak® analytical RP-HPLC column (5 µm particle size, 150 mm x 3.9 mm), and Acquity HSS T3 (2.1 × 150 mm; 1.8 µm particle size) UPLC columns were from Waters (Milford, USA). Falcon® tubes and Petri dishes, supplied by Becton Dickson Labware (Lincoln Park, USA) and Lasec (Cape Town, South Africa), respectively.

2.3 Methods

2.3.1 Production of the cyclodecapeptides

A. Pre-Culturing of B. parabrevis as a producer of tyrocidines

A freezer stock of *B. parabrevis* 8185 was plated onto TSB agar plates (3% *m/v* TSB,1.5% *m/v* agar) using sterile culturing techniques and incubated for ±48 hours at 37 °C. This was followed by the re-streaking of the fast-growing brown colonies on another TSB plate and the incubation at 37 °C for ±48 hours.

B. Production of the tyrothricin complex from B. parabrevis

Overnight cultures containing single colonies of *B. parabrevis* in 20 mL TSB media were used to inoculate TGS media supplemented by phenylalanine (20 mM) and tryptophan (10 mM). The inoculated media were left to incubate for 10 days at 37°C as described by Vosloo *et al*. [20].

C. Extraction of selected cyclodecapeptides from the tyrothricin complex

The optimised methodologies that were used to extract the crude peptide mixture from the *Br. Parabrevis* cultures were developed by the BIOPEP Peptide Group (Stellenbosch, South Africa) and cannot be discussed in detail as the technology is protected under a non-disclosure agreement. In short, the cultures were acidified, extracted with an organics solvent, precipitated, and polished to remove the brown pigments resulting in the extraction of a peptide complex (tyrothricin).

The tyrothricin extract contains a combination of Trcs and Grms [3, 21]. The gramicidins were removed by washing several times with a mixture of ether and acetone 1:1 (*v/v*) and centrifuging at 3000×*g* for 10 minutes to collect the pellet [11, 20]. The Trcs-containing pellet was first dried with nitrogen gas to remove the ether: acetone solution before it was re-suspended in 50% (*v/v*) acetonitrile: analytical quality water and freeze-dried for further analysis and purification. The removal of Grms was confirmed through UPLC-ESMS analysis.

2.3.2 Semi-preparative HPLC purification of selected cyclodecapeptides

Single analogues of TrcA, B, C, TpcB, and TpcC were obtained through semi-preparative RP-HPLC. The purification was done using a chromatographic system

controlled by Millennium software comprising of a Waters 717 Plus Autosampler, two Waters 510 pumps, and a Waters 440 detector set at 254 nm. The temperature of the column was set at 35°C.

Peptide extracts were dissolved in 50% (*v/v*) acetonitrile: analytical water at 10 mg/mL, centrifuged at 3000 *g* for 10 minutes to remove particulate matter and injected at 100 µL per purification run onto a reverse-phase semi-preparative C_{18} Nova-Pak® column (6 µm particle size, 60 Å pore size, 7.8 mm x 300 mm). Solvent A (0.1% *v/v* TFA: acetonitrile: analytical quality water) and solvent B (90% *v/v* ACN, 0.01% *v/v* TFA) were used forthe separation of the peptide in the Trcs extract using a gradient elution programme (Table 2.2) at 3.0 mL/min flow rate. Fractions were collected and dried in pyrolysed 20 mL vials and stored tightly closed at room temperature [22].

Table 2.2 The HPLC gradient program utilised for semi-preparative HPLC purification of the selected cyclodecapeptides from *Br. parabrevis.*

Minutes	% Eluent A	% Eluent B	Curve*
0.00	50	50	none
0.50	50	50	6 linear
23.0	20	80	5 concaves
24.0	0	100	6 linear
26.0	0	100	6 linear
30.0	50	50	6 linear
35.0	50	50	6 linear

* Curves 5 and 6 are from Waters™ gradient programmes

2.3.3 Characterisation of peptide extracts and purified peptides by ES-MS and UPLC-MS analysis

All fractions with more than 1.0 mg material from the purification steps were analysed using ESMS and UPLC-MS. All samples were subsequently centrifuged at 8600 x *g* for 10 min to remove any particulate material.

The system consists of a Waters Acquity® UPLC coupled to the high-resolution Waters Synapt G2 quadrupole time-of-flight (Q-TOF) mass spectrometer. For direct ESMS injections and detection during UPLC-MS, the instrument parameters were as follows: the cone and capillary voltages were set to 15 V and 3 kV respectively,

samples from direct injection (2-5 µL were injected via Acquity® UPLC system) and UPLC-MS were passed via a Z-spray electrospray ionisation source at a set temperature of 120 °C and flow of 300 µL/minute, desolvation at 275 °C and nitrogen gas at 650 L/hour flow rate into the mass analysers. Continuum data were collected in positive mode from *m/z* of 300-2000. For direct ESMS analysis, the concentration of peptide samples ranged between 250 -1000 µg/mL in 50% acetonitrile: analytical quality water, depending on purity.

For UPLC-ESMS 3 µL of the peptide sample, at 250 and 1000 µg/ in 50% acetonitrile: analytical quality water for purified HPLC fractions and crude extracts respectively, were injected onto an Acquity UPLC® BEH C_{18} column (130Å pore size, 1.7 µm particle size, 2.1 mm diameter X 50 mm length) at a flow rate of 0.3 mL/min and a set temperature of 60°C before introduction to the mass spectrometer. The separation was achieved using the linear-gradient program, given in Table 2.3 [11].

Table 2.3 The UPLC-ESMS gradient program peptide extracts and purified cyclodecapeptides

Minutes	% Eluent A	% Eluent B	Curve*
0.00	0	0	6
0.50	100	0	6
1.00	70	30	6
10.0	40	60	6
15.0	20	80	6
15.1	0	0	6
18.0	100	0	6

*6 depicts linear curve from Waters™ gradient programmes

The relative purity of the extracts was calculated from the peak area obtained from UPLC-ESMS, whereas the identity and integrity of peptides present in purified extracts were confirmed using high-resolution ESMS. The data obtained from ESMS and UPLC-ESMS was analysed using MassLynx™ software V4.1. In order to analyse the peptide identity and integrity, the *m/z* values in addition to the MaxEnt 3 calculated monoisotopic M_r of each peptide was assessed and evaluated using parts per million (ppm) mass error. The following equations were used to calculate the ppm mass error:

$$\text{ppm} = \frac{M\text{r (theoretical)} - M\text{r (experimental)}}{M\text{r (theoretical)}} \times 10^6$$

2.4 Results and discussion

2.4.1 Analysis of amino acid supplemented crude extracts

A complex mixture consisting of tyrocidines, tryptocidines, and phenycidines, as well as linear Grms, was successfully extracted from the tyrothricin complex produced by the soil bacterium *Br. parabrevis.* The exact composition of these crude extracts and the success of supplementation were monitored by UPLC-ESMS. The UPLC-ESMS chromatogram of each supplementation is shown in Figures 2.1-2.3.

Due to the highly conserved structure of tyrocidines, the analogues differ from one another by only one or two aromatic amino acids residues. The similarity between different tyrocidine analogues makes the purification of a single analogue a relatively challenging task [11]. Supplementation of the culture media with Phe and Trp shifted the profile of peptides produced by *Br. parabrevis ATCC 8185* towards TrcA and TpcC, analogues respectively and therefore simplify the purification. This result correlates with the previous findings by Vosloo *et al* [20].

Phe supplementation (20 mM Phe) of the bacterial culture media resulted in the production of a wide range of A analogues from the tyrocidine, tryptocidines, and phenycidine families with TrcA being the major peptide analogue (Figure 2.1). The low resolution between TrcA (Rt=10.21) and $TrcA_1$ (Rt=10.09) or TpcA (Rt=10.74) and PhcA (Rt=10.68) makes the purification difficult. However, TrcB is a good candidate to be subjected to RP-HPLC. Despite the small amount of TrcB (low signal intensity), there is no co-elusion if the production of TrcB' with the inversion of residues 3 and 4 is limited.

Table 2.4 shows that TrcA>TpcA>Grms/TrcB>$TrcA_1$>PhcA was the pattern of analogue abundancy presented in 20 mM Phe supplemented cultures. Furthermore, this culture had lower production of Grms when compared to cultures receiving no supplementation. $TrcA_1$ and PhcA are present in this culture while they are not in non-supplemented culture contrasting the Tpc analogues which are present in non-supplemented.

Trp-supplementation (10 mM Trp) of the bacterial culture media resulted in the production of C analogues of the tyrocidine and tryptocidine families with TpcC being the major peptide analogue (Figure 2.2). There is less co-elusion between different

analogues of Tpcs, therefore these bacterial culture extracts are good candidates to be subjected to RP-HPLC for TpcC, TrcC, and TpcB isolation. TrcB would have a low yield due to the very low amount present in the 10 mM Trp-supplemented culture (1% of the total culture mass) while TpcC is expected to have the highest yield after purification (27% of the total peptide). Furthermore, supplementation caused an increase in Grms production when compared to 10 mM Phe supplementation and un-supplemented cultures (Table 2.4). TpcC>Grms>TrcC>TpcB>TrcB was found to be the pattern of analogues abundancy presented in 10 mM Trp-supplemented cultures.

In contrast to the supplemented bacterial cultures, the culture which received no amino acid supplementation (Figure 2.3), did not favour the predominant production of analogues from any one of the A, B, and C groups. Instead, a mixture of A, B, and C analogues belonging to all three tyrocidine, tryptocidines, and phenycidine families was produced. However, TrcB was the most abundant analogue within the crude peptide mixture. The HLPC purification had sufficient resolution and different analogues present in this culture have been separated well from one another except PhcA (Rt=10.18) and TpcA (Rt=10.26). TrcB, TrcA are good candidates to be subjected to RP-HPLC as there are high amounts in the culture and there is no co-elusion. However, TpcC will have a low yield due to the very low amount present in the culture (4% of the total culture).

Table 2.4 shows that TrcB>TrcA>TpcB>TrcC>TpcA>TpcC is the pattern of analogues abundancy presented in extracts of non-supplemented cultures.

The abundancy pattern of Trcs analogue present within the supplemented cultures and the effect of supplementation on the production of Grms correlate with the literature [20].

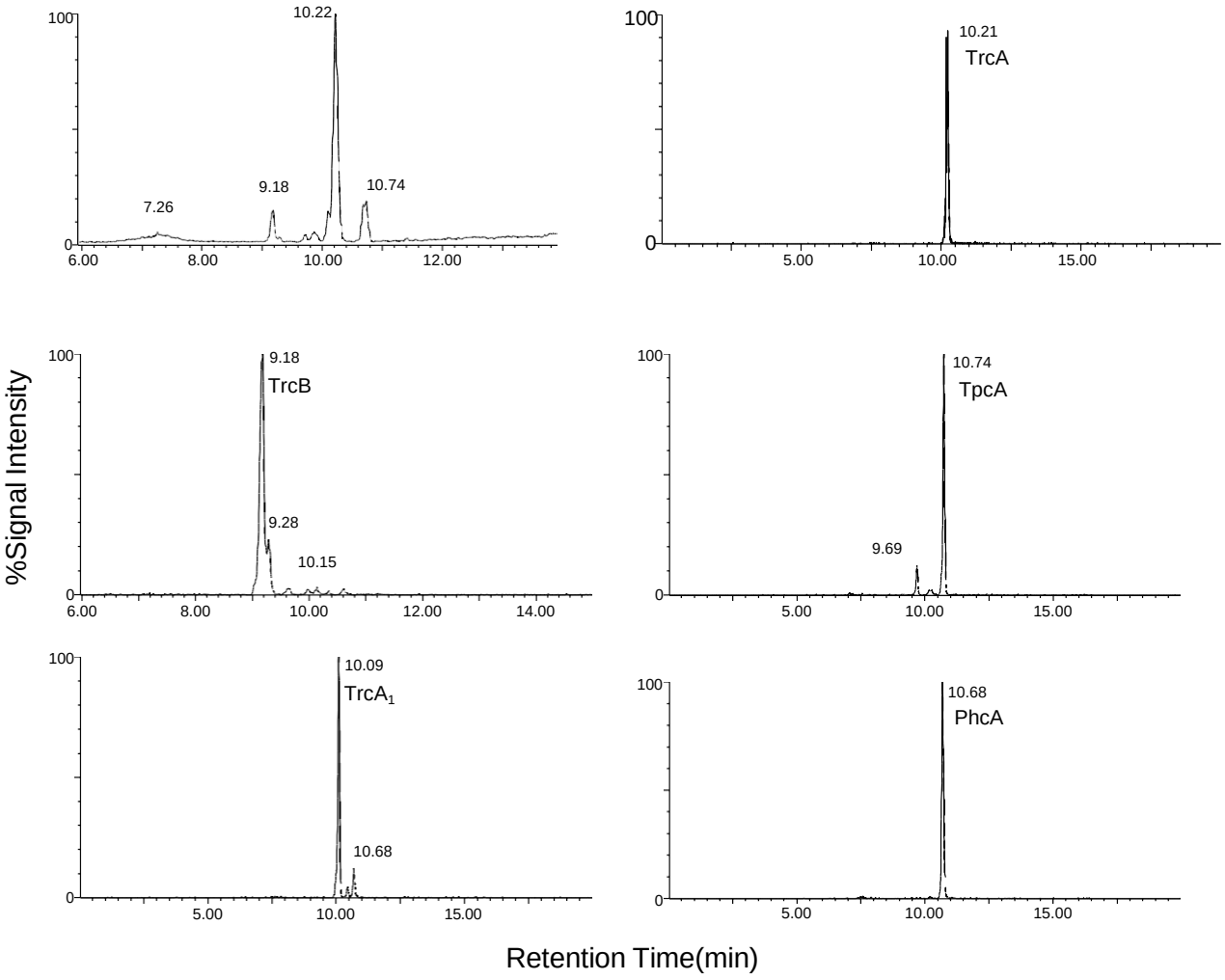

Figure 2.1 The UPLC-ESMS profile (top left) of all the different peptides present in crude extract from production in 20 mM Phe supplemented culture. Extracted *m/z* ($[M+2H]^{2+}$) chromatograms of component peaks in each of the crude extracts indicate the main analogue in the extracted peaks. The retention time and peptide identity for each of the single analogues are given for each of the *m/z* extracted peaks.

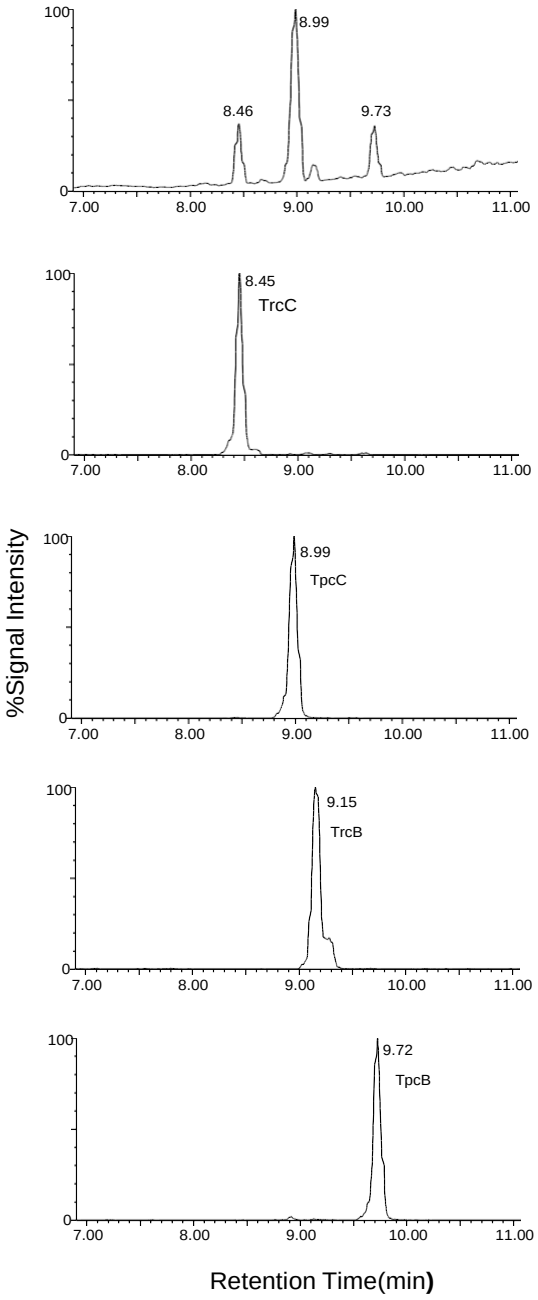

Figure 2.2 The UPLC-ESMS profile (top) of all the detected peptides and mass extracted chromatograms of crude extract from 10 mM Trp supplemented culture media. The single analogues present in the extracts are shown in the *m/z* extracted chromatograms below.

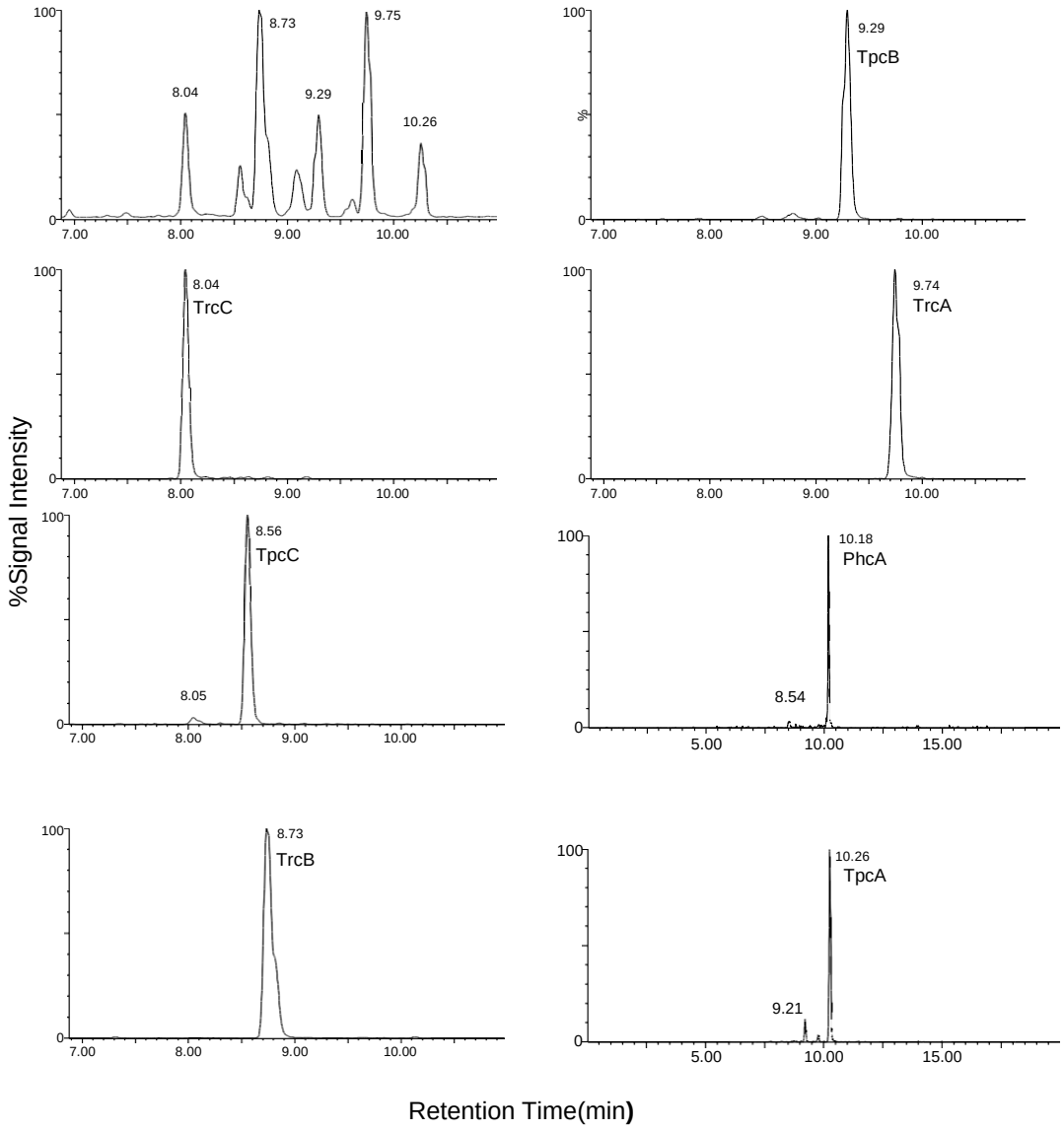

Figure 2.3 The UPLC-ESMS chromatogram (top left) of all the detected peptides and mass extracted chromatograms of crude extract from non-supplemented culture media. The single analogues present in the extract are shown in the rest of the *m/z* extracted chromatograms.

Table 2.4 Summary of percentage abundance of single analogues presents in the crude peptide mixtures extracted from amino acid supplemented and non-supplemented bacterial cultures of *Br. parabrevis.*

	% abundance [a]		
Peptide identity	**10 mM Trp supplemented**	**20 mM Phe supplemented**	**Un-supplemented**
TrcA	-	35.5	19.8
TrcA1	-	3.3	-
TrcB	1.1	4.2	30.7
TrcB1	-	-	-
TrcC	7.2	-	7.7
TrcC1	-	-	-
TpcA	-	4.9	7.0
TpcB	5.9	-	10.7
TpcC	27.4	-	3.7
PhcA	-	2.7	-
Grms	14.8	4.2	8.5
% Total peptide[b]	**41.6**	**50.6**	**79.6**

[a] % Abundance was calculated by expressing the peak area of each peptide as a percentage of the sum of the peak areas of all peptides present in the extract. It was assumed that the response factors of all peptides are similar due to their analogous structures.

[b] %Total peptide was determined by the sum of the peak areas of all the Trcs present in the crude extract.

2.4.2 Purification of cyclodecapeptides from culture extracts

Tyrocidines and analogues were extracted and purified through four different steps which resulted in the removal of linear Grms and non-peptide material. UPLC-ESMS analysis of non-supplemented bacterial culture, as an example, shows the resultant profile of each step (Fig. 2.4). The UPLC-ESMS analysis in Fig. 2.4 of stepwise purification showed that each step resulted in the removal of more of Grms (Rt=14-16.5 minutes) and non-peptide material (Rt=2.5-6.5 minutes). The organic solvent extraction resulted in a characteristic tyrothricin profile containing some non-peptide material, and the Trcs, Tpcs as well as the Grms (Fig. 2.4A) with TrcB being the major analogue. The precipitation step did not lead to a major change in the profile but did remove Grms and non-peptide contaminants (Fig 2.4B).

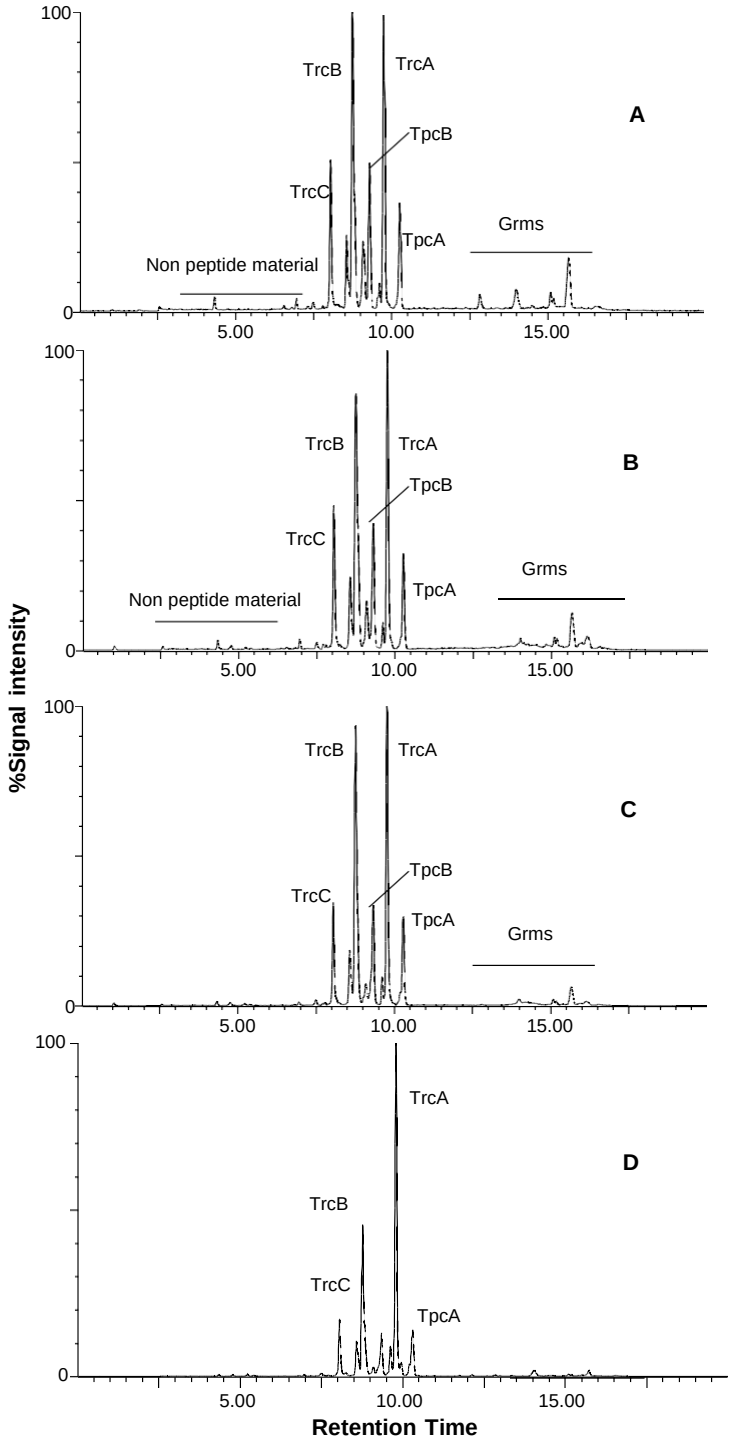

Figure 2.4 The UPLC-MS chromatography of stepwise purification of non-supplemented *Br. parabrevis* culture media. Peptide extract after **A.** organic solvent extraction **B.** precipitation **C.** polishing and **D.** ether: acetone wash steps.

The polishing step led to the loss of more polar peptides such, as TrcC and TrcB. The DEE-acetone precipitation removed most contaminants and Grms but led to a major loss of in particular the tryptocidines, with the tyrocidines (TrcA>TrcB>TrcC) remaining as the abundant analogues. The removal of Grms is essential as it complicates the purification of the other peptides (Trcs and Tpcs) during HPLC. The Grms are very hydrophobic and tend to stick and accumulate on the C_{18} matrix leading to leaching and loss of column resolution (unpublished results from BIOPEP™ Peptide Group).

A summary of the purification yields is given in Table 2.5. Although there is a significant decrease in the mass yield of the peptide extract, the purity of different Trc-fraction increases to above 95%. Isolation of TrcB and TrcC analogues via RP- HPLC from the crude extract before the polishing step is more feasible while the TrcA analogue can be isolated with a greater yield from the crude extract after being washed by DEE-acetone. The predicted mass yields of the major analogues within the un-supplemented culture are tabulated in Table 2.6. For the major peptide analogues, more than 60% of their mass were lost during the four steps in purification with losses of TrcB, TrcC, TpcA, and TrcA of 95%, 84%, 82%, and 62% respectively.

Table 2.5 Summary of the mass yields, % purity, and the relative yield % after four-step purification of a non-supplemented culture extract.

Step	Mass (mg)	% Peptide complex purity[a]	%Peptide complex yield[b]
Organic extraction	661.3	79.0	100
Precipitation	297.9	85.5	48.8
Polishing	235.4	92.2	41.6
DEE: Acetone wash	107.7	94.1	19.4

[a] The %purity was determined by the sum of the peak area of all peptides present in the crude extract after each step of organic solvent purification

[b] The % mass yield determined from the crude culture extracted after each step relative to the first step

Table 2.6 The predicted mass yields of the most predominant analogue in non-supplementedculture media.

	Theoretical mass (mg) yield of the major analogue [a]			
Step	**TrcA**	**TrcB**	**TrcC**	**TpcA**
Organic extraction	131	203	50.9	46.3
Precipitation	75.4	88.5	27.9	22.3
Polishing	71.1	50.9	19.8	21.7
DEE: Acetone wash	48.9	8.9	7.9	8.0

[a]The mass (mg) of the predominant analogues present in the non-supplemented culture was calculated by multiplying of % abundance by the total mass (mg) (refer to Table 2.7) of the crude extract after each step of the organic solvent purification

The percentage abundance of most Trcs analogue (TrcC, TpcA and TpcC) remained consistent through all four steps of purification unlike TrcB, which was lost by a further amount after each step of purification relative to the other analogue. TrcA was the only analogue that had a significant increase in percentage abundance after all four purification steps (Table 2.7).

In order to purify further amount of Trcs single analogues, commercial tyrothricin complex was washed with ether: acetone and subjected to RP-HPLC. The insolubility of Trcs analogues and solubility of the hydrophobic Grms in DEE-acetone due to their different hydrophobic properties allowed for the separation of the two groups of peptides from the tyrothricin mixture. However, as previously noted with non-supplemented culture, DEE-acetone wash, results in loss of the Trcs analogues. Therefore, each complex (tyrothricin, Trcs and Grms) were subjected to UPLC-ESMS to compare the abundance of different peptides analogues present within the preparation (Figure 2.5).

Table 2.7 The percentage abundance of Trc single analogues and Grms in non-supplemented *Br. parabrevis* culture media after each organic solvent step of extraction and purification.

	% abundance [a]			
Peptide identity	**Organic extract**	**Precipitation**	**Polished extract**	**DEE: Acetone**
TrcA	19.8	23.1	29.2	45.4
$TrcA_1$	-	-	-	-
TrcB	30.7	27.6	28.6	21.6
$TrcB_1$	-	-	-	-
TrcC	7.7	9.4	8.4	7.2
$TrcC_1$	-	-	-	-
TpcA	7.0	7.5	9.3	7.4
TpcB	9.1	15.7	12.8	8.3
TpcC	3.6	4.5	3.7	3.4
PhcA	-	-	-	-
Grms	8.5	6.7	3.0	2.8
%Total [b]	77.9	87.7	92.0	93.3

[a]% Abundance was calculated by expressing the peak area of each peptide as a percentage of the sum of the peak areas of all peptides present in the extract. It was assumed that the response factors of all peptides are similar due to their analogue structure.
[b] %Total peptide was determined by the sum of the peak areas of all the Trcs present in the crude extract after each step of purification.

The DEE-acetone wash resulted in complete loss of minor analogues and significant loss of some of the major analogues present within the culture despite increasing the total purity by removing the Grms. Table 2.8 compares the pattern of abundancy different Trcs analogues present in Trc mix and Grms extracted from the tyrothricin complex. In the tyrothricin complex, the major analogue was TrcB, if the peptide loss was even for all different Trcs analogues it was expected of TrcB to remain the major analogue present in extracted Trc complex and Grms. However, the major analogue present within the extracted Grms is TrcC. Therefore, it is concluded that the major losses are greater towards the more polar analogues.

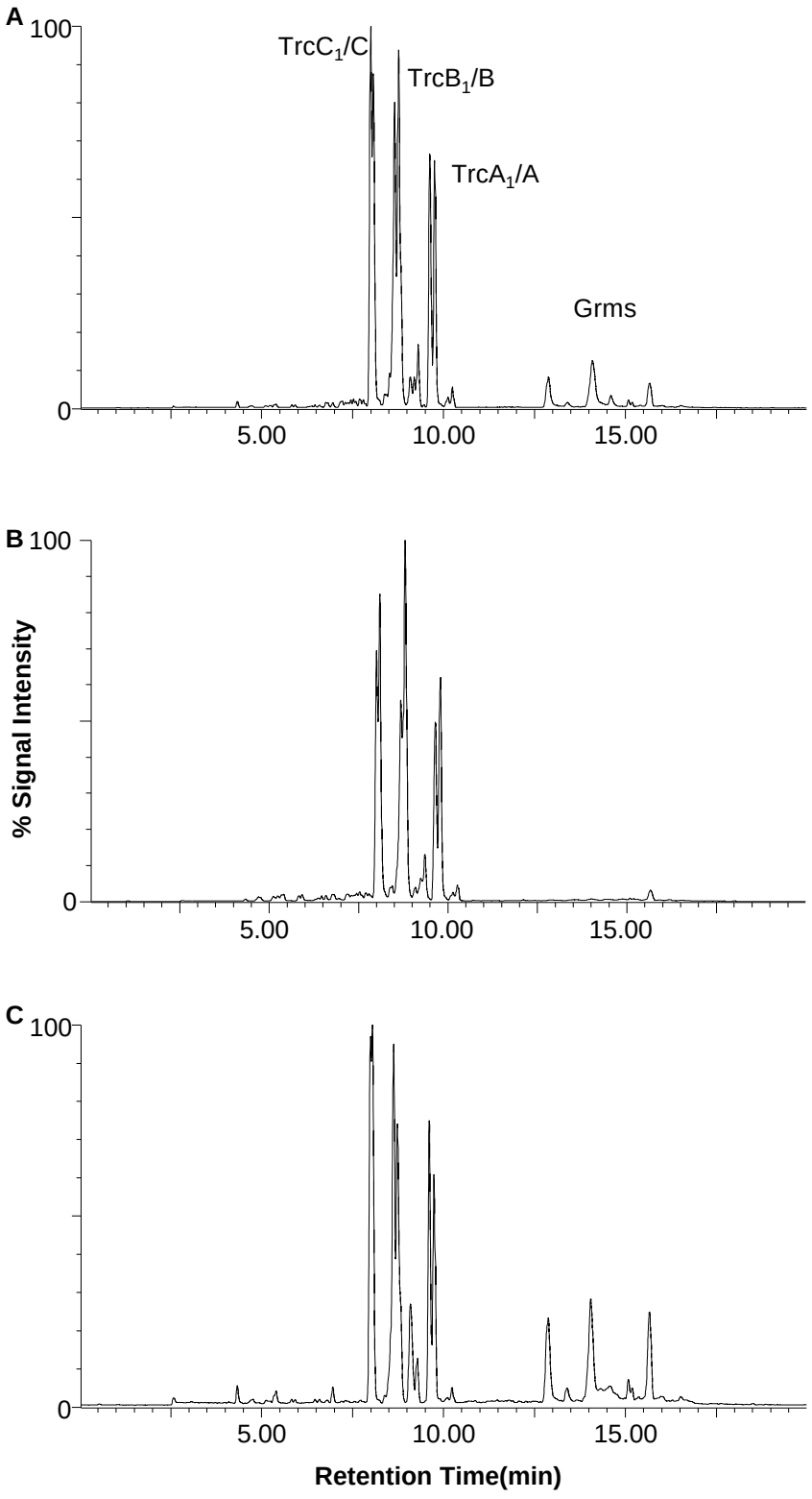

Figure 2.5 The UPLC chromatograms of commercial tyrothricin complex with **A.** the untreated tyrothricin, **B** the precipitate of the DEE: acetone wash containing the Trc mix, and **C.** the soluble of the DEE: acetone wash containing both the Trcs and the linear Grms.

Table 2.8 The percentage abundance and theoretical mass (mg) yield of the major analogue of Trc single analogues and Grms present within the commercial tyrothricin complex before and after the wash with DEE:acetone.

	%Abundance [a]			Theoretical mass (mg) yield of the major analogue [c]			%abundance Trc mix	
	Tyrothricin complex	Extracted Trc mix fraction	Extracted Grms fraction	Tyrothricin complex	Extracted Trc mix fraction	Extracted Grms	Vosloo [20]	Troskie *et al.* [6].
$TrcC_1$	14.2	12.4	11.2	2.13	1.27	0.52	1.6	12.5
TrcC	13.6	15.0	13.1	2.04	1.53	0.61	10.7	14.8
$TpcC_1$	1.1	1.2	0.5	0.17	0.12	0.02	0.3	-
TpcC	1.5	2.9	1.8	0.23	0.3	0.08	2.5	1.7
$TrcB_1$	14.4	9.3	13.1	2.16	0.95	0.61	3.5	19.2
TrcB	15.2	22.9	9.7	2.28	2.34	0.45	9.4	18.2
TrcB'	3.9	-	6	0.59	-	0.28	8.5	4.0
TpcB	2.7	3.8	1.7	0.41	0.27	0.08	6.2	1.0
$TrcA_1$	9.9	10.4	10.6	1.49	1.06	0.49	4.4	15.8
TrcA	9.6	13.0	9.3	1.44	1.32	0.43	21.1	12.9
TpcA	0.7	1.4	-	0.11	0.1	-	6.3	Trace
IGB	2.2	-	5.6	0.33	-	0.26	0.6	-
VGA	4.1	-	6.7	0.62	-	0.31	6.1	-
VGB	1.8	-	3.1	0.27	-	0.14	0.6	-
Total Trcs [b]	86.8%	92.1%	77.0%	13.05 mg	9.26 mg	3.,57mg	81.8 %	100.1%

[a] % Abundance was calculated by expressing the peak area of each peptide as a percentage of the sum of the peak areas of all peptides present in the extract. It was assumed that the response factors of all peptides are similar due to their analogue structure.
[b] %Total Trcs was determined by the sum of the peak areas of all the Trcs present in the tyrothricin complex and each of the extracts.
[c] The mass (mg) of the predominant analogues presents in the tyrothricin complex and each of the extracts were calculated by multiplying of % abundance by the total mass (mg) of in the tyrothricin complex and each of the extracts.

2.4.3 Effect of time on aggregation and purification

It has been shown by various studies [23, 24] that Trcs form oligomers in a variety of structures over a time which significantly complicates the purification and isolation of Trcs single analogues. Peptides with higher purity and hydrophobicity have a higher tendency of oligomerisation.

Trcs form different oligomers including dimers, trimers, and tetramers that can be detected by ESMS. The ESMS spectra in Figure 2.6 shows the oligomerisation profile of commercial Trc mix. As many of the dimers and higher oligomers are hetero-oligomeric which complicates the analysis as many heterodimers and homodimers, such as TrcA-TrcC and TrcB-TrcB, have the same mass. It is therefore difficult to distinguish the identity of different monomers present within a hetero-oligomeric complex without advanced mass spectroscopic analysis. When purifying Trcs it will typically take about 12 hours a day with 20 semi-preparative HPLC runs (35 minutes each) and peptides that are aggregating complicates purification. Highly aggregated peptides result in peak broadening in which different analogues of Trcs co-elute at the same time as well as a shift in retention time. Furthermore, aggregated peptide preparations can cause technical difficulties during the purification. Peptide aggregates tend to precipitate out of the solution and those that remain in solution as oligomers have an altered hydrophobicity which results in a shift in RP-HPLC chromatographic profile.

To test the time frame for dissolving and purification, samples were subjected to RP-HPLC over two time periods after being dissolved in 50% acetonitrile: analytical quality water. The chromatograph in Figure 2.7 shows the effect of aggregation on the elution time of the tyrocidines from the C_{18} column during one run of RP-HPLC. It seems that the formation of different oligomers of tyrocidines over six hours has resulted in more hydrophobic structures that caused broader peaks and later elusion from the C_{18} column when compared to the fresh sample with less oligomeric structures. However, the resolution between the three groups of Trc A_1/A, B_1/B, and C_1/C was maintained, indicating that the formation of hetero-oligomers did not have a major influence over the six hours.

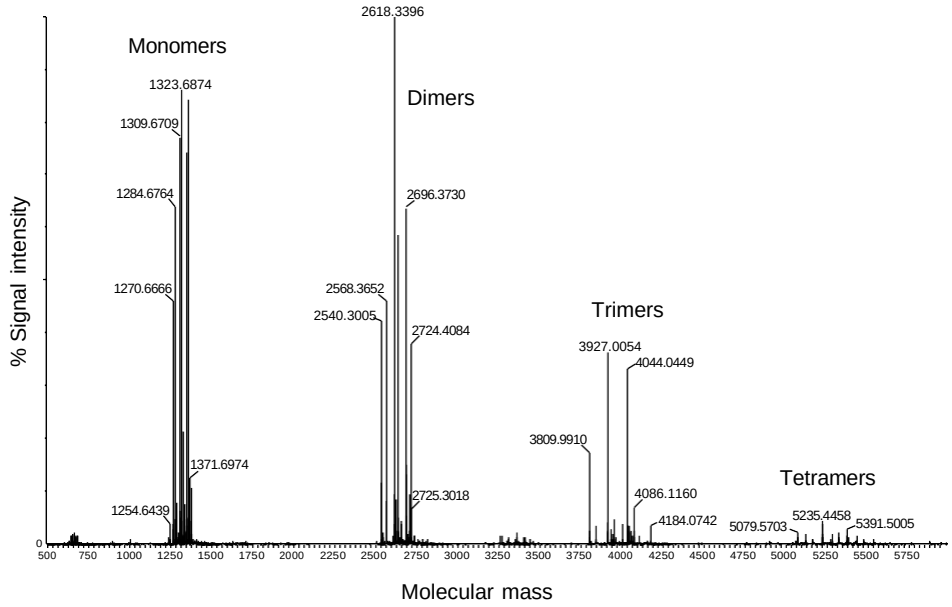

Figure 2.6 ESMS mass spectrum derived via MassLynx 4.01 MaxEnt 3 algorithm showing the oligomerisation profile of commercial Trc-mix (250 µg/mL)

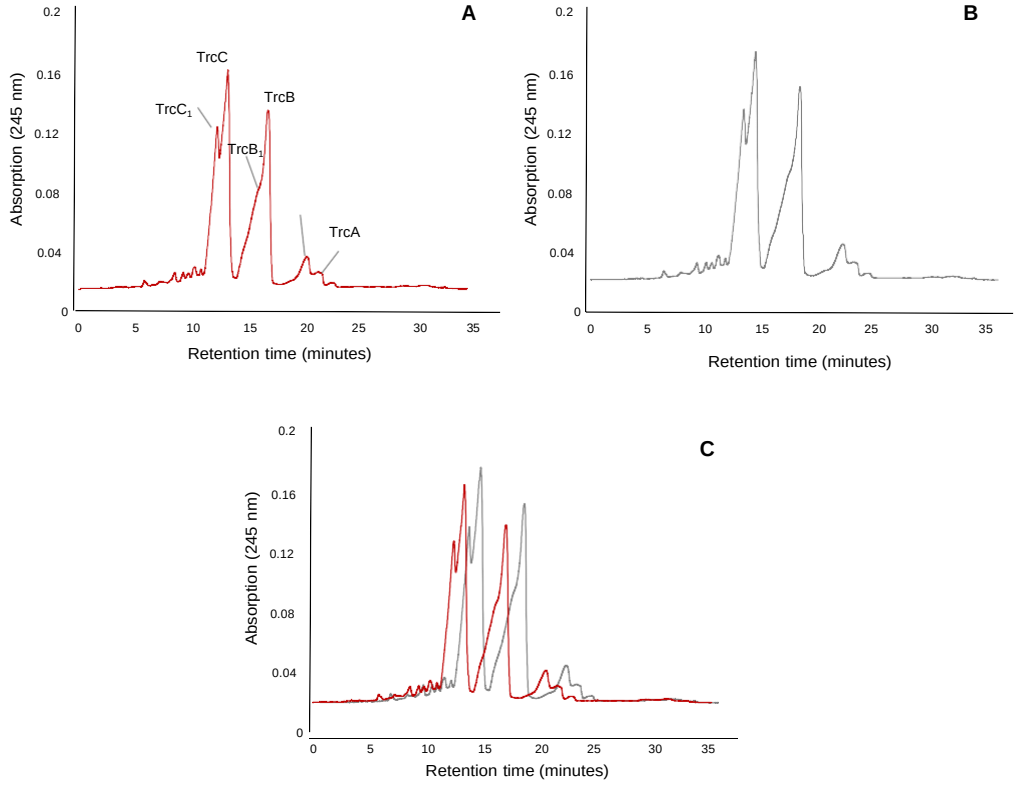

Figure 2.7 Semi-preparative HPLC chromatograms of a 100 µL injection of commercial Trc mixture (5 mg/mL). **A.** RP-HPLC profile of Trc mix directly after dissolving in in %50 acetonitrile: water **B.** RP-HPLC profile of Trc mix six hours after preparation **C.** The overlay of **A** (red) and **B** (grey) profiles shows the change in the time-dependent chromatographic result.

2.4.4 Semi-preparative RP-HPLC purification of single cyclodecapeptide analogues

The crude extracts and commercial Trc-mix were further purified using RP-HPLC based on a method developed by Rautenbach *et al.* [4] and Eyeghe-Bickong [21]. The protocol allows the earlier elution of most hydrophilic analogues and later elution of the most hydrophobic analogues, with the following elution sequence of the major peptides in this study: TrcC, TpcC, TrcB, TpcB, TrcA, and PhcA. The hydrophobicity of the peptide depends on the identity of aromatic residues at positions 3, 4, and 7. Figure 2.8 shows the collected fractions from the three different culture extracts in addition to the commercial Trc-mix.

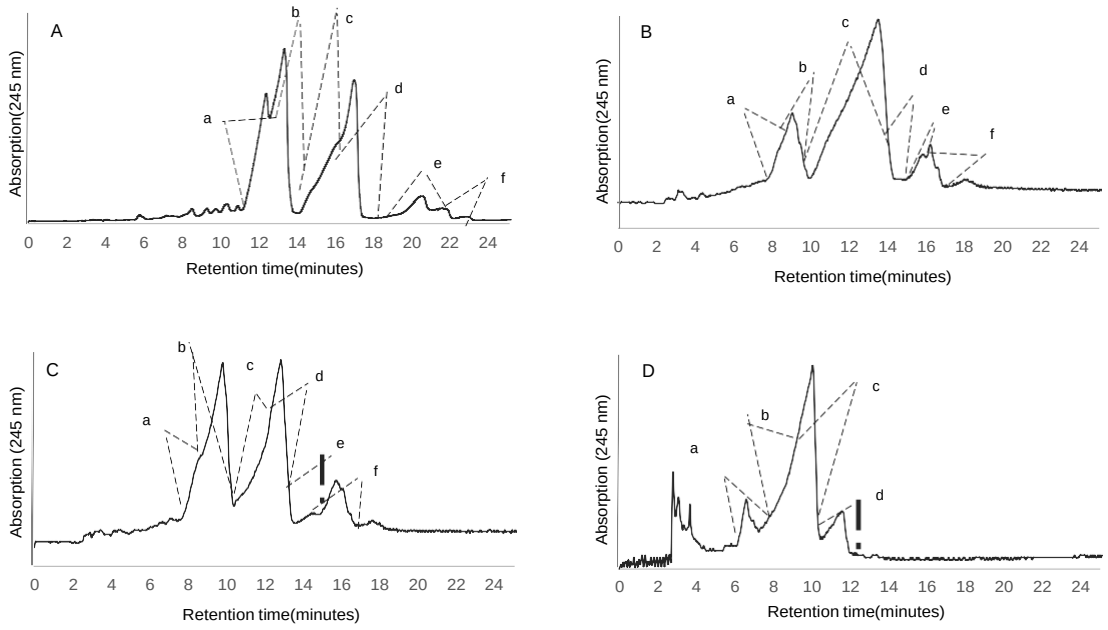

Figure 2.8 Semi-preparative HPLC chromatograms of **A.** commercial Trc-mix after the wash with DEE: acetone, **B.** 20 mM Phe supplemented **C.** non-supplemented. **D.** 10 mM Trp- supplemented cultures after the organic solvent extraction and precipitation step. The collected fractions are indicated with dashed lines and annotated with lower case a-f.

There is an elution time difference between Trcs single analogue present within commercial Trc-mix and biological culture about (4 minutes). This is because the biological culture extracts have been purified utilising a different more modern HPLC instrument than commercial Trc mix. The peptide composition of all collected fractions with more than 1.0 mg of mass was determined by ESMS analysis (Table 2.9).

Table 2.9 Summary of the ESMS analysis of each of the semi-preparative HPLC fractions from the different purified culture extracts and commercial Trc mix

HPLC fraction [a]	Major Peptide	Experimental [b] (Theoretical) monoisotopic M_r	Mass error [c] (ppm)	ESMS mass spectra of purified fraction	
A-a	ND	-		-	20 mM Phenylalanine-Supplemented
A-b	ND	-		-	
A-c	TrcB	1308.6636 (1308.6655)	1.5	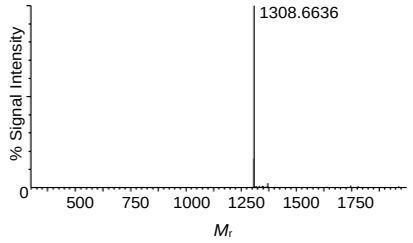	
A-d	ND	-	-	-	
A-e	ND	-	-	-	
A-f	TrcA	1269.6565 (1269.6546)	-1.5	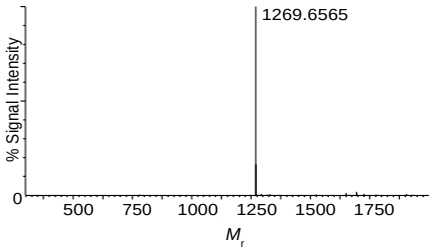	
B-a	TrcC	1347.6768 (1347.6764)	0.3	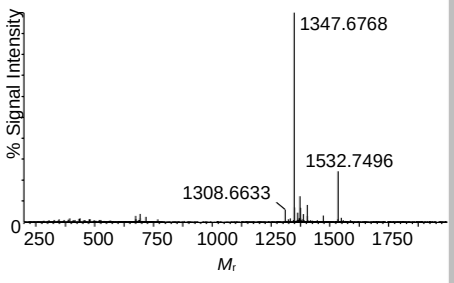	10 mM Tryptophan- supplemented
	TrcB	1308.6633 (1308.6655)	1.7		
	glycosylated TpcC	1532.7496 (1532.7407)	-5.8		
B-b	TpcC	1370.6920 (1370.6924)	0.3	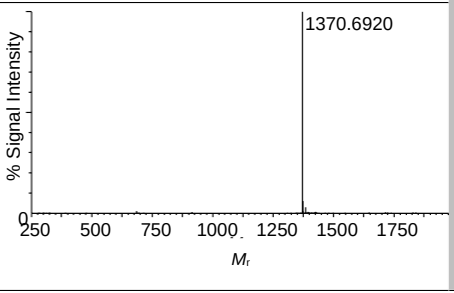	

Table 2.9 continued

B-c	TpcC	1370.6920 (1370.6924)	0.3	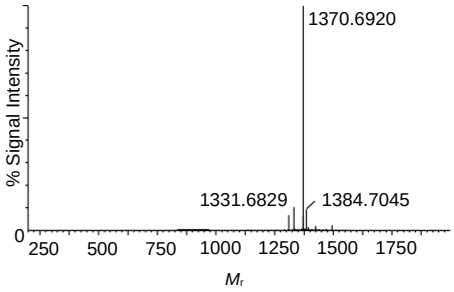	un-supplemented
	TpcB	1331.6829 (1331.6815)	-1.0		
	$TpcC_1$	1384.7045 (1384.7080)	2.57		
B-d	TpcB	1331.6840 (1331.6815)	-1.9	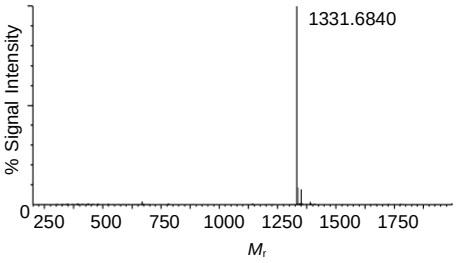	
C-a	TrcC	1347.6786 (1347.6764)	-1.6	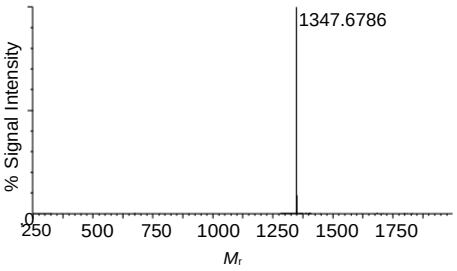	
C-b	ND	-	-	-	
C-c	ND	-	-	-	
C-d	TrcB	1308.6638 (1308.6655)	1.3	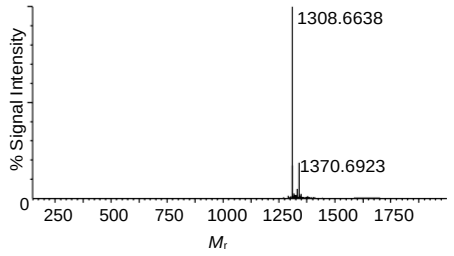	
	TpcC	1370.6923 (1370.6924)	0.1		
C-e	ND	-	-	-	

Table 2.9 continued

C-f	TrcA	1269.6544 (1269.6546)	1.6	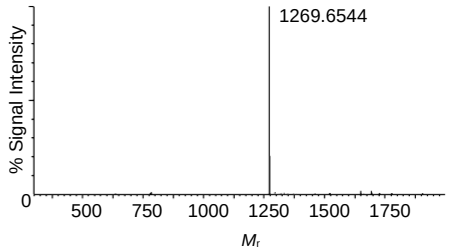	Trc mix
D-a	TrcC	1347.6768 (1347.6764)	0.3	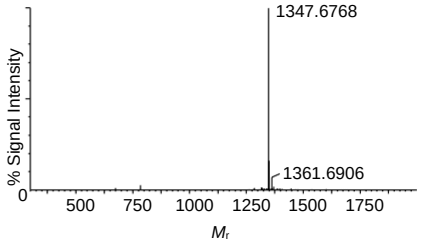	
	$TrcC_1$	1361.6906 ^{13}61.6921	1.1		
D-b	ND	-		-	
D-c	TrcB	1308.6700 1308.6655	-3.4	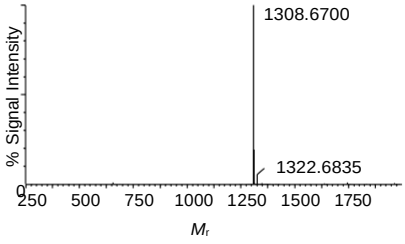	
	$TrcB_1$	1322.6835 1322.6812	-1.7		
D-d	ND	-		-	
D-e	TrcA	1269.6552 1269.6546	-0.5	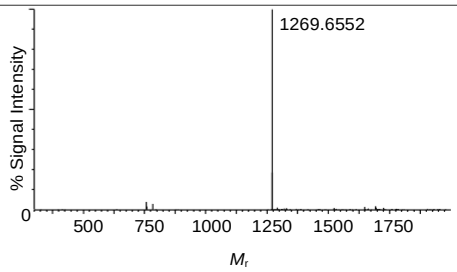	
D-f	ND	-		-	

[a] The fraction annotation refers to the chromatogram in Fig 2.8 (A, B, C or D) and fraction (a-f)
[b] Experimental M_r calculated using the following equation: $M_r = (m/z\ x\ z) - z\ x\ 1.007825$.
[c] Parts per million error or ppm errors were calculated using the following equation:
ppm = 10^6 x {M_r(theoretical) – M_r(experimental)}/M_r(theoretical).
ND - Not Determined: The amount of collected fraction was too low for ESMS analysis, therefore the peptide identity in the collected fraction is unknown.

From the initial ESMS analysis (Table 2.9) it was found that fractions **c** and **f** (from 20 mM Phe-supplemented culture extract) containing pure TrcB and TrcA, respectively, fractions **b** and **d** (from 10 mM Trp-supplemented culture extract) containing pure TpcC and TpcB, fractions **a** and **f** (from non-supplemented culture extract) containing pure TrcC and TrcA and fraction **c** and **e** (from commercial Trc-mix)

containing pure TrcB and TrcA. Therefore, they were subjected to UPLC-ESMS to determine the purity of the single analogues. One example UPLC-MS from each of the purified peptides is shown (Figures 2.10).

Our group previously showed that Trcs tend to deaminate at the Glu and/or Asn residues and as many peptides, they have a tendency of K^+ or Na^+ adducts formation during ESMS. These aspects could influence the purity and UPLC-MS purity determination of the purified Trcs and Tpcs. ESMS results revealed that none of the pure peptides in the collected fractions were deaminated. Interestingly, a novel glycosylated analogue of TpcC was detected in fraction **a** purified from the 10 mM Trp-supplemented culture extract. Calculated mass error for all analogues present within different collected fractions was below 6 ppm confirming the correct identification of the peptides in the tyrothricin complex (Tables 2.9 and 2.10). The UPLC-MS chromatography correlated with similar reported studies [21, 24, 25] (Table 2.10).

Fraction **a,** containing mainly TrcC, and fraction **c** containing mainly TpcC from the 10 mM Trp supplemented culture were contaminated by small amounts of Trc B and TpcB, respectively. Fraction **d,** mainly containing TrcB, purified from non-supplemented culture contained a small amount of TpcC as shown in the UPLC-ESMS chromatogram in Figure 2.3. The retention time of TrcB (8.73) and TpcC (8.56) is very close therefore some co-elution of the two peptides was to be expected in the lower resolution semi-preparative RP-HPLC.

Fractions **a** and **c** containing mainly TrcB and TrcC (from Trc mix) contained a small amount of the Lys analogues, $TrcB_1$ and $TrcC_1$, respectively. Separation of TrcC from $TrcC_1$ and TrcB from $TrcB_1$ is difficult as the two analogues only differ in a CH_2 group due to the substitution of Orn by Lys. In order to obtain a better separation analytical RP-HPLC can be utilised with lower loading concertation, lower flow rate, and higher resolution [5, 24].

The purification of five different Trcs single analogues from the crude extracts and commercial Trc mix was successful. All analogues had a purity of higher than 90%, as determined with UPLC-MS (Table 2.10).

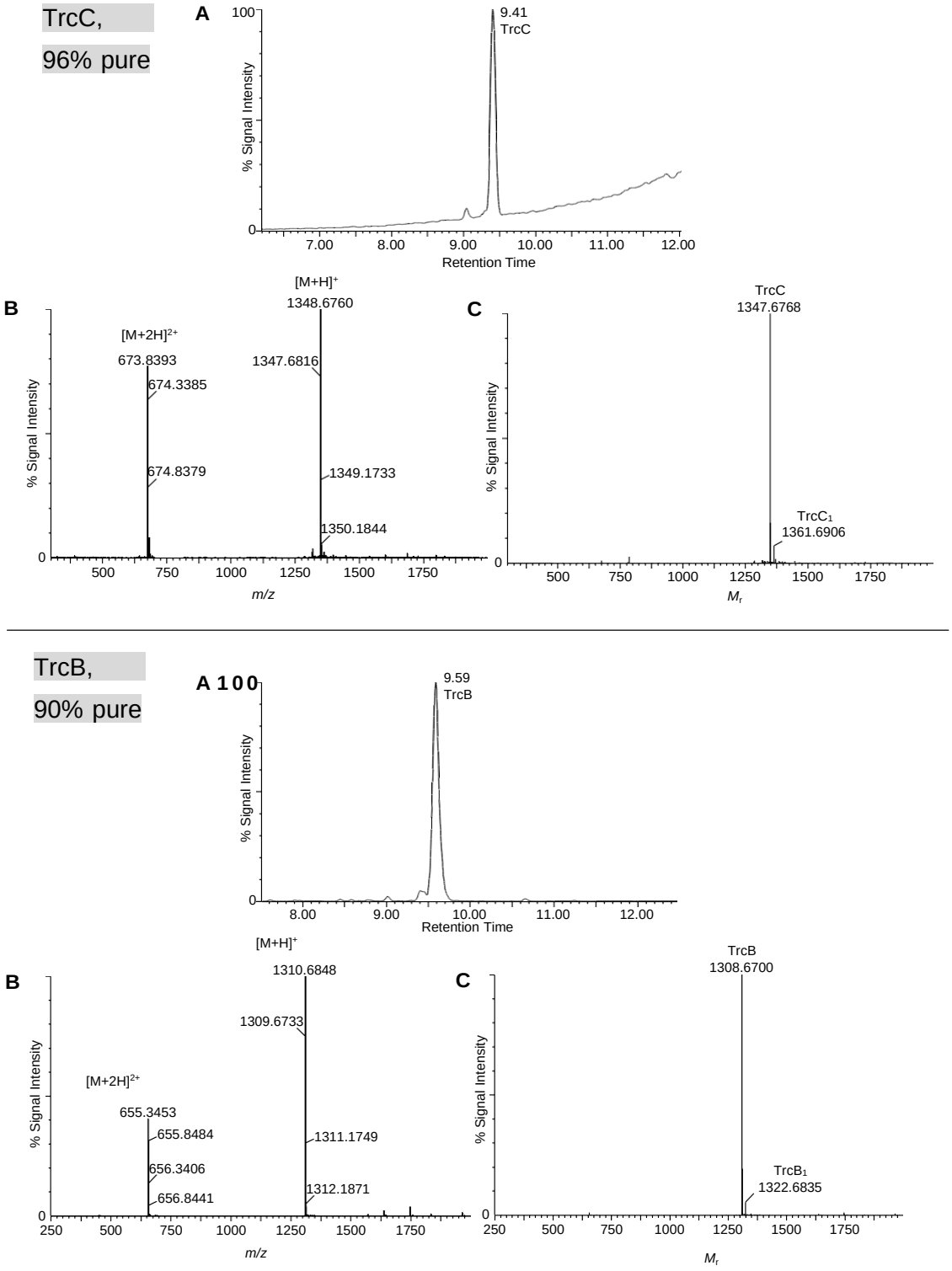

Figure 2.9. UPLC-MS results of the purified peptides with **A.** the UPLC profile of the purified peptide. **B.** ESMS positive ion spectrum of the major peak indicating singly charged molecular ions $[M+H]^+$ and doubly charged molecular ions $[M+2H]^{2+}$ and **C.** the MaxEnt 3 generated mass spectrum showing the peptide monoisotopic M_r.

Figure 2.9. Continued

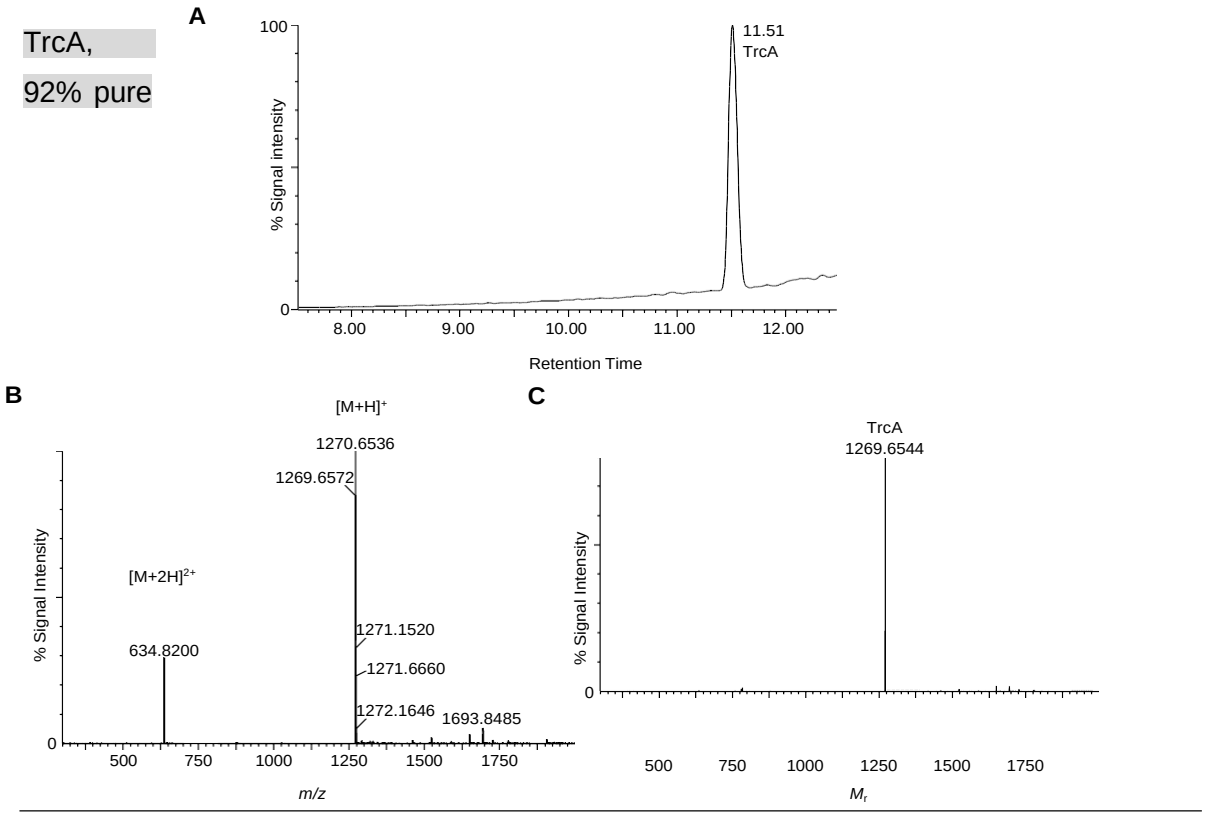

Figure 2.9 Continued

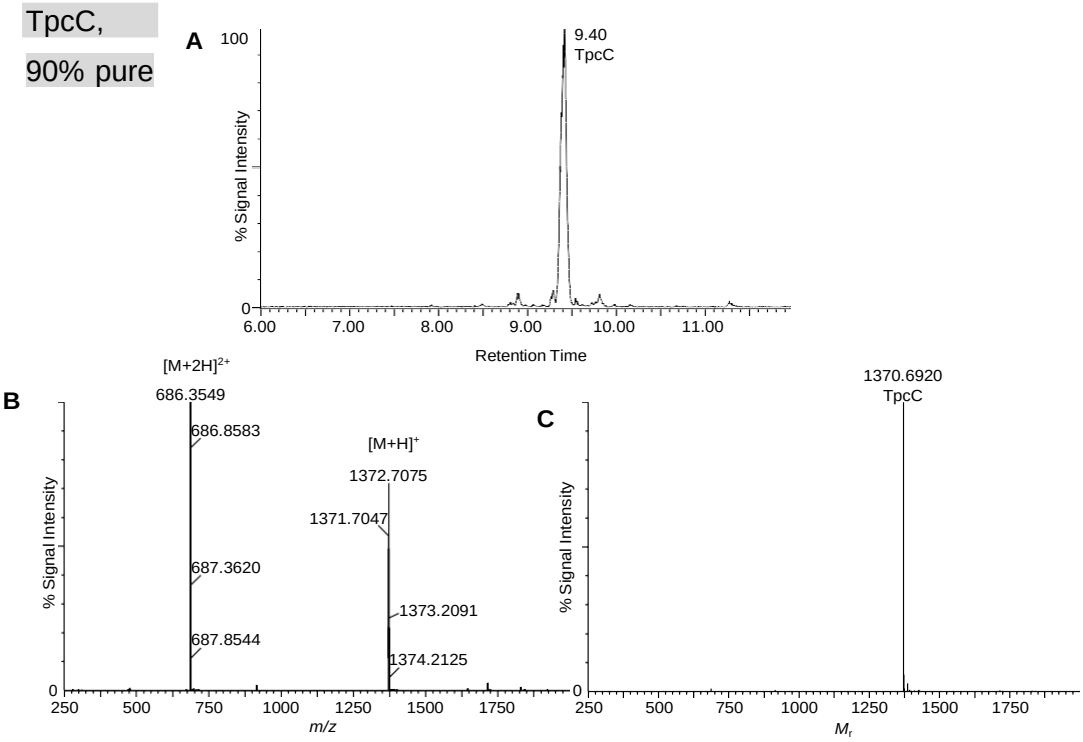

Mass spectrometric analyses revealed that all five single analogues of Trcs have a high tendency of forming singly and doubly charges species which is due to the single and double protonation of the peptide (Figure 2.9). It is clear from the mass spectrometry analysis that the five Trcs analogue that were purified are of high purity with expected M_r (Figure 9.2, Table 2.10).

Table 2.10 Summary of the purified peptides in this study.

Peptide identity	Source of extraction	HPLC fraction	Mass (mg)	M_r (Exp) (ppm) [a]	UPLC Rt (minute)	Purity (%)[b]
TrcA	F-sup/Trc mix	f	10.3	0.1	11.51	92
TrcB	Un-sup/Trc mix	d	1.4	-3.5	10.24	90
TrcC	Un-sup	a	1.6	-0.3	9.41	96
TpcB	W-sup	e	2.6	-1.9	10.22	94
TpcC	W-sup	d	4.2	0.3	10.70	90

[*] F-sup, W-sup and un-sup depicts Phe, Trp and non-supplemented cultures, respectively.
[a] Experimental monoisotopic mass was determined by ESMS and the MaxEnt3 algorithm of each peptide.
[b] % Purity was calculated by expressing the peak area of each peptide as a percentage of the sum of the UPLC-MS peak areas of all compounds present in the extract. It was assumed that the response factors of all peptides are similar due to their analogue structure.

2.5 Conclusion

Trcs tend to self-assemble at high concentrations and over time which severely complicates the RP-HPLC purification of these closely related cyclodecapeptides. Aggregation results in inconsistent retention and peak broadening of different Trc analogues during the RP-HPLC purification. Regardless of these aggregation issues, five single analogues, TrcA, TrcB, TrcC TpcB and TpcC, with the purity of above 90% were successfully isolated from the tyrothricin complexes produced by *Br. parabrevis* and commercial tyrothricin complex. The supplementation of the *Br. parabrevis* culture broths with 20 mM Phe and 10 mM Trp shifted the production towards TrcA and TpcC, respectively. This correlated with previous studies by Vosloo *et al*. [20]. Furthermore, UPLC-ESMS showed the presence of minor Lys containing analogues, $TrcA_1$, $TrcB_1$ and the rare $PhcA_1$, Orn containing including Tpcs (TpcA, TpcB, TpcC) and Trcs (TrcA, TrcB, TrcC) in crude culture extracts. The effect of supplementation on the Trp-rich Grms was to be expected with 10 mM Trp-supplementation increasing Grms production, in contrast to 20 mM Phe-supplementation decreasing Grms production. The reason for this is probably the high Phe concentration promoting Phe-containing Trc synthesis, while the Trp-rich Trcs, Tpcs, and Grms being compromised. Although supplementation eased the isolation of single Trc analogues, it had a negative effect on the amount of peptide being produced, compared to the non-supplemented extract which was higher than the Trp/Phe-supplemented extracts.

The four purification steps on the crude extracts resulted in the removal of linear Grms and non-peptide material, however, the peptide yield decreased drastically after each step of purification due to the loss of Trcs, some analogues were lost more than others. The major Trc analogues in the extract change drastically after the polishing step and more so after the DEE-acetone precipitation step. For example, TrcB was the major analogue after organic solvent extraction, while TrcA was the major analogue when the extract went through all four steps. The DEE-acetone precipitation step resulted in the removal of all linear Grms from the tyrothricin complex, however, it caused major Trcs analogue loss with TrcA being the major lost peptide during this step. It can be concluded that care must be taken as some rare analogues can be lost during these purification steps.

The isolated Trc single analogues will be used in a formulation study with a focus to improve their selectivity towards *Candida albicans* and *Candida glabrata* reported *in* Chapter 5. Furthermore, the effect of the formulants consisting of cellulose derivatives on the self-assembly of pure Trcs and Tpcs will be reported.

2.6 References

1 Rautenbach, M., Troskie, A. M., and Vosloo, J. A. (2016) Antifungal peptides: To be or not to be membrane active*. Biochimie 130*, 132–145.

2 Hotchkiss, R.D., and Dubos, R. J. (1941) The isolation of bactericidal substances from cultures of *Bacillus brevis*. *J. Cell*. *Biol. 141*, 155-162.

3 Dubos, R. J. (1939) Studies on a bactericidal agent extracted from a soil *Bacillus*: III Preparation and activity of a protein-free fraction. *J. Exp. Med*. *70*, 249–256.

4 Rautenbach, M., Vlok, N. M., Stander, M., and Hoppe, H. C. (2007) Inhibition of *malaria* parasite blood stages by tyrocidines, membrane-active cyclic peptide antibiotics from Bacillus brevis. *Biochim. Biophys. Acta Biomembr*. *1768*, 1488–1497.

5 Leussa, N. A. (2014) Characterisation of small cyclic peptides with anti-*listerial* and anti-*malarial* activity. PhD Thesis, Department of Biochemistry, University of Stellenbosch, Stellenbosch, South Africa, http://hdl.handle.net/100191/86161

6 Troskie, A. M., de Beer, A., Vosloo, J. A., Jacobs, K., and Rautenbach, M. (2014) Inhibition of agronomically relevant fungal phytopathogens by tyrocidines, cyclic antimicrobial peptides isolated from *Bacillus aneurinolyticus. Microbiology*. *160*, 2089–2101.

7 Rautenbach, M., Troskie, A. M., Vosloo, J. A., and Dathe, M. E. (2016) Antifungal membranolytic activity of the tyrocidines against filamentous plant fungi. *Biochimie 130*, 122–131.

8 Troskie, A. M., Rautenbach, M., Delattin, N., Vosloo, J. A., Dathe, M., Cammue, B. P. A., and Thevissen, K. (2014) Synergistic activity of the tyrocidines, antimicrobial cyclodecapeptides from *Bacillus aneurinolyticus*, with amphotericin B and caspofungin against *Candida albicans* biofilms. *Antimicrob. Agents Chemother*. *58*, 3697–3707.

9 Brewer, D., Hunter, H., and Lajoie, G. (1998) NMR studies of the antimicrobial salivary peptides histatin 3 and histatin 5 in aqueous and nonaqueous solutions. *J. Cell. Biol*. *76*, 247–256.

10 Dubos, R. J., and Hotchkiss, R. D. (1941) The production of bactericidal substances by aerobic sporulating *bacilli*. *J. Exp. Med*. *73*, 629–640.

11 Vosloo, J. A., Stander, M. A., Leussa, A. N. N., Spathelf, B. M., and Rautenbach, M. (2013) Manipulation of the tyrothricin production profile of *Bacillus aneurinolyticus*. *Microbiology. 159*, 2200–2211.

12 Tang, X. J., Thibault, P., and Boyd, R. K. (1992) Characterisation of the tyrocidine and gramicidin fractions of the tyrothricin complex from *Bacillus brevis* using

liquid chromatography and mass spectrometry. *Int. J. Mass Spectrom. 122*, 153–179.

13 Dorsey, J. G. (1996) Liquid chromatography: Theory and methodology *Anal. Chem. 68,* 515-568

14 Wheeler, J. f. (1993) Phase-transitions of reversed-phase stationary phases-cause and effects in the mechanism of retention. *J. Chromatogr. 656*, 317-333

15 Tchapala, a. (1993) General view of molecular interaction mechanisms in reversed-phase liquid chromatography. *J. Chromatogr. 656*, 81-112

16 Hufmer, A. F. (1997) separation and analysis of peptides and protein*. Anal. Chem. 69,* 29R-57R

17 Veenstra, T. D. (1999) electrospray ionization mass spectrometry: A promising new technique in the study of protein/DNA noncovalent complex *Biochem. Biophys. Res. Commun. 257*, 1-5

18 Jonscher, K. R., and Yates, J. R., (1997) The quadropole ion trap mass spectrometer-a small solution to a big challenge. *Anal. Chem 245,* 1-15

19 Allen, D. R, and McWhinney, B. C. (2019) Quadrupole Time-of-Flight Mass Spectrometry: A paradigm shift in toxicology screening applications. *Clin Biochem Rev. 40,* 135-146

20 Vosloo, J. A. (2016) Optimised bacterial production and characterisation of natural antimicrobial peptides with potential application in agriculture. Ph.D. Thesis, Department of Biochemistry, University of Stellenbosch. http://hdl.handle.net/10019.1/98411

21 Eyéghé-bickong, H. A. (2011) Role of surfactin from *Bacillus subtilis* in protection against antimicrobial peptides produced by *Bacillus* species. Ph.D. Thesis, Department of Biochemistry, University of Stellenbosch. http://hdl.handle.net/10019.1/6773

22 Paladini, A., and Craig, L. C. (1954) The chemistry of tyrocidine. III. The structure of tyrocidine A. *J. Am. Chem. Soc. 76*, 688–692.

23 Breslow, R., and Chipman, D. (1964) The use of tyrocidines for the study of conformation and aggregation behaviour. *J. Am. Chem. Soc. 55*, 4195–4196.

24 Spathelf, B. M. (2010) Qualitative structure-activity relationships of the major tyrocidines, cyclic decapeptides from *Bacillus aneurinolyticus*. Ph.D. Thesis, Department of Biochemistry, University of Stellenbosch, http://scholar.sun.ac.za/handle/10019.1/4001

25 Troskie, A. M. (2013) Tyrocidines, cyclic decapeptides produced by soil *bacilli*, as potent inhibitors of fungal pathogens. Ph.D. Thesis, Department of Biochemistry, University of Stellenbosch, http://hdl.handle.net/10019.1/86162

Chapter 3

The influence of formulants on anti-*Candida* activity of the tyrocidine complex

3.1. Introduction

Tyrocidines are small cyclic antimicrobial peptides with proven anti-*Candida* activity [1]. These molecules are well-known for forming a variety of oligomeric structures, especially in aqueous environments [2, 3]. The activity of the tyrocidines is proposed to be dependent on their oligomerisation profile [2, 3, 4]. Modification of a peptide's amphipathicity, hydrophobicity, and conformational flexibility in solution, either via chemical modification or conformational changes due to specific interactions with media components or oligomerisation, can influence the peptide's activity [5, 6, 7]. It is therefore hypothesised that formulation of tyrocidines could alter their conformation, oligomerisation, and biological activity [3].

In this study, the tyrocidine peptide complex or tyrocidine mixture (Trc mix) was formulated with cellulose derivatives to limit the formation of large Trc oligomers [8, 9], therefore allowing peptide, specifically dimers, to act on the target organism which would enhance the overall biological activity. Formation of big aggregates/oligomers would result in the loss of peptide activity due to the loss of peptide from solution and possibly the loss of dimeric peptide that is proposed to be the active structures [7, 8]. Most of the dimeric structures, which were found by Munyuki *et al*. [8] via a modelling study, retain their amphipathic properties allowing interaction and destabilising of the target cell membrane [2, 7, 8, 9].

Six different cellulose derivatives and soluble chitosan were used to formulate of the Trc mix. In addition to A4M and E4M formulant of pure TrcA and A4M formulant of TpcC. All cellulose derivatives formulants utilised in this study have a cellulose backbone with different modifications including, methyl, propyl, and hydroxyl groups (Table 3.1). The activity of the formulations and peptides was tested against *Candida albicans* (*C. albicans*) and *Candida glabrata (C. glabrata)* and human erythrocytes for toxicity. To compare the activity of Trcs with the antifungal drugs, caspofungin and fluconazole, the % metabolic inhibition of *C. albicans* was compared with that induced by Trc mix and its cellulose-type formulations.

Table 3.1. Summary of commercial modified cellulose and saccharide derivatives utilised as formulants for the tyrocidine mixture (Trc mix) in this study. The colours in this table will be used to aid the identification of formulants in Chapters 3 and 4.

Saccharide derivative	Commercial ID abbreviation	Modification	Viscosity cps	Colour code*
Methyl-cellulose	A4M	$-CH_3$	3500-5600	
Hydroxy-propyl-methyl- cellulose	E4M	$-CH_2OH$/ $-CH_2CH(OH)CH_3$	2700-5040	
Hydroxy-propyl-methyl- cellulose	E10M	$-CH_2OH$/ $-CH_2CH(OH)CH_3$	7500-14000	
Hydroxy-propyl-cellulose	KLUE	$-CH_2OH$	200-600	
Hydroxy-propyl-cellulose	KLUL	$-CH_2OH$	75 - 150	
Chitosan	CHS	-	Not available	
Hydroxy-propyl-methyl-cellulose	K15M	$-CH_2OH$/ $-CH_2CH(OH)\ CH_3$	10000-18000	

* The colour code was used in all graphs to ease the comparative interpretation

3.2. Materials

Commercial tyrothricin extract was supplied by Sigma-Aldrich (St Louis, USA). Trc mix was extracted from commercial tyrothricin using an optimised diethyl ether and acetone precipitation protocol [10]. Ethanol (EtOH), diethyl ether (DEE), and acetone were supplied by Merck (Darmstadt, Germany). Tyrocidine a (TrcA) and tryptocidine C (TpcC) were purified to >95% from Trc mix and *Brevibacillus parabrevis* culture extracts (refer to Chapter 2 for more details on purification). Chitosan, gramicidin S (GS), fluconazole and caspofungin was purchased from Sigma-Aldrich (St Louis, USA). Analytical grade water (MQH_2O) was prepared by filtering water from a reverse osmosis plant through a Millipore-Q® water purification system (Milford, USA). The 96-well black and transparent flat-bottom plates were supplied by Thermo Fisher Scientific (Denmark). Benecel A4M (A4M), Benecel E4M (E4M), Benecel E10M (E10M), Benecel K15M (K15M) Klucel E IND (KLUE), Klucel I IND (KLUI) were donated by ASHLAND, Covington, Kentucky America. Sterile Petri dishes were obtained from Lasec (South Africa) and Falcon tubes were supplied by Becton Dickson Labware (Lincoln Park, USA). Agar, sodium chloride, hydrochloric acid, tryptone, and yeast extract were obtained from Merck (Darmstadt, Germany). RPMI 1640 medium was from Lonza (Walkersville, USA) and resazurin sodium salt was from Sigma Aldrich (St Louis, USA). Mixed cellulose syringe filters (0.22 µm) were purchased from Merck-Millipore (Massachusetts, USA). *C. albicans CAB1653,* an environmental isolate from the Western Cape, South Africa*,* was obtained from the culture collection of Prof. Alf Botha in the

Department of Microbiology, Stellenbosch University, South Africa. *C. glabrata BG19,* a clinical isolate, was donated by Dr Bahareh Bagheri, Tygerberg Medical School, Stellenbosch University, South Africa.

3.3. Methods

3.3.1 Culturing of *C. albicans* and *C. glabrata*

Yeast cells from freezer stocks of *C. albicans* and *C. glabrata* were plated onto YPD agar plates (yeast extract 1%, peptone 2% (*m/v)* agar, glucose 2% (*m/v)* agar, 1.5% *m/v* agar) using sterile culturing techniques and incubated for ±48 hours at 37°C. This was followed by the inoculation of a single representative colony in 20 mL YPD broth and maturation for 17 hours at 37°C on a shaker at 150 rpm. RPMI media was then used to subculture the yeast at a final cell concentration of $5.5x10^5$ cells/mL.

3.3.2 Preparation of formulations of Trc mix and purified peptides

Seven different cellulose derivatives were prepared to stock concentrations of 1.00, 2.00, and 4.00 mg/mL in MQH_2O. The sample solutions were then sonicated for ± 5 minutes allowing for a complete dissolution of the cellulose derivatives. The solutions were filter-sterilised using a 0.2 µm sterile filter. Trc mix, TrcA and TpcC were made up to the concentration of 1000 µg/mL in 15% (*v/v)* ethanol in MQH_2O. Trc mix and the formulants (cellulose derivatives) were mixed in varying ratios (1:1, 1:2, 1:4, *m/m*) and matured for 1 and 20 hours. TrcA and TpcC were formulated with A4M to 1:4 (*m/m*) ratio and TrcA was also formulated with E10M to 1:4 (*m/m*) ratio and matured for 1 and 20 hours. The formulations were mixed and incubated in a 96-well microtiter plate (dilution plate) and were serially diluted to the desired concentration. A 10 µL aliquot of the Trc mix formulations were transferred to another 96-well microtiter plate (assay plate) followed by the addition of 90 µL RPMI media containing *Candida* cell culture. Table 3.2 shows different formulants of Trc mix at 500 µg/mL in the stock solution were prepared with different ratios of cellulose derivatives.

Table 3.2. Summary of the preparation parameters for different Trc mix formulants assaystudies targeting two *Candida* species.

	Formulants	Trc mix: formulant Ratio (*m/m*)	Final concentration of the formulant (µg/mL)	Target organism
1 hour of maturation	Water	-	500	*C. albicans*
	A4M	1:1	500	
	E4M	1:1	500	
	E10M	1:1	500	
	KLUE*	1:1	500	
	KLUI*	1:1	500	
	CHS*	1:1	500	
	K15M	1:1	500	
20 hours of maturation	Water	-	500	*C. albicans*
	A4M	1:1	500	
	E4M	1:1	500	
	E10M	1:1	500	
	K15M	1:1	500	
1 hour of maturation	A4M	1:2	1000	*C. albicans*
	E4M	1:2	1000	
	E10M	1:2	1000	
	K15M	1:2	1000	
20 hours of maturation	A4M	1:2	1000	*C. albicans*
	E4M	1:2	1000	
	E10M	1:2	1000	
	K15M	1:2	1000	
1 hour of maturation	A4M	1:4	2000	*C. albicans*
	E4M	1:4	2000	
	E10M	1:4	2000	
	K15M	1:4	2000	
20 hours of maturation	A4M	1:4	2000	*C. albicans* and *C. glabrata*
	E4M	1:4	2000	
	E10M	1:4	2000	
	K15M	1:4	2000	

*Activity was measured at selected concentrations of Trc mix

GS, caspofungin and fluconazole, as known antifungal controls were made up to 1000 µg/mL and were serially diluted to the desired concentration, with 10 µL added to the 90 µL *C. albicans* culture to a 96-well plate. The rest of the procedure was followed as above.

3.3.3 Metabolic inhibition anti-*Candida* assay

Planktonic *Candida* cultures, exposed to Trc mix, pure TrcA and pure TpcC and their formulations, as well gramicidin S, caspofungin and fluconazole, were incubated for 24 hours at 37 °C and 90% humidity in 96-well microtiter plates. This was followed by the addition of 10 µL resazurin reagent (0.30 mg/mL) to each well and further maturation of 90 minutes for *C. albicans* and four hours for *C. glabrata* (at 37 °C). The inhibition of metabolic activity was determined by measuring fluorescence emission of the metabolic dye using the Tecan Spark 10M Multimode Microplate Reader. Excitation and emission wavelengths were set at 560 nm and 590 nm (Em590), respectively. The measured fluorescence was converted to % inhibition of metabolism as described by the following equation:

$$\%\ \text{metabolic inhibition} = 100 - \frac{100\text{X}\ (Em590\ \text{of well} - mean\ \text{of}\ Em590\ \text{of}\ blank)}{(mean\ \text{of}\ Em590\ \text{of}\ growth\ metabolism - mean\ \text{of}\ Em590\ blank)}$$

The negative control (0% metabolic inhibition) was cell cultures treated with 1.5 % ethanol and the background (blank) was RPMI medium containing no cells and only the solvent control.

3.3.4 Data analysis of metabolic inhibition assay

Dose-response assays were done using three to four individual starter cultures, each divided into eight to twenty sub-cultures. All data analysis was performed using GraphPad Prism® V 5.0 software (San Diego, CA, USA). Non-linear regression to calculate the inhibition parameters utilised sigmoidal curves with variable slope (Hill slope constrained to less than 7) were fitted to the dose-response data using the following equation:

$$y = \frac{bottom + (top - bottom)}{1 + 10^{\log IC_{50}\ \text{x activity}\ slope}}$$

The top and bottom of the curve represent the percentage metabolic inhibition at the highest and lowest concentrations of different formulants of Trc mix, respectively. Using the method described by Rautenbach *et al.* [11], MIC (minimum metabolic inhibition concentration), IC_{50} (concentration that gives 50% metabolic inhibition) of the *Candida* species exposed to Trc mix and its formulations were determined.

3.3.5 Haemolytic toxicity

The assays were performed by Dr. W. van Rensburg (Stellenbosch University) and the methodology is described in brief. Packed erythrocytes from a consenting anonymous A+ donor was obtained adhering to the relevant ethics and legislation. The haemolysis assays were done according to Rautenbach *et al*.[12] with a few adaptations. Trc mix formulations 1:4 (*m/m*) with the different saccharides were prepared in class vials as above and 10.0 μL of doubling dilutions, starting at 500 μg/mL, were transferred to a 96-well plate. Washed erythrocytes in RPMI media at 1% haematocrit (100 μL) were then added to each well and incubated at 37°C for 2 hours. The plates were then centrifuged (900×*g* for 10 minutes) to remove the intact erythrocytes. An aliquot of 10 μL of each well's supernatant was transferred to a 96-well plate containing 90 μL phosphate buffered saline. The released haemoglobin of the lysed erythrocytes was measured at 415 nm using a BioRad Model 680 Microplate reader. The haemolytic toxicity was calculated using the following equation:

$$\%\ \text{Haemolytic activity} = 100 \times \frac{Abs\ \text{of}\ sample\ - mean\ \ Abs\ \text{of}\ background}{mean\ Abs\ \text{of}\ \ fully\ lysed - mean\ \ Abs\ \ \text{of}\ background}$$

The full lysis was determined with 10 μg gramicidin S, translating to 100 μg/mL in the assay in the lysis control wells. The negative control (background, 0% lysis) were erythrocytes in RPMI medium.

3.4. Results and discussion

This chapter aimed to find the best cellulose derivative as formulants for Trc mix, with a specific focus to obtain with the highest potency and specificity against *C. albicans* and *C. glabrata.* To achieve this aim, anti-*Candia* activity assays were performed on the various Trc mix formulation. Furthermore, fluorescence assays were performed on the most active formulants of Trc mix to investigate the effect of cellulose derivatives and maturation time on oligomerization profile of Trc mix which will be reported in chapter four.

3.4.1 Assessing formulations of Trc mix targeting *C. albicans*

To assess the activity of Trc mix in water containing 1.5% ethanol as control formulation. The activity of the Trc mix remained relatively constant between12.5- 25 μg/mL when we considered only the MIC as inhibition parameter (Figure 3.1A), but when the full dose-response was considered the activity was variable (Figure 3.1B). At the low Trc mix concentrations, the *Candida* cells were metabolically stressed and showed high metabolic

activity detected as “negative” inhibition (Figure 3.1B). At medium, to high concentration 6.25-25 μg/mL there was a variable response that could be the consequence of the *Candida* response and the variable oligomerisation of the peptides in the control preparations [2] (Figure. 3.1B).

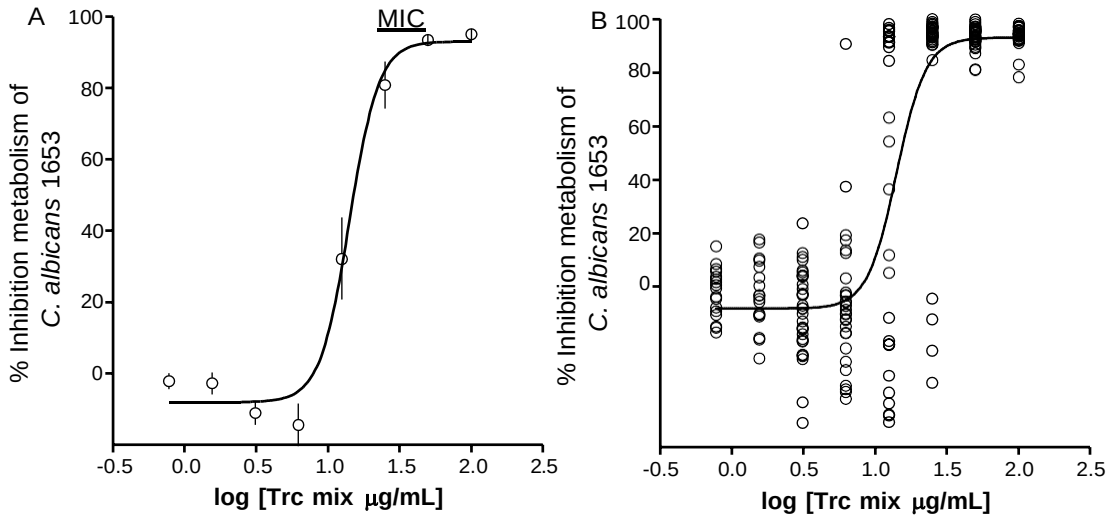

Figure 3.1. The combined dose-response showing the activity Trc mix against *C. albicans* with [Trc mix] ranging from 100 μg/mL to 3.125 μg/mL. The dose response curve in A was fitted to the 220 determinations from 11 biological repeats and 33 dose response ranges shown in B. All data points are shown in B with the average of 33 data points at each concentration and standard error of the mean is (SEM) shown in A.

These results not only emphasised the importance of multiple biological repeats to get reliable data but also how important the stability of Trc mix preparation can be. To improve the Trc mix preparation, eight different of Trc mix preparations were prepared, namely, six formulations combined with commercial cellulose derivatives, one with chitosan and the control with Trc mix in 1.5% EtOH in water (*m/v*). The anti-*Candida* activity was measured for three concentrations to assess the data variability and facilitate the selection of the best formulant to stabilise the Trc mix. The three concentrations used were deduced from the full dose-response using Trc mix control preparation (Figure 3.1A). The selected concentrations were chosen as 50.0 μg/mL as it was the MIC* of Trc mix, 12.5 μg/mL as it is the approximate highest $IC_{50,}$ and the Trc mix MIC at 25.0 μg/mL*.

An exploratory experiment was designed to investigate the influence of cellulose derivatives on Trc mix potency against *C. albicans* cells, with the selected concentrations of Trc mix: cellulose derivatives at 1:1 *(m/m)* ratio. Figure 3.2 shows the metabolic inhibition caused by different formulants of Trc mix at three different concentrations. The culture survival data from Figure 3.2 has been summarised in Table 3.3. We equated the lack of conversion of

the metabolic dye resazurin to resorufin as cell death, while survival was equated to the conversion in our assay.

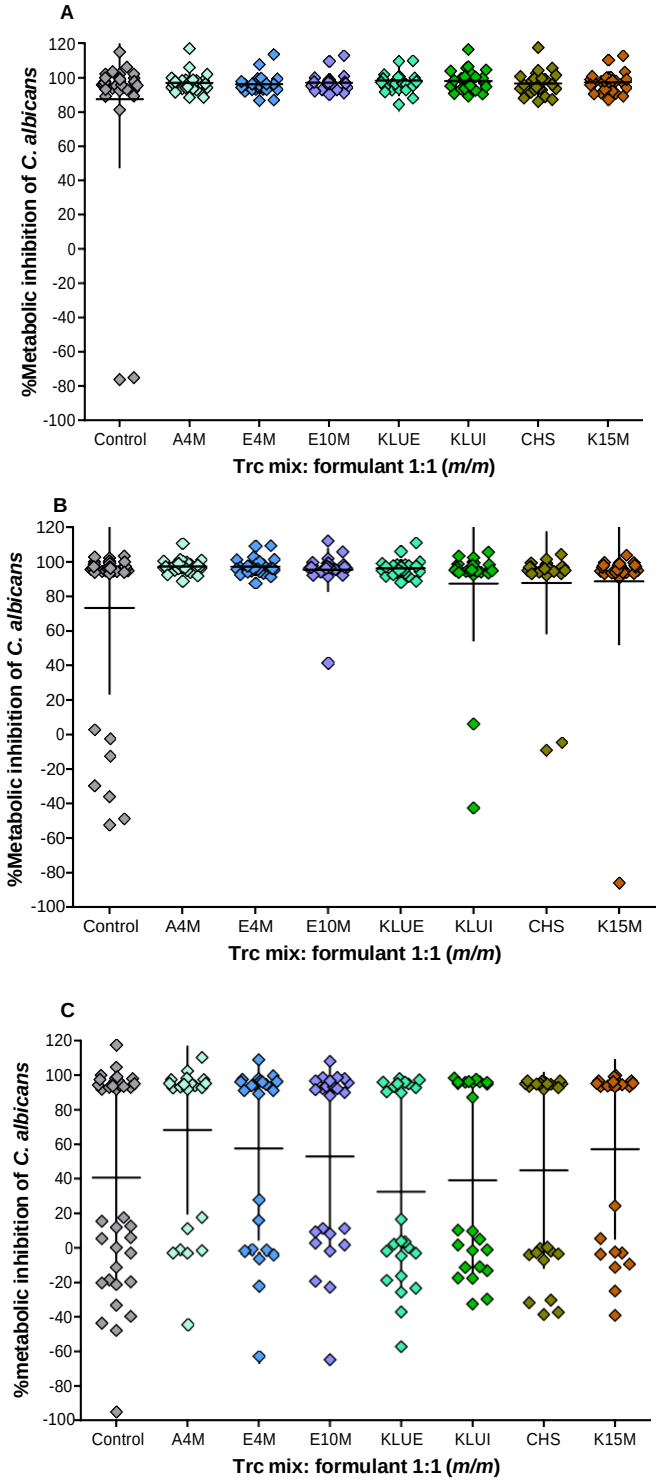

Figure 3.2. Metabolic inhibition of *C. albicans* cultures treated by **A.** 50 µg/mL formulated Trc mix, **B.** 25 µg/mL formulated Trc mix, and **C.**12.5 µg/mL formulated Trc mix. Each data point represents one culture. The mean %metabolic inhibition is shown for each condition with standard deviation (SD).

At Trc mix of 50.0 µg/mL, 100% inhibition of metabolism for the seven different Trc mix preparations were obtained, with the control showing 2/36 cultures that survived the treatment (Figure 3.2A**)**. It is hypothesised that the survival of some treated cultures may be due to the presence of persister cells [12]. This result suggests that the formulated Trc mix at 50 µg/mL is sufficient to eradicate persister and normal population of *C. albicans*, while Trc mix on its own only inhibited the normal population of *C. albicans*, and it was less effective or ineffective against these so-called persister cells.

At 25.0 µg/mL Trc mix shows some scatter of data with the negative inhibition values, therefore only metabolic stress was induced (Figure 3.2B**)**. It was calculated that 4-25% of cultures survived some of the treatments (Table 3.3), but the cells in these cultures were stressed which increased their metabolism and conversion of resazurin to resorufin. The Trc mix control preparation showed the most scatter and culture stress (19% survival), while there was no survival or 4-8% survival of cultures in the saccharide formulations, indicating saccharide formulants did enhance the anti-*Candida* activity of Trc mix.

Table 3.3. Survival (%) of 24 cultures after exposure to Trc mix and its formulations with a variety of saccharides at the three selected concentrations.

Peptide's formulants	Trc mix 50µg/mL	Trc mix 25µg/mL	Trc mix 12.5µg/mL
Control	0.6*	19*	50*
A4M	0	0	29
E4M	0	0	37
E10M	0	4	42
KLUE	0	0	58
KLUI	0	8	54
CHS	0	8	46
K15M	0	4	37

* 36 cultures were treated for the control

We observed the most stressed cells at the lowest concentration of 12.5 µg/mL Trc mix in the preparations, and 29-58% survival (Figure 3.2C, Table 3.3). Cultures treated with Trc mix formulated by cellulose derivatives with lower viscosity such as KLUE and KLUL, in addition to CHS show the highest survival meaning these cellulose derivatives did not enhance the activity of Trc mix at this concentration. The formulations of Trc mix at 12.5 µg/mL in A4M and E4M followed by E10M and K15M, exhibiting the same or better activity than the control preparation, were selected for further investigation (Figure 3.2 C).

3.4.2 Optimising the formulation of Trc mix

Formulation of Trc mix with A4M, E4M, E10M, and K15M enhanced the Trc mix activity as shown in Table 3.3 and Figure 3.2. To further assess these formulations full dose-response assays were performed. Trc mix was formulated with cellulose derivatives at 1:1 (*m/m*) ratio, as well as increased ratios of Trc mix: cellulose derivatives at 1:2 and 1:4 (*m/m*) ratio. The formulations were also allowed to mature over time for 1 hour (assumed as fresh) and 20 hours (matured formulation). Furthermore, the best ratio and maturation time of the formulation components were selected to be tested against another species of *Candida,* namely *C. glabrata.* Table 3.4 gives a summary of the representative dose responses and comparative IC_{50} and MIC, values. Statistical comparison between IC_{50} and MIC values of Trc mix (matured for 1 and 20 hours) and IC_{50} and MIC values of formulated Trc mix are summarised in the supplementary tables S1 to S4. From the Unpaired student t-test of fresh versus matured preparation pairs indicated that there were significant differences for the Trc mix alone as well as some of the 1:1 and 1:2 (*m/m*) formulations, showing that the formulation ratio and time have an influence on the activity (Table S1 and S2). When all the datasets were compared using One-way Anova with Bonferroni correlation test, we found fewer differences as this statistical method considers all the variability over this large dataset (Tables S3 and S4). This, however, indicated that the activity of Trc mix was preserved in these formulations.

At specific ratios of formulated Trc mix in the cellulose derivatives, we observed significantly smaller IC_{50} values and/or MIC values (Table 3.4, Tables S1-S4). Depending on the concentration and the ratio, the cellulose derivatives enhance or support the activity of the Trc mix. From this E4M and E10M was revealed as two of the best formulants of Trc mix. MIC and IC_{50} values of formulated Trc mix by E10M at 1:1 and 1:4 ratios and E4M at 1:1 and 1:2 ratios were consistently lower than 10 μg/mL regardless of the maturation time.

Matured Trc mix (20 hours of maturation) had statistically lower IC_{50} and MIC values than fresh Trc mix preparations (1 hour of maturation) (Table 3.4, Tables S1 and S2). Longer maturation of the preparations was observed to generally enhance the activity of the Trc mix and the formulations if data pairs are considered (Tables S1 and S2).

Table 3.4. Comparative activity data of formulated Trc mix targeting *C. albicans and C. glabrata*, Bar-graphs show the IC_{50} and MIC in µg/mL against *C. albicans and C. glabrata*. Errors bars represent SEM for a minimum of three biological and six technical repeats. The average MIC and IC_{50} in µg/mL are shown above each bar. Refer to tables S1-4 for details and statistical comparisons.

Trc-mix: formulant ratio (*m/m)*	Fungal target	Comparison of IC_{50} and MIC values
		1-hour maturation (fresh)
1:1	*Candida albicans*	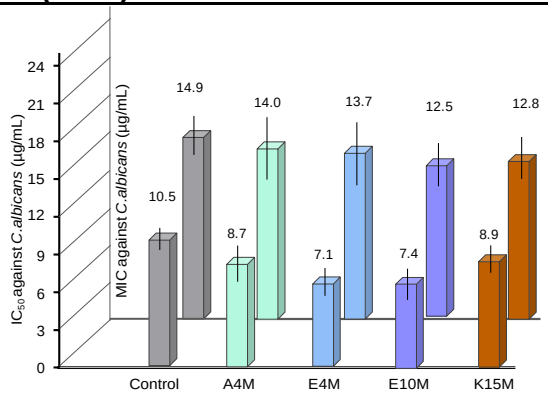
1:2	*Candida albicans*	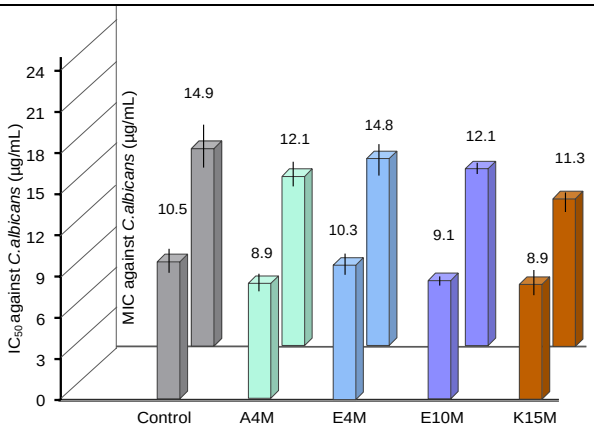
1:4	*Candida albicans*	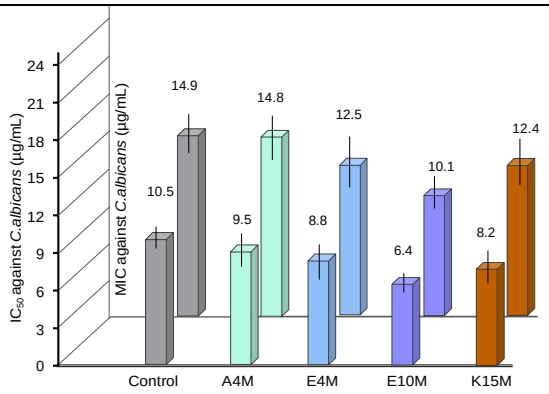

Table 3.4 Continued

Trc-mix: formulant ratio (m/*m*)	Fungal target	Comparison of IC_{50} and MIC values
		20-hours maturation (matured)
1:1	*Candida albicans*	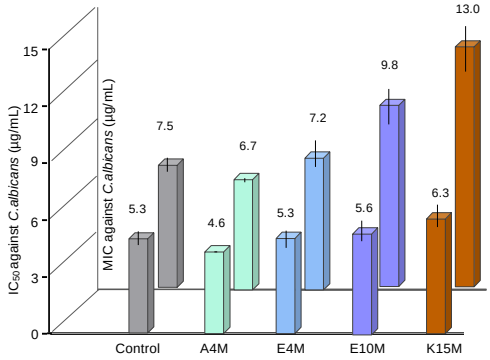
1:2	*Candida albicans*	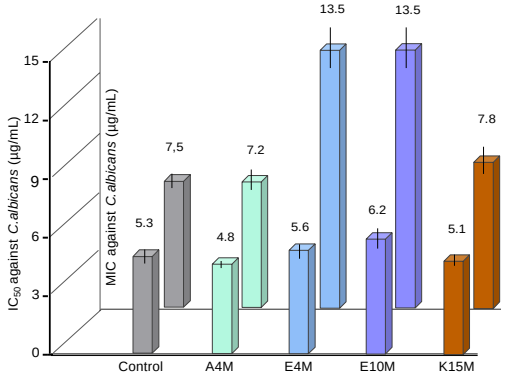
1:4	*Candida albicans*	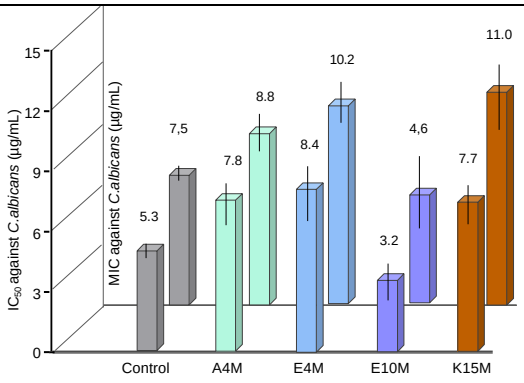
1:4	*Candida glabrata*	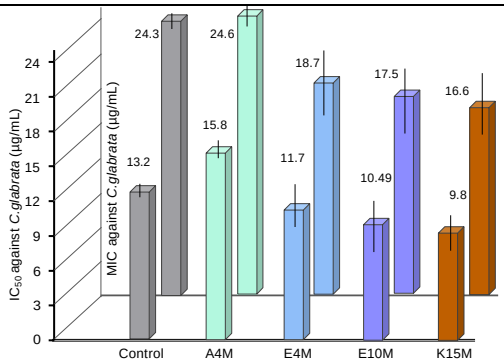

3.4.3 The effect of cellulose derivatives on Trc mix anti-*C. glabrata* activity

The four most promising formulations were also tested against a second *Candida* specie, namely *C. glabrata* at the same cell density as *C. albicans*. In general, MIC and IC_{50} values of 20-hour matured Trc mix preparations against *C. glabrata* were statistically higher than *C. albicans* except for E4M and K15M preparations (Table 3.2, Figure 3.3).

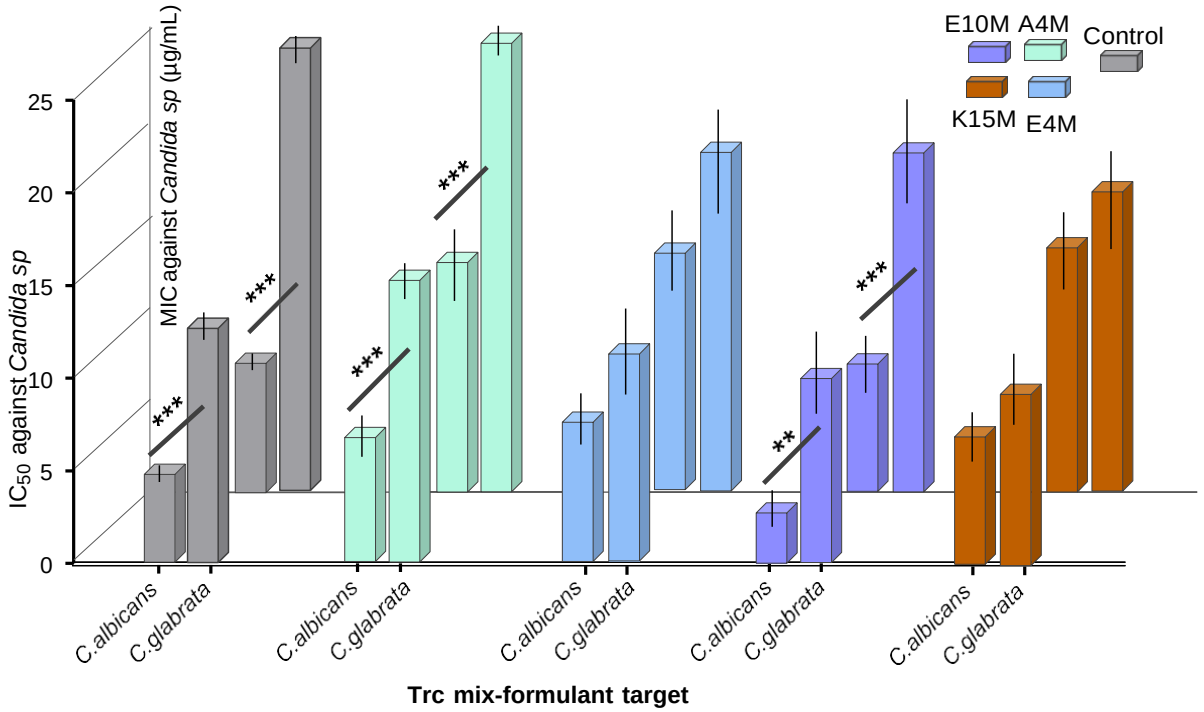

Figure 3.3. Comparison of the IC_{50} µg/mL against *C. albicans* and *C. glabrata* of 20 hour matured preparations (1:4 ratio). Data represent the mean of 3 biological repeats and 6-14 technical repeats with SEM. Unpaired Student t-test was done on each of the analysed groups, with ** P<0.01 and ***P<0.001.

Trc mix and Trc mix formulated with A4M and E10M had significantly smaller IC_{50} values when targeting *C. albicans*, than IC_{50} values against *C. glabrata.* As different target cells have different growth rates, differences in MIC or IC_{50} values are to be expected. Interestingly, the activity of K15M and E4M preparations of the Trc mix was observed to be similar against the two strains of *Candida*. This is an indication that the formulation modulated the activity to a point that different growth or different organisms had a minor influence.

3.3.4 The effect of cellulose derivatives on Trc mix haemolytic activity

When we considered the haemolytic activity of the different formulations, there was no clear distinction between the different formulations. All of the 1:4 *(m/m)* formulations showed similar haemolytic toxicity than the Trc mixture alone (Figure. 3.4). This implies that the formulation

with the cellulose derivatives had a minor impact on the selectivity towards the erythrocyte membrane but did change the activity towards two *Candida* strains.

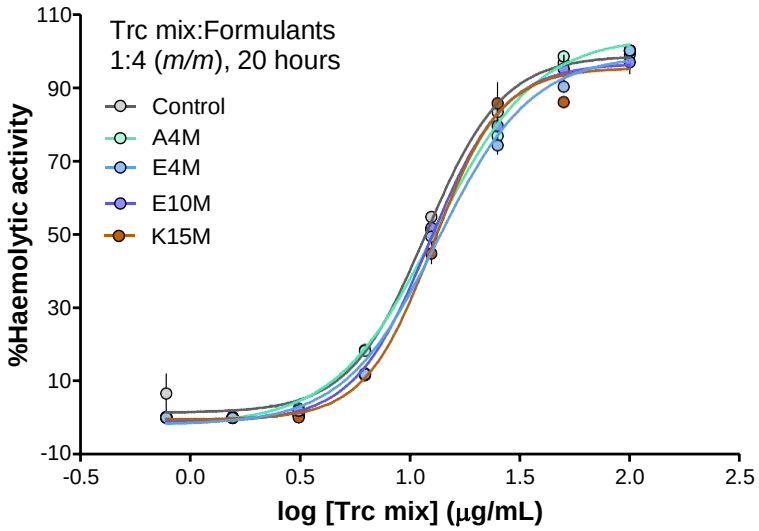

Figure 3.4. Comparison of the haemolytic activity against human erythrocytes of the 20 hours matured 1:4 Trc mix formulations. Data represent the mean of three biological repeats with SEM. Data is courtesy of W van Rensburg (Stellenbosch University).

3.3.5 Anti-*Candida* of purified TrcA and TpcC and their formulations

After testing the biological activity of different preparations of Trc mix, we investigated the anti-*Candida* activity of purified TrcA and TpcC. (Refer to chapter two for purification and isolation of Trcs single analogue).

Due to the time constraints and limited access to laboratory facilities during CoVID-19 lockdown, the focus was only on these two peptides and two cellulose formulants, A4M and E4M.

We chose one of the most hydrophobic (TrcA) and one of the most polar Trcs analogue (TpcC) to see whether formulation can improve the activity of these two analogues. As the hydrophobicity of the peptide depends on the identity of aromatic residues at positions 3, 4, and 7, TrcA containing two Phe is one of the most hydrophobic Trcs analogues, while TpcC containing three Trp is one of the most hydrophilic analogues. Previous research illustrated that Both TrcA and TpcC exhibit high activity against *Aspergillus fumigates* in addition to *C. albicans* [1, 13].

Therefore, the anti-*Candida* activity of TrcA and TpcC was determined and compared with that of Trc mix, and standard anti-fungal drugs available on market, the antifungal lipopeptide

caspofungin (an echinocandin [14]) and an antifungal azole, fluconazole [15]. The activity parameters are summarised in Table 3.5.

Table 3.5 Summary of the IC_{50} and MIC values of different preparations of the purified, peptides, selected formulations and two antifungal drugs against *C. albicans*. The n in brackets indicates the number of full dose responses.

		IC_{50}±SEM µM (n)		MIC±SEM µM (n)	
Formulant (Ratio, *m/m*)	Peptide or compound	Fresh, 1 hour	Matured, 20 hours	Fresh, 1 hour	Matured, 20 hours
1.5% EtOH	Trc mix	7.9±0.6(12)	4.0±0.2(12)	11.3±1.1 (12)	5.6±0.3 (12)
A4M (1:4)	Trc mix	7.2±0.9(12)	5.9±0.6(12)	11.2±1.2 (12)	6.6±0.6 (12)
E4M (1:4)	Trc mix	6.6±0.9(12)	6.3±0.8(12)	9.4±1.4(12)	7.7±1.3(12)
1.5% EtOH	TrcA	3.9±0.3 (9)	4.4±0.2 (17)	6.1±0.6 (9)	7.3±0.6 (17)
A4M (1:4)	TrcA	nd	5.4±0.5 (7)	7.8±0.0 (6)	7.0±0.7 (14)
E4M (1:4)	TrcA	nd	5.5±0.6 (5)	5±0.6 (6)	8.90±0.8 (5)
1.5% EtOH	TpcC	nd	10±1.1 (7)	22±3.2 (6)	22±2.7 (14)
A4M (1:4)	TpcC	nd	9.8±1.4 (4)	20±3.8 (4)	19.3±3.5 (9)
water	Caspofungin	nd	nd	>45.7 (6)	nd
water	Fluconazole	nd	nd	>326.5 (6)	nd

The concentration of the peptides from Trc mix was calculated from the average M_r of 1318 for the peptide complex as calculated from the peptide contribution in the Trc mix determined in Chapter 2.

TrcA has significantly lower IC_{50} and MIC values when compared to TpcC indicating a better overall antifungal activity of TrcA towards this environmental strain of *C. albicans* (refer to Table S5 in supplementary data). This correlates with results obtained by Troskie *et al*. [1]. The difference between the anti-*Candida* activities of the two analogues can be due to their difference in hydrophobicity, or that TrcA forms more active higher oligomers compared to TpcC. Furthermore, the difference in the activity of these two analogues can be due to the difference in the peptide sequence and structure. The fact that TrcA has two Phe residues in positions 3 and 4 instead of two larger and more polar Trp residues may result in higher activity. It has been shown that Phe has a higher affinity for lipid membranes and inserts itself deeper that Trp into target cell membranes [17, 18].

The anti-*Candida* activity of Trc mix and the purified TrcA and TpcC and selected formulations were compared with two antifungal drugs used in treatment for *C. albicans,* namely fluconazole and caspofungin (Table 3.5 and Figure 3.5). It is concerning that the *Candida* strain used in this study is fully resistant to fluconazole and resistant to caspofungin. Based on reported antifungal susceptibility testing of yeasts from standard clinical laboratories, MICs

higher than 64 and 2 µg/mL for fluconazole and caspofungin are considered resistant [19]. (Table 3.5). However, it is highly susceptible to TrcA and Trc mix. Fluconazole, caspofungin and the less active TpcC resulted in the induction of metabolic stress in the *Candida* cells as is illustrated in Figure 3.5. Resazurin is an oxidation-reduction (REDOX) indicator dye that undergoes a colorimetric change in response to cellular metabolic reduction [19]. Resazurin is a blue dye with low fluorescence and its reduced form, resorufin, is pink with high fluorescence [19]. The high conversion of resazurin to resorufin is associated with either cellular vitality or cellular stress response (Figure 3.5).

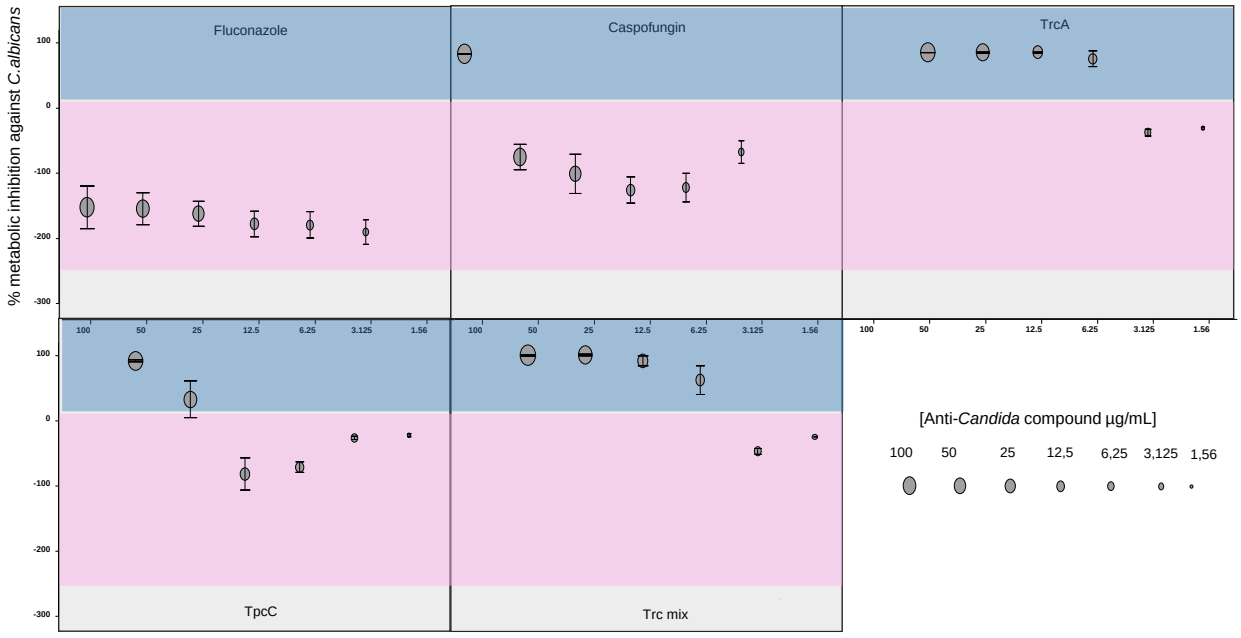

Figure 3.5 Comparative activity data of different anti-fungal compounds targeting *C. albicans*. The pink/white and blue panels are representative of metabolically stressed and inactive of dead *Candida* cells, respectively. Errors bars represent SEM for a minimum of three biological and six technical repeats. The concentration in µg/mL is presented as scaled filled circles (scale bar indicated on left).

This is observed as “negative” metabolic inhibition, indicated as pink (colour of reduced dye) in Figure 3.5. When *Candida* cells are more stressed, they reduce resazurin faster and can result in the further bleaching of the dye due to further conversion of resazurin to resorufin [20]. Upon induction of such stress signals, *Candida* cells can start to form biofilms [21] or they express multidrug-resistant (MDR) pumps to keep the anti-fungal compound out of the cells [22]. These rapid adaptations and the fact that the yeast target is eukaryotic make the treatment of *Candida* infections especially difficult. However, TrcA and Trc mix did not result in an increase in metabolic stress. This means that there is a significantly smaller chance that *Candida* cells develop a resistance mechanism against these peptides due to rapid and multiple modes of action of Trcs.

For the formulation of the purified peptides, two of the promising cellulose derivatives were initially chosen namely A4M and E4M and formulations were prepared at peptide: cellulose derivatives 1:4 (*m/m*) matured over 1 and 20 hours. Both Trc A and TpcC were first formulated with A4M in a 1:4 (*m/m*) ratio. Neither the A4M formulated TpcC or TrcA exhibited better activity than the peptides alone after 1 hour or 20 hours of maturation (Table 3.5). TrcA maintained activity in E4M, but some activity was lost in A4M at 1-hour maturation. TpcC activity was also similar alone and in formulation (Table S5). This indicated preservation of the antifungal activity for TpcC and A4M. The activity of TrcA was preserved in E4M, but not stabilised over time (Table 3.5). TrcA showed a significant loss of activity in the A4M formulation, but this activity was preserved over time (Table S5). Increasing hydrophobicity of Trcs would result in the formation of bigger self-assembly/oligomers structures [6] and could lead to change in the activity. Therefore, if the dimers proposed by Loll *et al.* [7] and Munyuki *et al.* [8] are the active moieties, the Trc activity would be dependent on a critical concentration of oligomerisation. Oligomers in solution have to be in a certain size range for the optimum availability of dimers and activity. In the case of the more hydrophobic TrcA seems there may have been a minor disturbance of the oligomer population is a solution by A4M leading to the higher MIC values. Alternatively, it could be that active groups in the TrcA structure were masked by the formulants leading to lower activity, but also the stabilisation.

3.5. Conclusion

The biological activity of tyrocidines is highly dependent on the oligomerisation profile and the amphipathicity of the molecule [2, 3]. However, *Candida* cells exposed to low concentrations of Trc mix, where less oligomerisation is expected, had an enhanced metabolic activity which resulted in the bleaching of the resazurin dye. These cells experience a substantial increase in aerobic metabolism and redox potential that could be an indication of cellular stress. These metabolically stressed cells could signal and induce *Candida* persister cells. Persister cells tend to form biofilms which makes it difficult for the antimicrobial agent to reach the target [20]. These cells could survive while the Trc peptides kill the normal *Candia* population.

It is hypothesised, that the oligomerisation profile of Trc mix is dynamic and peptide arranges and rearranges until it gets into the most favoured oligomer conformations and therefore in the ideal formulation, longer maturation (20 hours) resulted in oligomers that supported the release of dimer or more dimer in solution and therefore enhanced activity. Furthermore, we found that the formulation of Trc mix by cellulose derivatives and longer maturation of formulation components resulted in better activity, including the inhibition of potential persister

cell induction. The biological activity of Trc mix was therefore successfully enhanced through formulation with more viscous cellulose derivatives. Among seven different cellulose derivative formulants of Trc mix utilised in this study, Trc mix formulated with E10M at 1:4 (*m/m*) had significantly enhanced activity when targeting *C. albicans* and a minor enhancement in selectivity from 2- to 3-fold (results not shown). On the other hand, none of the formulations proved to be more selective, namely presenting reduced haemolytic activity. In contrast, pure TrcA or TpcC did not follow that same activity behaviour as Trc mix when matured longer. This could be that TrcA has a relatively stable oligomer population in solution because of its hydrophobicity, therefore, longer maturation does not result in a major change in oligomerisation and biological activity. TpcC is more polar but parallel studies by our group [22] showed that it formed large oligomers. Again, prolonged maturation did not result in enhanced activity, probably because this peptide is inherently less active or that the formulants are unable to modulate the oligomerisation to improve activity. This is in contrast to Trc mix which contains a complex mixture of different analogues, including TrcA and a small amount of TpcC. It is possibly that longer incubation is needed to form stable homo-oligomers and hetero-oligomers that has high activity towards *Candida* cells. It is hypothesised that the formulation of Trc mix by cellulose derivatives causes a conformational change of the oligomeric structures. The rearrangement of oligomers in the formulation form more active structures from which the proposed active amphipathic dimers [8] can be released or that more dimers remain in solution for interacting with the *Candida* target cell wall and membrane. It can be concluded that the formulation of Trc mix was successful as they enhanced the biological activity of Trc mix over time which indicated the increased stability of the active moieties in the formulations. This hypothesis will be further explored in chapter 4 utilising fluorescence studies of the Trc preparations.

3.6. References

1 Troskie, A. M., Rautenbach, M., Delattin, N., Vosloo, J. A., Dathe, M., Cammue, B. P. A., and Thevissen, K. (2014) Synergistic activity of the tyrocidines, antimicrobial cyclodecapeptides from *Bacillus aneurinolyticus*, with amphotericin B and caspofungin against *Candida albicans* biofilms. *Antimicrob. Agents Chemother. 58*, 3697–3707.

2 Ruttenberg, M., King, T., and Craig, L. (1966) The chemistry of tyrocidine. VII. Studies on association behavior and implications regarding conformation. *Biochemistry 5*, 2857–2864.

3 Breslow, R., and Chipman, D. (1964) The use of tyrocidines for the study of conformation and aggregation behavior. *J. Am. Chem. Soc.* 55, 4195–4196.

4 Powers, J. P. S., and Hancock, R. E. W. (2003) The relationship between peptide structure and antibacterial activity. *Peptides* 24, 1681–1691.

5 Prenner, E. J., Kay, C. M., Mcelhaney, R. N., and Hodges, R. S. (2002) Conformation and interaction of the cyclic cationic antimicrobial peptides in lipid bilayers. *J Pept Res* 60, 23–36.

6 Marques, M. A., Citron, D., and Wang, C. (2007) Development of tyrocidine A analogues with improved antibacterial activity. *Bioorg. Med. Chem.* 15, 6667–6677.

7 Loll, P., Uptona, E., Nahouma, V., Economoua, C., Cocklina, S. (2012) The high resolution structure of tyrocidine A reveals an amphipathic dimer Patrick. *Biochem Biophys Acta* 40, 1301–1315.

8 Munyuki, G., Jackson, G. E., Venter, G. A., Kövér, K. E., Szilágyi, L., Rautenbach, M., Spathelf, B. M., Bhattacharya, B., and Van Der Spoel, D. (2013) β-sheet structures and dimer models of the two major tyrocidines, antimicrobial peptides *from Bacillus aneurinolyticus*. *Biochemistry* 52, 7798–7806.

9 Paradies, H. H. (1979) Aggregation of Tyrocidine in aqueous solutions. *Chemistry* 88, 810–817.

10 Vosloo, J. A. (2016) Optimised bacterial production and characterisation of natural antimicrobial peptides with potential application in agriculture. PhD Thesis, Department of Biochemistry, University of Stellenbosch. https://scholar.sun.ac.za/handle/10019.1/98411

11 Rautenbach, M., Kulenkampff, J., and Westerhoff, H. (2006) Analyses of dose – response curves to compare the antimicrobial activity of model cationic α-helical peptides highlights the necessity for a minimum of two activity parameters. *Anal. Biochem*. 350, 81–90.

12 Rautenbach, M., Vlok, N.M., Stander, M., and Hoppe, H.C. (2007) Inhibition of malaria parasite blood stages by tyrocidines, membrane-active cyclic peptide antibiotics from *Bacillus brevis. Biochim. Biophys. Acta* 1768, 1488–1497.

13 Mamhende, P. G. M (2019) Investigation of the antifungal activity of tryptophan-rich cyclic peptides. MSc Thesis, Department of Biochemistry, University of Stellenbosch. https://scholar.sun.ac.za/handle/10019.1/105718

14 Keating, G. M., and Figgitt D. P. (2003) Caspofungin. *Drugs 63,* 2235–2263.

15 Shao, P. L., Huang, L. M., and Hsueh, P. R. (2007) Recent advances and challenges in the treatment of invasive fungal infections, Int. J. Antimicrob. Agents 30, 487– 495

16 Troskie. A.M (2014) Tyrocidines, cyclic decapeptides produced by soil bacilli, as potent inhibitors of fungal pathogens. PhD Thesis, Department of Biochemistry, University of Stellenbosch. https://scholar.sun.ac.za/handle/10019.1/86162

17 Braun, P., and von Heijne, G. (1999) The aromatic residues Trp and Phe have different effects on the positioning of a transmembrane helix in the microsomal membrane. *Biochemistry 38,* 9778–9782

18 Shai, Y. (2002). Mode of action of membrane-active antimicrobial peptides. *Biopolymers 66,* 236–248.

19 Allexander, B. D., Procop, G. W., Dufresne, P., Fuller, F., Ghannoum, M. A., Hanson, K. E., Holliday, D., Kovanda, L., Lockhart, S. R., Ostrosky-Zeichner, L., Schuetz, A. N., Wiederhold, N. P., and Zelazny A. M. (2017) Reference method forbroth dilution antifungal susceptibility testing of yeasts,

Approved standard M27, Clinical and Laboratory Standards Institute USA, *https://clsi.org/media/1897/m27ed4_sample.pdf*

20 Rampersad, S. N. (2012) Multiple applications of Alamar Blue as an indicator of metabolic function and cellular health in cell viability bioassays. *Sensors (Basel). 12,* 12347-12360.

21 Li, P., Seneviratne, C. J., Alpi, E., and Vizcaino, J. A. (2015) Delicate metabolic control and coordinated stress response critically determine antifungal tolerance of *Candida albicans* biofilm persisters. *Antimicrob. Agents Chemother.* 59, 6101–6112.

22 Lewis, K. (2008) Multidrug tolerance of biofilms and persister cells*. Curr. Top. Microbiol. Immunol* 322,107-131

23 Rautenbach, M., Kumar, V., Vosloo, J. Masoudi, Y., Wyk, R., and Stander M. (2021) Oligomerisation of tryptocidine C, a Trp-rich cyclodecapeptide from the antimicrobial tyrothricin complex, *Biochimie,* 181, 123-133

3.7. Supplementary data

Table S1 Summary of the IC_{50} and MIC values of different preparations of Trc mix against *C. albicans*.

		IC_{50}±SEM in µg/mL		MIC±SEM in µg/mL	
Formulant	Trc mix: formulant (*m/m*)	Fresh (1 hour)	Matured ** (20 hours)	Fresh (1 hour)	Matured (20 hours)
Control	-	(n=34)10.5±0.8	(n=20)5.3±0.3	(n=34)14.9±1.5	7.5±0.5
A4M	1:1	(n=20)8.7±1.4	(n=12)4.6±0.3	(n=2014.0±2.4	(n=12)6.7±0.5
E4M	1:1	(n=20)7.1±1.1	(n=12)5.3±0.4	(n=2013.7±2.5	(n=12)7.2±0.7
E10M	1:1	(n=16)7.4±1.1	(n=12)5.6±0.5	(n=16)12.5±1.7	(n=12)9.8±0.9
K15M	1:1	(n=16)8.9±1.0	(n=12)6.3±1.2	(n=16)12.8±1.6	(n=12)13.0±1.2
A4M	1:2	(n=16)8.9±0.6	(n=12)4.8±0.1	(n=16)12.1±0.1	(n=12)7.2±0.7
E4M	1:2	(n=16)10.3±0.7	(n=12)5.6±1.1	(n=16)14.8±1.2	(n=12)6.2±0.7
E10M	1:2	(n=16)9.1±0.3	(n=12)6.2±0.5	(n=16)12.1±0.3	(n=12)13.5±1.0
K15M	1:2	(n=16)8.9±0.9	(n=12)5.1±0.2	(n=16)11.3±0.6	(n=12)7.8±0.8
A4M	1:4	(n=16)9.5±1.3	(n=12)7.8±0.8	(n=16)14.8±1.6	(n=12)8.8±0.9
E4M	1:4	(n=16)8.8±1.3	(n=12)8.4±1.1	(n=16)12.5±1.9	(n=12)10.2±1.7
E10M	1:4	(n=16)6.4±0.5	(n=12)3.2±1.0	(n=16)10.1±1.2	(n=12)4.6±0.8
K15M	1:4	(n=16)8.2±1.3	(n=12)7.7±1.08	(n=16)12.4±1.9	(n=12)11.0±1.8

Table S2 Statistical comparison of IC_{50} between different Trc mix of fresh (1 hour) and matured (20 hours) formulations. The analysed IC_{50} and MIC values represent the mean of 3-4 biological repeats and 12-32 technical repeats with SEM. Unpaired Student t-test was done on each of the analysed pairs and only those with significant differences are shown.

Formulant 1	Formulant 2	IC50 ± SEM (µg/mL) 1	IC50± SEM (µg/mL) 2	P value
Control 1h matured	Control 20h matured	10.5±0.8	5.3±0.3	<0.0001
Tmix E4M (1:2) 1h matured	Tmix E4M (1:2) 20h matured	10.3±0.7	5.6±1.1	<0.0001
Tmix E10M (1:2) 1h matured	Tmix E10M (1:2) 20h matured	9.1±0.3	6.2±0.5	<0.0001
Tmix E10M (1:4) 1h matured	Tmix E10M (1:4) 20h matured	6.4±0.5	3.2±1.0	0.0021
Tmix K15M (1:2) 1h matured	Tmix K15M (1:2) 20h matured	8.9±0.9	5.1±0.2	0.0017
Formulant 1	Formulant 2	MIC ± SEM (µg/mL) 1	MIC± SEM (µg/mL) 2	P value
Control 1h matured	Control 20h matured	14.9±1.5	7.5±0.5	0.007
Tmix A4M (1:1) 1h matured	Tmix A4M (1:1) 20h matured	14.0±2.4	6.7±0.5	0.0203
Tmix A4M (1:4) 1h matured	Tmix A4M (1:4) 20h matured	14.8±1.6	8.8±0.9	0.0065
Tmix E10M (1:4) 1h matured	Tmix E10M (1:4) 20h matured	10.1±1.2	4.6±0.8	0.0023

Table S3 Statistical comparison of IC_{50} between different formulations of Trc mix. The IC_{50} values analysed were the mean of 3-4 biological repeats and 12-32 technical repeats with SEM. One way Anova with Bonferroni correlation test was done between each of the selected data sets groups

			20 hours of maturation												
			1:4				1:2				1:1				
			K15M	E10M	E4M	A4M	K15M	E10M	E4M	A4M	K15M	E10M	E4M	A4M	Control
1 hour of maturation	1:4	K15M	ns	<0.05	ns	ns	ns	ns	ns	ns	ns	ns	ns	ns	ns
		E10M	ns	<0.05	ns	ns	ns	ns	ns	ns	ns	ns	ns	ns	ns
		E4M	ns	<0.05	ns	ns	ns	ns	ns	ns	ns	ns	ns	ns	ns
		A4M	ns	<0.01	ns	ns	ns	ns	ns	ns	ns	ns	ns	ns	ns
	1:2	K15M	ns	<0.05	ns	ns	<0.01	ns	ns	ns	ns	ns	ns	ns	ns
		E10M	ns	<0.01	ns	ns	ns	0.001	ns	ns	ns	<0.01	ns	ns	ns
		E4M	ns	0.001	ns	ns	ns	ns	<0.01	<0.05	ns	ns	<0.05	<0.05	ns
		A4M	ns	<0.05	ns	ns	ns	ns	ns	<0.05	ns	ns	ns	<0.01	ns
	1:1	K15M	ns	<0.05	ns	ns	<0.05	ns	ns	ns	ns	ns	ns	ns	ns
		E10M	ns	0.001	ns	ns	ns	ns	ns	ns	ns	ns	ns	ns	ns
		E4M	ns	ns	ns	ns	ns	ns	ns	ns	ns	ns	ns	ns	ns
		A4M	ns	<0.01	ns	ns	ns	ns	ns	<0.05	ns	ns	ns	<0.05	ns
		Control	ns	0.001	<0.05	<0.05	<0.01	<0.05	<0.05	<0.01	ns	<0.05	0.001	0.001	0.001

			1 hour of maturation												
			1:4				1:2				1:1				
			K15M	E10M	E4M	A4M	K15M	E10M	E4M	A4M	K15M	E10M	E4M	A4M	Control
1 hour of maturation	1:4	K15M		ns	ns	ns	ns	ns	ns	ns	ns	ns	ns	ns	ns
		E10M			ns	ns	ns	ns	ns	ns	ns	ns	ns	ns	<0.01
		E4M				ns	ns	ns	ns	ns	ns	ns	ns	ns	ns
		A4M					ns	ns	ns	ns	ns	ns	ns	ns	ns
	1:2	K15M						ns	ns	ns	ns	ns	ns	ns	ns
		E10M							ns	ns	ns	ns	ns	ns	ns
		E4M								ns	ns	ns	ns	ns	ns
		A4M									ns	ns	ns	ns	ns
	1:1	K15M										ns	ns	ns	ns
		E10M											ns	ns	<0.05
		E4M												ns	ns
		A4M													ns

			20 hours of maturation												
			1:4				1:2				1:1				
			K15M	E10M	E4M	A4M	K15M	E10M	E4M	A4M	K15M	E10M	E4M	A4M	Control
20 hours of maturation	1:4	K15M		ns	ns	ns	ns	ns	ns	ns	ns	ns	ns	ns	ns
		E10M			ns	ns	ns	0.001	ns	ns	ns	0.001	ns	ns	<0.01
		E4M				ns	ns	ns	ns	ns	ns	ns	ns	ns	ns
		A4M					ns	ns	ns	ns	ns	ns	ns	ns	ns
	1:2	K15M						ns	ns	ns	ns	ns	ns	ns	ns
		E10M							ns	ns	ns	ns	ns	ns	ns
		E4M								ns	ns	ns	ns	ns	ns
		A4M									ns	ns	ns	ns	ns
	1:1	K15M										ns	ns	ns	ns
		E10M											ns	ns	ns
		E4M												ns	<0.05
		A4M													ns

Table S4 Statistical comparison of determined MICs against *C. albicans* between different formulations of Trc mix. The MIC values analysed were the mean of 3-4 biological repeats and 12-32 technical repeats with SEM. One-way Anova with Bonferroni correlation test was done between each of the selected data sets groups.

			20 hours of maturation												
			1:4				1:2				1:1				
			K15M	E10M	E4M	A4M	K15M	E10M	E4M	A4M	K15M	E10M	E4M	A4M	Control
1 hour of maturation	1:4	K15M	ns	ns	ns	ns	ns	ns	ns	ns	ns	ns	ns	ns	ns
		E10M	ns	ns	ns	ns	ns	ns	ns	ns	ns	ns	ns	ns	ns
		E4M	ns	ns	ns	ns	ns	ns	ns	ns	ns	ns	ns	ns	ns
		A4M	ns	ns	ns	ns	ns	ns	ns	<0.01	ns	ns	ns	<0.01	<0.05
	1:2	K15M	ns	ns	ns	ns	ns	ns	ns	ns	ns	ns	ns	ns	ns
		E10M	ns	<0.05	ns	ns	ns	ns	ns	ns	ns	ns	ns	ns	ns
		E4M	ns	ns	ns	ns	ns	ns	ns	ns	ns	ns	<0.05	ns	ns
		A4M	ns	ns	ns	ns	ns	ns	ns	ns	ns	ns	ns	ns	<0.05
	1:1	K15M	ns	ns	ns	ns	ns	ns	ns	ns	ns	ns	ns	ns	ns
		E10M	ns	<0.01	ns	ns	ns	ns	ns	ns	ns	ns	ns	ns	ns
		E4M	ns	ns	ns	ns	ns	ns	ns	ns	ns	ns	<0.05	ns	ns
		A4M	ns	ns	ns	<0.05	ns	ns	ns	ns	ns	ns	0.001	0.001	0.001
		Control	ns	ns	ns	<0.05	ns	ns	ns	<0.05	ns	ns	ns	<0.01	0.001

			1 hour of maturation												
			1:4				1:2				1:1				
			K15M	E10M	E4M	A4M	K15M	E10M	E4M	A4M	K15M	E10M	E4M	A4M	Control
1 hour of maturation	1:4	K15M		ns	ns	ns	ns	ns	ns	ns	ns	ns	ns	ns	ns
		E10M			ns	ns	ns	ns	ns	ns	ns	ns	ns	ns	ns
		E4M				ns	ns	ns	ns	ns	ns	ns	ns	ns	ns
		A4M					ns	ns	ns	ns	ns	ns	ns	ns	ns
	1:2	K15M						ns	ns	ns	ns	ns	ns	ns	ns
		E10M							ns	ns	ns	ns	ns	ns	ns
		E4M								ns	ns	ns	ns	ns	ns
		A4M									ns	ns	ns	ns	ns
	1:1	K15M										ns	ns	ns	ns
		E10M											ns	ns	ns
		E4M												ns	ns
		A4M													ns

			20 hours of maturation												
			1:4				1:2				1:1				
			K15M	E10M	E4M	A4M	K15M	E10M	E4M	A4M	K15M	E10M	E4M	A4M	Control
20 hours of maturation	1:4	K15M		ns	ns	ns	ns	ns	ns	ns	ns	ns	ns	ns	ns
		E10M			ns	ns	ns	<0.01	ns	ns	ns	ns	ns	ns	ns
		E4M				ns	ns	ns	ns	ns	ns	ns	ns	ns	ns
		A4M					ns	ns	ns	ns	ns	ns	ns	ns	ns
	1:2	K15M						ns	ns	ns	ns	ns	ns	ns	ns
		E10M							ns	ns	ns	ns	ns	ns	ns
		E4M								ns	ns	ns	ns	ns	ns
		A4M									ns	ns	ns	ns	ns
	1:1	K15M										ns	ns	ns	ns
		E10M											ns	ns	ns
		E4M												ns	ns
		A4M													ns

Table S5 Statistical comparison of MIC values between different formulations of TrcA and TpcC. One-way Anova with Bonferroni correlation test was done between each of the selected data setsgroups.

			20 hours of maturation				
			TrcA			TpcC	
1 hour of maturation	Peptide	Formulant	Control	A4M	E4M	Control	A4M
	TrcA	Control	ns	ns	ns	0.001	0.001
		A4M	ns	ns	ns	<0.01	0.001
		E4M	ns	ns	ns	0.001	0.001
	TpcC	Control	0.001	0.001	0.001	ns	ns
		A4M	0.001	0.001	0.001	ns	ns

			1 hour of maturation				
			TrcA			TpcC	
1 hour of maturation	Peptide	Formulant	Control	A4M	E4M	Control	A4M
	TrcA	Control	ns	ns	ns	0.001	0.001
		A4M	ns	ns	ns	0.001	<0.01
		E4M	ns	ns	ns	0.001	0.001
	TpcC	Control	0.001	0.001	0.001	ns	ns
		A4M	ns	ns	ns	ns	ns

			20 hours of maturation				
			TrcA			TpcC	
20 hours of maturation	Peptide	Formulant	Control	A4M	E4M	Control	A4M
	TrcA	Control	ns	ns	ns	ns	ns
		A4M	ns	ns	ns	ns	ns
		E4M	ns	ns	ns	ns	ns
	TpcC	Control	0.001	0.001	0.001	ns	ns
		A4M	ns	ns	ns	ns	ns

Chapter 4

Fluorescence studies on the tyrocidine formulation with cellulose derivatives

4.1 Introduction

During the purification and isolation of Trc mix single analogues reported in Chapter 2, we observed the known oligomerisation of the peptides [1, 2, 3]. It was hypothesised that the peptides in Trc mix interact with glucose moieties in polysaccharides, as previously found by Juhl *et al* [4]. In Chapter 3 the formulation of Trc mix with polysaccharides led to changes in activity against *C. albicans* and human erythrocytes. It was shown that Trc mix formulations containing certain cellulose derivatives have an enhanced anti-*Candida* activity. Furthermore, we found that 20 hours matured Trc mix-cellulose derivative preparations are significantly more active against *Candida* species. Considering the tendency of the peptides to oligomerise, we decided to investigate the interaction of the aromatic amino acid residues in Trc mix with cellulose derivatives and their influence on the fluorescence properties of the Trcs.

Most of the dimeric structures that were found by Munyuki *et al.* [5] and Loll *et al.* [6] via modelling studies, retain their amphipathic properties allowing for the interaction of the peptide and the target cell membrane and therefore, destabilising of the membrane. it is proposed that the dimeric peptide is the bioactive structure. Therefore, it was hypothesised that the presence of specific functional groups on cellulose moieties may weaken the interaction between the peptide molecules to limit the formation of larger peptide oligomers that form over 20 hours of maturation. In this, the formulation could support oligomer conformation(s) that allows the release of membrane-active dimers and other oligomers or aid the solution retention. This chapter reports the influence of maturation and cellulose derivatives on biophysical properties of the Trc mix. We aimed to monitor and compare the formation of self-assembly structures of Trc mix and formulated Trc mix by cellulose derivatives after 1, 4 and 20 hours of maturation. Formulants, identical to those used in the activity studies against *Candida* species, were used, namely soluble celluloses with different cellulose derivatives containing methyl, ethyl, propyl, and hydroxyl side chains resulting in varying hydrophobicity of the formulant (Figure 4.1A and B).

The presence of 4/10 aromatic amino acids such as Trp, Tyr and Phe in the structure of the cyclic peptides, allows the tracking of these peptides via fluorescence spectroscopy (Figure 4.1C).

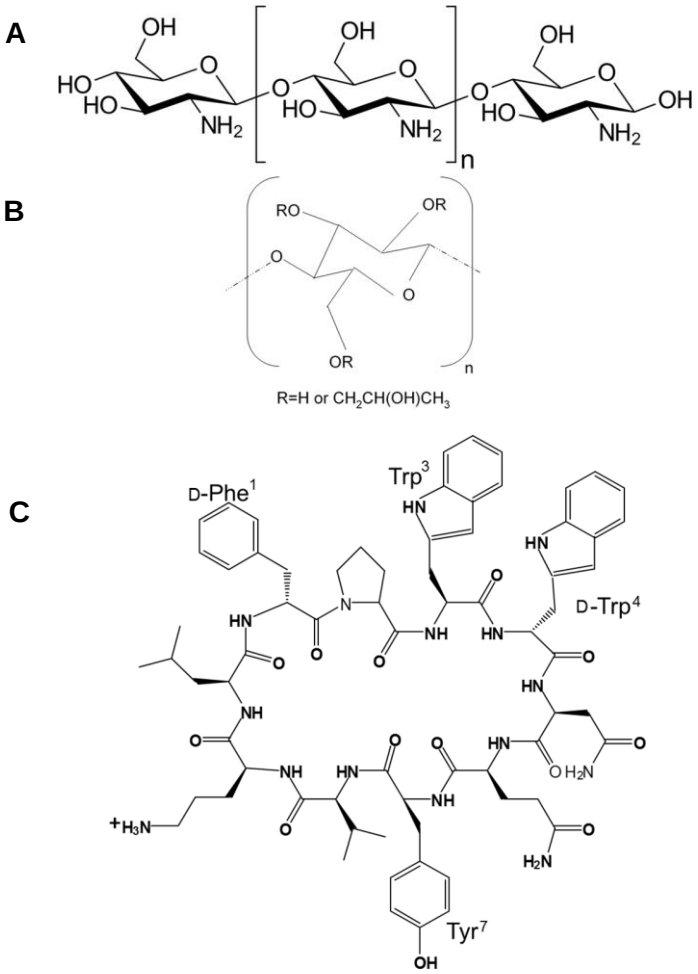

Figure 4.1. Examples of cellulose derivatives and Trcs studied in this chapter with **A.** chitosan polymer, **B.** core of hydroxyl and methylcellulose derivatives, and **C.** primary structure of Trc C indicating the four aromatic amino acids in the cyclic peptide structure.

Rigid chromophores such as aromatic amino acids (Trp, Tyr and Phe) have a limited range of vibrational energy level [7]. When these chromophores absorb light, they will return to the ground estate by emitting photons. This phenomenon is called fluorescence and such molecules are called fluorophores [7]. Fluorescence is the result of a three-state electronic transition namely, excitation (light absorption), excited estate lifetime (an extremely short time in which fluorophore stays in the excited state), emission (release of the photon bythe fluorophore and returning to the ground state) [7] (Figure 4.2). As some of the light absorbed is always lost during the transition from the excited to the emitted state, the emitted spectrum lies at a lower energy level/longer wavelength than the excited spectrum[8]. Furthermore, the emitted spectrum can be quenched due to two other processes namely: internal and external quenching [7, 8, 9]. Internal quenching/self-quenching is due to some intrinsic features of the excited molecules such as the tendency of the molecule for structural rearrangement or oligomerisation/aggregation. External quenching arises when another

molecule present in the sample (polar solvent) absorbs the emitted energy. All forms of quenching results in non-radiative energy emission. However, if a fluorescent molecule is excited into a more polar environment (e.g., a high concentration of cellulose derivatives), the solvent molecules immediately adjust to the electron distribution in the fluorophore. The adjustment of the solvent molecules with the excited fluorescent molecule's electron distribution does not happen instantaneously thus the solvent molecules react using dielectric relaxation until the corresponding excited state is reached. The same process occurs during emission, which results in the fluorescent spectrum experiencing a red shift. If a molecule is excited into a less polar environment, the emitted fluorescent spectrum experiencing a blueshift [7, 8, 9, 10, 11, 12].

Fluorescence spectrometry is generally utilised in biophysical and biochemical studies of peptides and proteins as the frequency in which the light is absorbed is affected by the environment and the structure of the molecules. Therefore, the influence of the environment on the fluorophore, the components of a solvent, and the molecular interaction/stability can be identified via fluorescence spectrometry. Furthermore, as this technique is highly sensitive there is only a small quantity of the sample needed [7, 8, 9, 10].

As mentioned before, aromatic amino acids are good fluorophores, due to their absorbing aromatic ring structures and high resonance energy. Trp is the best fluorophore of the aromatic amino acid residue with $\lambda_{excitation}$ at 282 nm and $\lambda_{emission}$ at 348 nm [9]. Trp is highly solvatochromic, meaning, the fluorescence of Trp is influenced by the environment (solution) and the proximity of other protonated groups of nearby residues as these can cause fluorescence quenching [7, 9]. Therefore, the nearby charged amino acid groups can transfer electrons from protonated carboxyl groups, electron transfer can occur by peptides bonds, and electrons can be accepted by the formulation components. All of these can then lead to the fluorescence signal quenching [9, 11, 12].

Tyr with $\lambda_{excitation}$ is at 267 nm and $\lambda_{emission}$ at 350-303 nm is the second-best fluorophore in proteins and the tyrocidines. The emitted spectrum is quenched in a polar environment. Furthermore, Tyr fluorescence has been observed to be quenched by the presence of nearby tryptophan moieties via resonance energy transfer [9]. Phe is a weak fluorophore with $\lambda_{excitation}$ at 256 nm and $\lambda_{emission}$ at 282 nm [9]. Its emitted spectrum can be only observed in the absence of both Trp and Tyr. Trp is, therefore, a major fluorophore in the tyrocidines and tryptocidines as it has greater resonance energy transfer, absorptivity and higher quantum yield compared to Tyr and

Phe [9], hence chosen as the main fluorophore for the biophysical studies reported in this chapter.

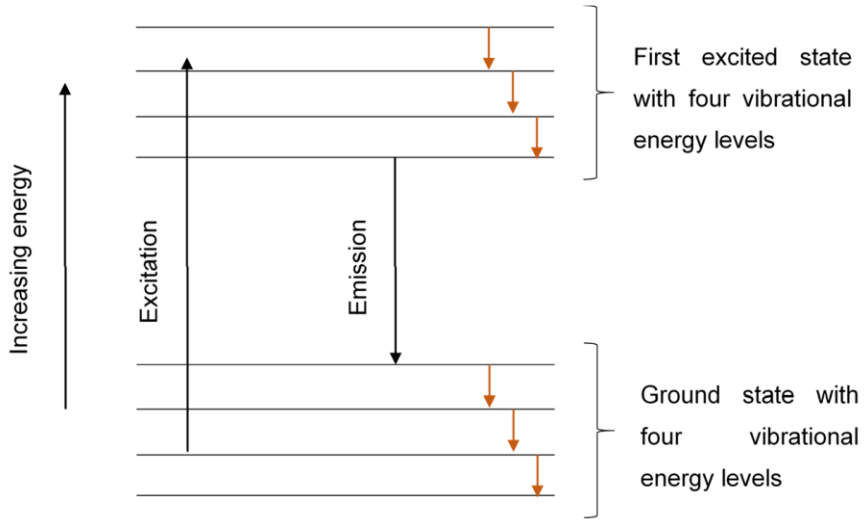

Figure 4.2. Physical basis of fluorescence. As aromatic amino acid residues are rigid molecules with few vibrational levels (four levels are shown in this scheme) the released energy from the excited estate to the ground estate is in form of a photon [7].

To assess the formulant stability-activity relationships, the Trp fluorescence was utilised, as many of the cyclodecapeptides in Trc mix contain Trp such as Trc B, B_1, C and C_1 with minor contribution by TpcA, A_1, B, B_1, C and C_1. Trp fluorescence would allow the monitoring of localised changes in oligomerisation of the peptide in the Trc mix and formulations.

4.2 Materials

TpcC was purified from *Brevibacillus parabrevis* culture extracts (refer to chapter two for more details). Commercial tyrothricin extract was supplied by Sigma-Aldrich (St Louis, USA). Ethanol, diethyl ether and acetone were supplied by Merck (Darmstadt, Germany). Analytical grade water (MQH_2O) was prepared by filtering water from a reverse osmosis plant through a Millipore-Q® water purification system (Milford. USA). The 96-well black and transparent flat-bottom plates were supplied by Thermo Fisher Scientific (Denmark). Benecel A4M(A4M), Benecel E4M (E4M), Benecel E10M (E10M), Benecel K15M (K15M) Klucel E IND (KLUE). Klucel L IND (KLUL) were donated by ASHLAND, Covington, Kentucky America. Chitosan was purchased from Sigma-Aldrich (St Louis. USA). Tyrocidine mixture (Trc mix) was extracted from commercial tyrothricin using diethyl ether and acetone [13] (also refer to Chapter 2 for details on the Trc mix preparation)

4.3 Methods

4.3.1 Fluorescence spectroscopy

To determine the biophysical characteristics of formulated Trc mix, formulants were prepared as described before (chapter three) in 15% ethanol (*v/v)* followed by a 10-fold dilution by adding 90 µL of filter-sterilized MQH_2O. The Trc mix formulation preparation and analysis parameters are summarised in Table 4.1.

Table 4.1. Summary of the composition and the preparation of different formulation of Trc mix and the parameters used in the fluorescence monitoring of their stability.

Formulants	Readings interval (hours)	Trc mix: formulants ratio (*m/m)*	[Trc mix] µg/mL	Excitation. emission range (nm)
Control*	1, 4, 20	-	50	280, 320-400
A4M	1, 4, 20	1:1	50	280, 320-400
E4M	1, 4, 20	1:1	50	280, 320-400
E10M	1, 4, 20	1:1	50	280, 320-400
KLUE	1, 4, 20	1:1	50	280, 320-400
KLUI	1, 4, 20	1:1	50	280, 320-400
CHS	1, 4, 20	1:1	50	280, 320-400
K15M	1, 4, 20	1:1	50	280, 320-400
A4M	1, 4, 20	1:2	50	280, 320-400
E4M	1, 4, 20	1:2	50	280, 320-400
E10M	1, 4, 20	1:2	50	280, 320-400
K15M	1, 4, 20	1:2	50	280, 320-400
A4M	1, 4, 20	1:4	25,50	280, 320-400
E4M	1, 4, 20	1:4	25,50	280, 320-400
E10M	1, 4, 20	1:4	25,50	280, 320-400
K15M	1, 4, 20	1:4	25,50	280, 320-400
Control*	Continual 60 minutes	1:4	100-1.25	280, 340
A4M	Continual 60 minutes	1:4	100-1.25	280, 340
E4M	Continual 60 minutes	1:4	100-1.25	280, 340
Control*	Continual 60 minutes	1:4	50	280, 320-400
A4M	Continual 60 minutes	1:4	50	280, 320-400
E4M	Continual 60 minutes	1:4	50	280, 320-400

***** 1.5% Ethanol in MQH_2O (*v/v*)

In all assays, the excitation wavelength was 280 nm. However, the emission parameters differed between different assays. For assays with 50 µg/mL Trc mix, fluorescence emission was scanned from 320 nm to 400 nm, while for assays with the titrated concentrations of Trc mix (ranging from 100 to 1.2 µg/mL), fluorescence emission was measured at 340 nm. The emission bandwidth was 20 nm with 10 flashes and Z position of 2000 µm. All fluorescence readings were collected using the Tecan Spark 10M Multimode Microplate Reader. Readings were taken after 1, 4 and 20 hours of maturation. Continuous readings over 60 minutes were taken for titrated Trc mix and formulated Trc mix with A4M and E4M.

Readings were taken with six to twelve repeats to allow the statistical comparison of the preparations.

The titrated concentration of TpcC (95% purity), ranging from (1000 to 30 µM) were prepared as described before in 20% acetonitrile (*v/v*) followed by a 10 times dilution by adding 90 µl of 20% acetonitrile (*v/v*). Readings were taken continuously for 60 minutes. The excitation wavelength was 280 nm and emission 340 nm. The emission bandwidth was 20 nm with 10 flashes and Z position of 2000 µm. All fluorescence readings were collected every two minutes, using the Tecan Spark 10M Multimode Microplate Reader. Readings were taken with three technical repeats to minimise the possible technical errors.

4.4 Results and discussion

4.4.1 Fluorescence spectrometry of Trc mix and its formulations

Various non-covalent and hydrophobic interactions play important roles in the formation of higher/larger oligomers. The presence of four aromatic amino acid residues and three hydrophobic residues in tyrocidines would drive hydrophobic interactions in aqueous systems between the peptides to form oligomers that may lead the change in their optical characters such as a change in absorption and fluorescence emission. Trcs have three aromatic fluorophores namely Phe, Tyr and Trp. As mentioned, Trp was chosen for this study as a fluorophore as it is a major fluorophore with greater resonance energy transfer, absorptivity and higher quantum yield [9].

Trc mix at 50 µg/mL in 1.5% ethanol: analytical grade water (*v/v*) was used as control. The formulation stability, when combined with six different cellulose derivatives and chitosan 1:1 *(m/m),* was studied utilising fluorescence spectrometry. The concentration of 50 µg/mL Trc mix was chosen as the *Candida* cultures treated with the different Trc mix formulations showed 100% metabolic inhibition at this concentration. The Trp fluorescence was considered as the major contributor to the detected fluorescence emission between 320-400 nm, which was determined after 1, 4 and 20 hours of maturation. The change in total fluorescence of formulated Trc mix at the three time points of maturation is shown in Figure 4.3. Each preparation was monitored individually as technical repeats may not have identical behaviour due to the sensitivity of the Trc oligomerisation to the plastic surface contact [14], the time during pipetting, time after mixing, the sequence of adding components and small temperature variations. The formation of unstable oligomers and dynamic

changes in oligomerisation can therefore be monitored and compared by assessing the scattering of data points (Figure 4.3).

For all the preparations, the fluorescence scattering of Trc mix formulations increased dramatically from 1 to 4 hours. This then remained relatively stable for all the preparations except for the control in 1.5% ethanol: water (*v/v*) and formulation with A4M that both exhibited increased scattering at 20 hours (Figure 4.3C). The other formulations of Trc mix showed less scatter after an hour of incubation and after 20 hours when compared to the control, considering a scatter parameter that was defined as: Average of 12 repeats/standard deviation = signal/noise = S/N. This was discussed in more detail below in the discussion on a global comparison of all the datasets (refer to Figure 4.6B in discussion below). This stabilisation of fluorescence can be contributed to the interaction of cellulose derivatives and Trc mix which prevents/slows down the formation and dynamic rearrangement of oligomers. However, the concentration of cellulose derivatives at 50 µg/mL may not fully stabilise all the Trc molecules at 50 µg/mL and they still aggregate/oligomerise over 20 hours resulting in a larger scattering. The aggregation/oligomerisation is supported by the lower total fluorescence or quenching for all twelve technical repeats at 20 hours versus 1 hour of maturation (Figure 4.3, refer to Figure 4.6 in discussion below). The lower quantum yield of Trp could be due to either the exposure of the Trp residue to the polar solvent, polar groups in the celluloses, interaction with polar groups [7] (Lys, Orn, Gln, Asn and Tyr side chains) and/or due to aromatic stacking [7, 9]. Comparing the mean of percentage fluorescence loss over 20 hours of maturation, Trc mix lost close to half the Trp signal intensity while formulated Trc mix lost about a third of the Trp signal intensity (Table 4.2).

Table 4.2. Summary of %relative fluorescence unit (RFU) loss measured for each of the eight formulants of Trc mix 1:1 (*m/m*) from 1 to 4 and 1 to 20 hours of maturation. The relative loss is also indicated as a heat map with blue the lowest lost and red the highest loss.

	Mean of % RFU loss from 1 hour	
Cellulose derivatives	**4 hours of maturation**	**20 hours of maturation**
Control	23	45
A4M	22	32
E4M	20	25
E10M	24	31
KLUE	19	26
KLUI	22	30
CHS	25	35
K15M	20	27

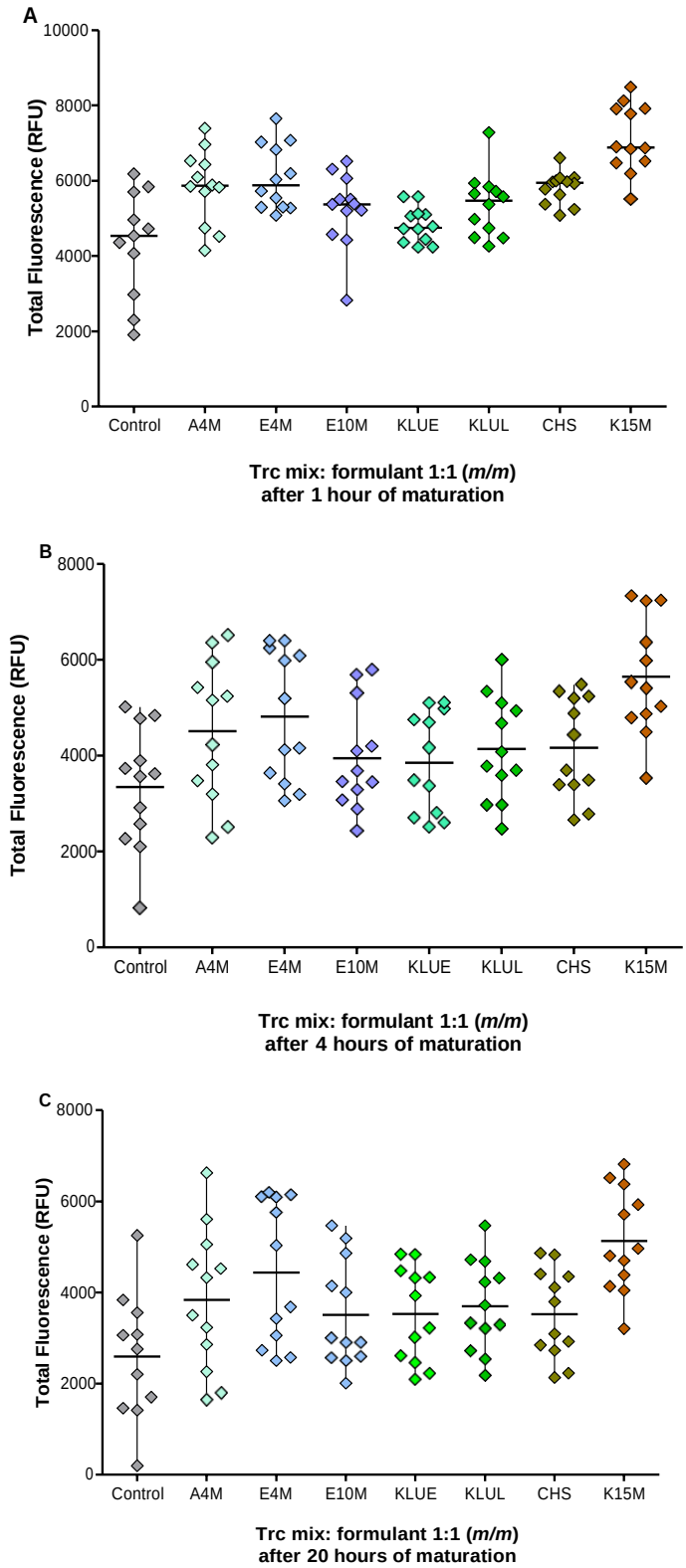

Figure 4.3. Comparison of Trp total fluorescence in relative fluorescence units (RFUs) of the 50 µg/mL Trc mix preparations after **A.**1, **B.** 4, and **C.**20 hours of maturation in solution with different cellulose derivatives at 1:1 (*m/m*) ratio. Twelve preparations of each formulation are shown with the range and mean.

The most stable formulations in terms of Trp fluorescence contained CHS and K15M, followed by KLUE and KLUL. Interestingly, CHS, KLUE and KLUL followed by E4M had very high S/N after one hour of maturation which significantly decreased over 20 hours of maturation (Figure 4.3, refer to Figure 4.6F). These four formulants have the lowest viscosity, which indicates that viscosity may be important in the time-dependent maturation and stabilisation. This result further indicates that cellulose derivatives do influence and possibly delay the formation of the large oligomers. However, it also seems that too much stabilisation or the low viscosity correlates with the weaker activity of the formulants against *C. albicans* as reported for CHS, KLUE and KLUL in Chapter 3. It is hypothesised that highly stable oligomers may not have a high enough affinity to bind to the cell membrane of the target organism, possibly because of the masking of active groups and/or thermodynamic stability of the formulant-peptide oligomers that traps the peptides. Therefore KLUE, KLUL and CHS were omitted from the rest of the biophysical studies.

In the following studies, we considered the formulation of 50 μg/mL Trc mix with increased concentrations at 100 μg/mL and 200 μg/mL of A4M, E4M, E10M and K15M to yield formulation ratios of 1:2 and 1:4, respectively (Figures 4.4 and 4.5). The Trp signal loss of formulated Trc mix by cellulose derivatives at 1:2 (*m/m*) ratio was less than formulations at 1:1 (*m/m*) ratio further confirming the influence of cellulose derivatives on prevention/slowing down the formation of oligomers (Figure 4.4). The S/N ratios for all the 1:2 formulations were above 6 which is higher than control and Trc mix: cellulose derivatives at 1:1 (*m/m*) ratio, except for K15M at 1 hour (refer to Figure 4.6D). There was no significant increase in the scattering of the data as none of the preparation's S/N ratio decreased, except for the control, at 20 hours of maturation (refer to Figure 4.6D).

As 100 μg/mL of cellulose derivatives per 50 μg/mL Trc mix stabilised the Trp fluorescence over 20 hours of maturation, we increased the formulants concentration even further (200 μg/mL per 50 μg/mL Trc mix) yielding a ratio of 1:4 (*m/m)* to investigate any other possible changes in Trp fluorescence over 20 hours of maturation (Figure 4.5 A-C). The 200 μg/mL of cellulose derivatives per 50 μg/mL Trc mix yielded stable formulations with much less scatter and the Trp fluorescence signal loss was significantly lower when compared to Trc mix by formulated 50 μg/mL of cellulose derivatives (refer to addendum Tables S1-S4 for statistical analyses). The S/N ratios for the 1:4 formulations are higher for all preparations compared to 100 μg/mL of cellulose derivatives and remains constant over 20 hours of maturation for all preparations (refer to Figure 4.6F).

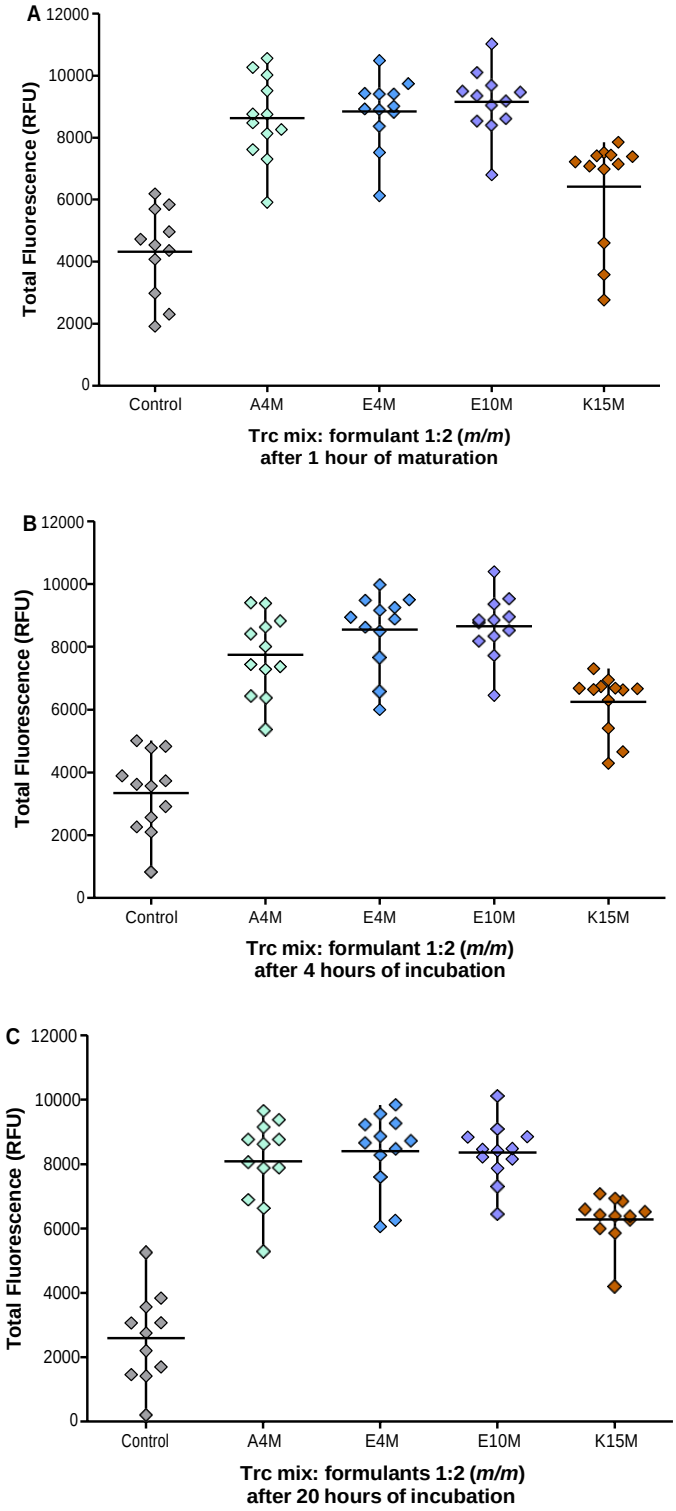

Figure 4.4. Comparison of Trp total fluorescence in RFUs of the 50 µg/mL Trc mix preparations after **A**.1 hour, **B**. 4 hours, and **C**. 20 hours of maturation in solution with different cellulose derivatives at 1:2 (*m/m*) ratio. Twelve preparations of each formulation are shown with the range and mean.

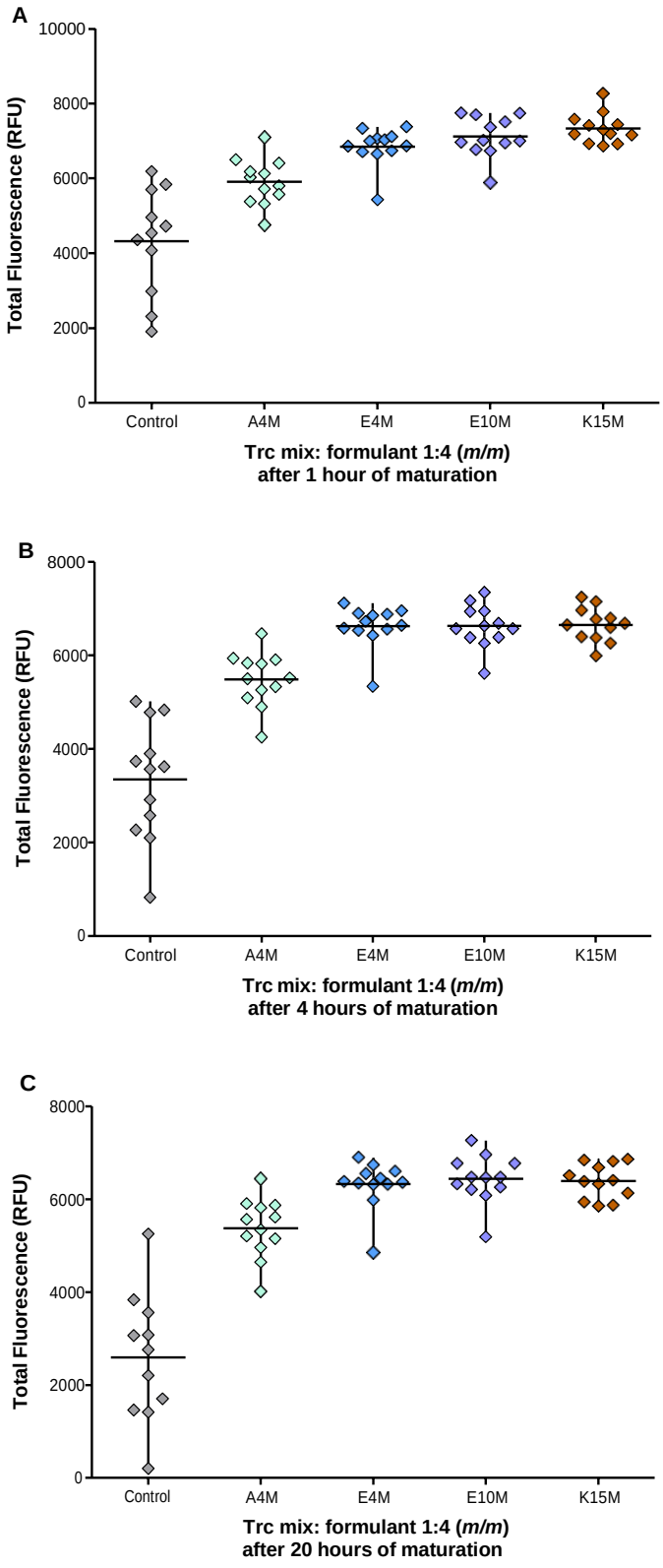

Figure 4.5. Comparison of Trp total fluorescence in RFUs of the 50 µg/mL Trc mix preparations after **A**.1, **B**. 4, and **C**.20 hours of maturation in solution with different cellulose derivatives at 1:4 (*m/m*) ratio. Twelve preparations of each formulation are shown with the range and mean.

An increased ratio of cellulose derivatives resulted in the increased S/N ratio, signifying more stable formulations up to 20 hours (refer to Table 4.3 and Figure 4.6). As an example, 50 and 100 µg/mL of K15M, had significantly different S/N after 1, 4 and 20 hours of maturation, but 200 µg/mL of K15M had a constant S/N over 20 hours with a 130% improvement in S/N for the 1:2 formulation (Figure 4.6D and Table 4.3). A comparative summary of the results is given in Figure 4.6 and Table 4.3.

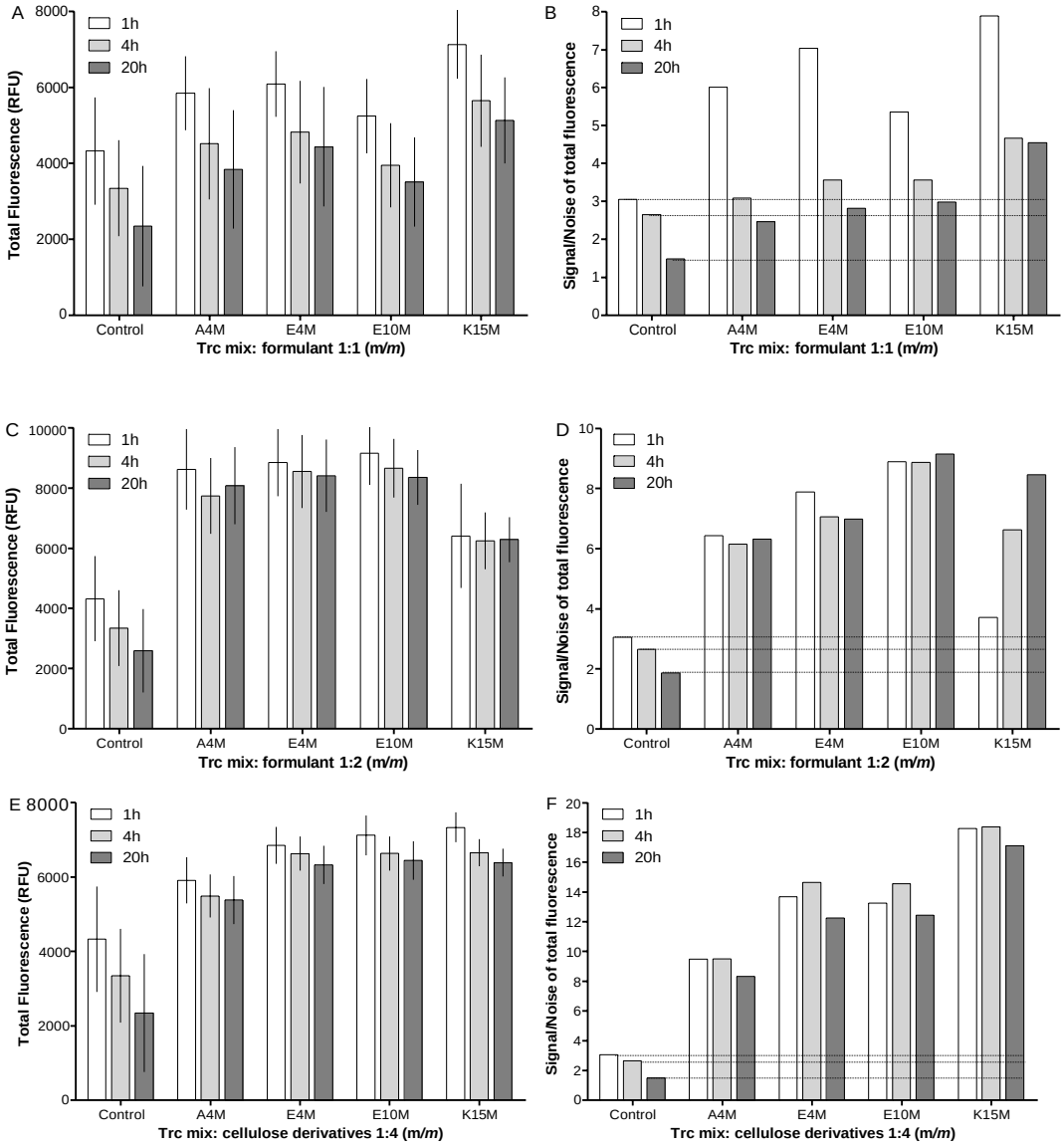

Figure 4.6. Comparison of the total fluorescence changes of formulated Trc mix at 50 µg/mL and different ratios of cellulose derivatives over time with **A.** 1:1 (*m/m*) ratio, **C.** 1:2 (*m/m*) ratio and **E.**1:4 (*m/m*) ratio. Each bar represents the mean of 12 preparation and their determinations with SD. **B**, **D** and **F** show the S/N comparison of the respected datasets. The dotted lines show the comparison with the controls at 1, 4 and 20 hours.

Table 4.3. Summary of %S/N loss, indicating instability, measured for each of the five formulants of Trc mix 1:1, 1:2 and 1:4 *(m/m)* from 1 to 20 hours of maturation.

	% loss of S/N over 20h of maturation		
	Trc mix: cellulose derivatives 1:1 *(m/m)*	Trc mix: cellulose derivatives 1:2 *(m/m)*	Trc mix: cellulose derivatives 1:4 *(m/m)*
Control	39	39	39
A4M	60	2	13
E4M	55	11	11
E10M	44	2 (gain)	7
K15M	46	130 (gain)	7

As seen in Figure 4.6, the Trc mix (control) lost close to half of the Trp fluorescence signal over 20 hours. This significant signal loss is mostly attributed to the stacking of the aromatic residue peptide molecules, specifically quenching of the Trp fluorescence (refer to tables S2-4 in supplementary data). Upon addition of the cellulose derivatives to the Trc mix preparation at 50 µg/mL, the signal loss decreased significantly (Figure 4.6A and B, Table 4.3, Table S1, refer to Tables S2-4 for statistical analyses). It is assumed that cellulose derivatives inhibit the aromatic stacking in oligomers resulting in less quenching of the total Trp signal. However, the concentration of the cellulose derivatives is too low in the 1:1 formulants to form stable formulation therefore after 20 hours of maturation the signal loss can still be observed. In Figure 4.6 C, D and E, F it can be seen that the Trp signal fluorescence measured for Trc mix formulations at ratios of 1:2 and 1.4 are significantly more stable over 20 hours of maturation (refer to Tables S3 and S4 for statistical analyses).

It is hypothesised that in addition to slowing down the formation of large oligomers, the higher concentration of the cellulose derivatives results in the formation of smaller and more stable oligomers over 20 hours maturation. The cellulose derivatives “interfere” with the stacking of aromatic amino acid residues, with the latter resulting in Trp fluorescence signal loss. This could happen via direct interaction with certain residues, specifically involving residues 4 and 9 (D-Trp^4 or D-Phe^4 and Orn^9/Lys^9) in the peptides as shown by Juhl *et al*. [4]. Alternatively, the formulants may have a chaotropic effect in which oligomerisation via hydrogen bonding of the peptide molecules, form β-sheet type oligomers [5, 6], direct steric hindering of aromatic stacking or the hydrophobic forces are disrupted. The latter could be directly related to water preferentially interacting with the cellulose OH-groups (hydration of formulants). This effectively will lower the water activity reducing the hydrophobic clustering of the aromatic and hydrophobic groups. As these oligomers in the 1:2 and 1:4 formulations are possibly an optimal size and stability to remain in solution, they do not constantly rearrange resulting in a constant high S/N ratio over 20 hours of maturation (refer to Figure 4.6 D and F). Therefore, it is concluded that increased concentration of cellulose derivatives

results in a more stable Trp fluorescence meaning the solution conformation and oligomers of the peptides in the Trc mix were better stabilised.

4.4.2 Effect of time and concentration on the formation of oligomers

Maturation time had a major influence on the total Trp fluorescence signal observed for Trc mix and its formulations. To further investigate the conformational changes of the Trp-containing peptides in the Trc mix and formulated Trc mix fluorescence was monitored continuously over the first 60 minutes at 50 and 6.25 µg/mL Trc mix (Figure 4.7). Trc mix in the control solution (1.5% ethanol in analytical grade water. *v/v*) and in A4M (200 and 25 µg/mL) showed a large Trp fluorescence loss in the first 6 minutes. This indicates a rapid change in the solution conformation/oligomerisation or rapid settling out of the solution. Visual inspection of the solutions did not reveal any opacity or over precipitation of the components. It was assumed that interaction with the surface will be similar to the % signal loss. Therefore, it was assumed that the major change in Trp fluorescence signal, is due to the conformational reorganisation of the peptide molecules (Figure 4.7). However, Trc mix (50 and 6.25 µg/mL) in E4M (200 and 25 µg/mL), did not show a rapid Trp fluorescence loss in the first six minutes (Figure 4.7E), which can be due to two reasons. First, the oligomers may have already formed before measuring started (the time from preparing the formulation until measuring the fluorescence) and second, that E4M stabilised the formation of the oligomers, therefore the rapid stacking of aromatic amino acids did not occur in the first six minutes of the maturation.

The initial and final fluorescence observed of different preparations of 6.25 µg/mL Trc mix which were relatively similar, indicating similar changes in Trp environment at the low concentration of Trc mix and that the formulants did not have an influence. However, the observed initial and final fluorescence (fluorescence at 12 minutes and 60 minutes, respectively) of different preparations of 50 µg/mL Trc mix were very different from one another, with control having the highest and E4M having the lowest starting/ending fluorescence. This indicated that the Trp residues were in different environments in the three formulations with 50 µg/mL Trc mix. The Trp environment, in contrast with 6.25 µg/mL Trc mix, was both influenced by the formulant and concentration, indicating that concentration-driven oligomerisation plays an important role in these observed differences in Trp fluorescence.

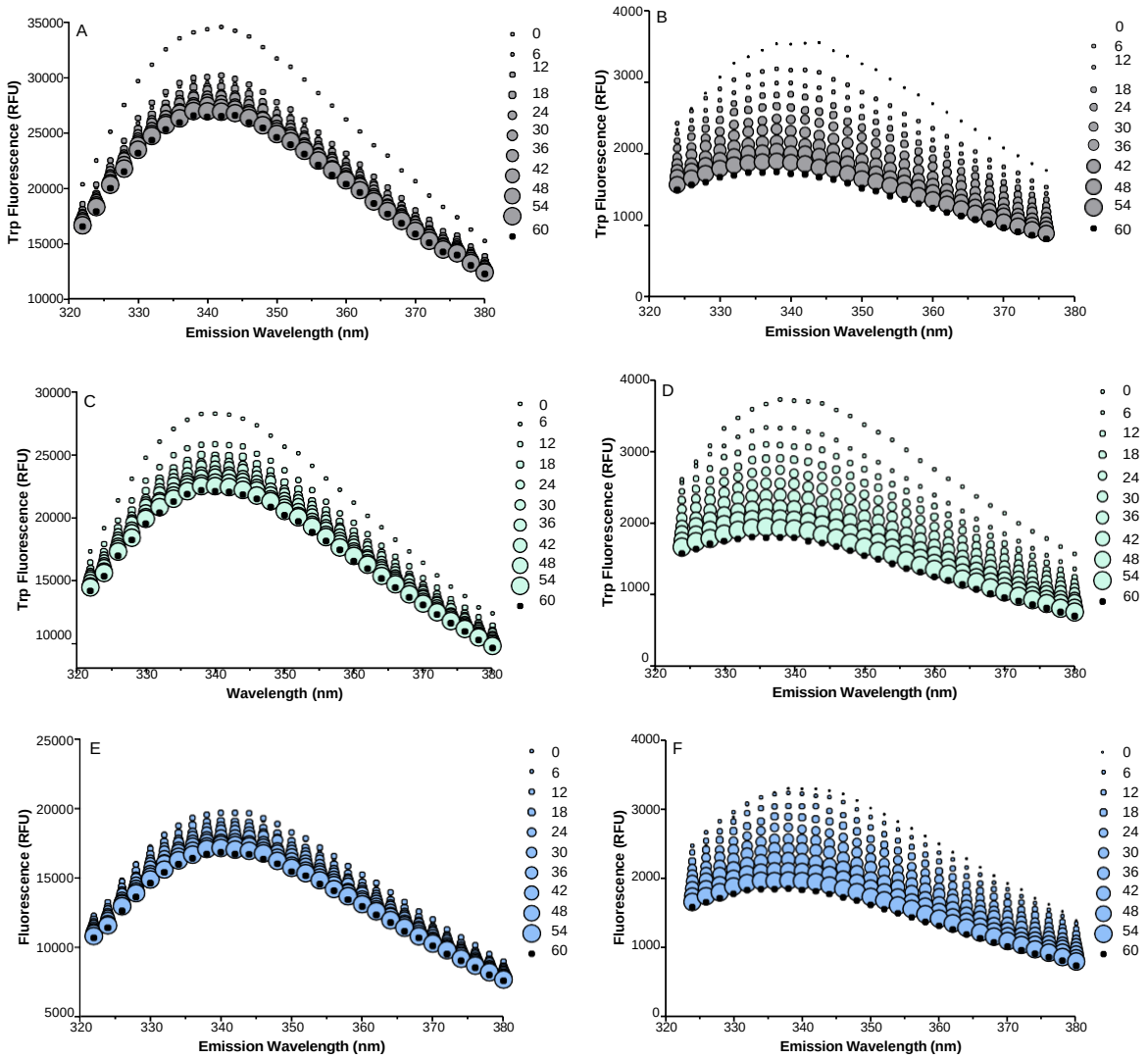

Figure 4.7. Fluorescence emission spectra (excitation at 280 nm) over time with **A**. Trc mix at 50 µg/mL in control solution, **C** formulated with 200 µg/mL A4M and E 200 µg/mL E4M and **B** Trc mix at 6.25 µg/mL **D** formulated with 200 µg/mL A4M and **F** 200 µg/mL E4M. Each data point is the mean of three replicates.

By plotting the Trp fluorescence at 12-60 minutes for control and formulations with 50 and 6.25 µg/mL of Trc mix, the ΔRFU/minute (ΔRFU = change in relative fluorescence units) was calculated using the slope of Trp fluorescence decrease from 12-60 minutes and was attributed to the rate of the formation of oligomers at a certain concentration (Figure 4.8A and B).

Although different formulations of Trc mix at the same concentration had the same aggregation/oligomerisation rate, this rate was different between 50 and 6.25 µg/mL of control and cellulose derivatives preparation of Trc mix. This result indicated that at the higher concentration of 50 µg/mL Trc mix oligomers are formed at a 2-3-fold higher rate

when compared to the lower concentration of 6.25 µg/mL Trc mix (Figure 4.8A). This confirmed that the Trc mix concentration was the main driver in fluorescence loss and that oligomerisation is concentration-dependent, as expected.

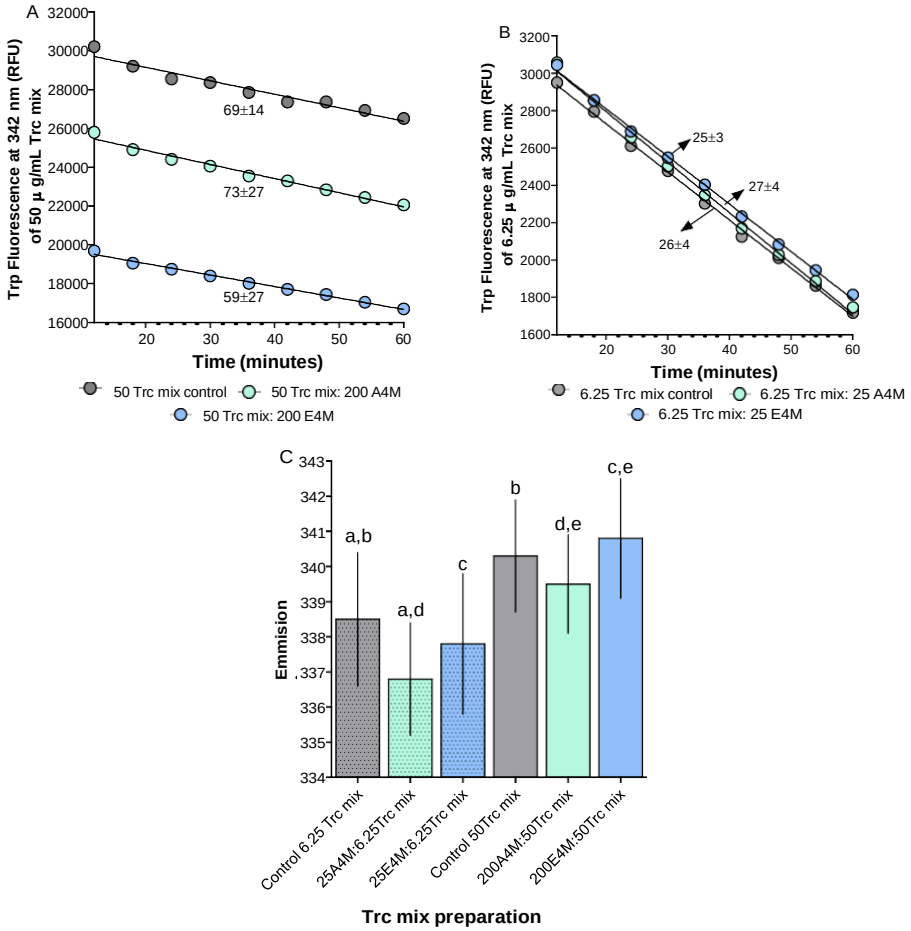

Figure 4.8. Monitoring the influence of the formulation on the aggregation rate of **A.** 50 µg/mL and **B.** 6.25 µg/mL Trc mix. The numbers on the graphs indicated the slope and aggregation/oligomerisation rates (∆RFU/minute) from 12-60 minutes. SD shows the error of three repeats. **C.** Comparison of emission averages as calculated over 33 time points (n=33) with SD. Statistical comparison of λ_{max} was done via One-way Anova and Bonferroni's Multiple Comparison Test with a = P<0.01; b, c, d =P<0.001; e = P<0.05.

The emission λ_{max} of different formulations of Trc mix differed between the two concentrations of 50 and 6.25 µg/mL (Figures 4.7 and 4.8C). The emission λ_{max} at 50 µg/mL Trc mix is red-shifted when compared to 6.25 µg/mL of Trc mix (Figure 4.8C). This indicated that the Trp residues were in a more polar environment in the structures that formed at 50 µg/mL than those that exist at 6.25 µg/mL of Trc mix. The redshift and the quenching that were observed would be correlated if there is an interaction of some of the Trp side chains with the polar residues of the peptide in the oligomers. There is a blue shift for 6.25 µg/mL Trc mix formulated by A4M, as these preparations have significantly a lower λ_{max} than the

control. This indicated that the Trp residues are in a more hydrophobic environment as A4M is a methylated cellulose and the most hydrophobic formulant.

Monitoring of Trp fluorescence over a broader concentration range of Trc mix and formulated Trc mix revealed the critical concentration in which Trp environment changes, which would be related to the critical concentration of oligomerisation/aggregation. The relation of the initial changes and oligomerisation over the first 60 minutes was investigated by measuring the total Trp fluorescence over a biological concentration range (100 to 1.25 µg/mL) of Trc mix and formulated Trc mix. From this, it was again shown that Trc mix concentration has a major influence on oligomerisation behaviour (Figure 4.8). Formation of oligomers takes place at high rates with multiple reactions that are far from equilibrium, therefore it was not feasible to determine the initial oligomerisation rate for each of the concentrations [11]. To simplify the analysis, the data from the first 10 minutes were ignored because of large fluctuations (low S/N). At a low concentration of Trc mix, total Trp fluorescence is low as expected, and errors will be larger. Increasing the concentration of Trc mix will result in increased total fluorescence intensity and more reliable readings. However, this depends on if the peptide remains in solution and does not oligomerise, which both will lead to quenching and influence on the total Trp fluorescence and data reliability. However, the change of Trp fluorescence at a specific concentration with the increase in the Trc mix concentration can be used to determine the critical oligomerisation concentration as the linear correlation with the total fluorescence intensity will be lost. That is because the concentration of Trc mix is high enough to result in the formation of large oligomers that can lead to settling out of solution (not visible to the naked eye) and/or quenching of Trp fluorescence due to aromatic stacking of aromatic amino acid residues (π-π interactions) [1]. This can cause a loss in signal intensity that depends on the Trc mix concentration and type of side chains present in the cellulose derivatives and solvent. The change in the environment of the peptide molecules can result in a change in hydrogen bonded structures, weak non-covalent interaction, and aromatic amino acid stacking, leading to different critical oligomerisation concentration. From these studies, we determined the Trc mix critical oligomerisation concentration of the Trp-containing peptide as 8 µg/mL (~ 6 µM). The Trc mix formulation with A4M and E4M presented critical oligomerisation concentrations as 17 µg/mL (~13 µM) and 15 µg/mL (~12 µM) respectively. Therefore, a higher concentration of peptide is needed in the A4M and E4M formulations for the formation of oligomers and stacking of the aromatic amino acids.

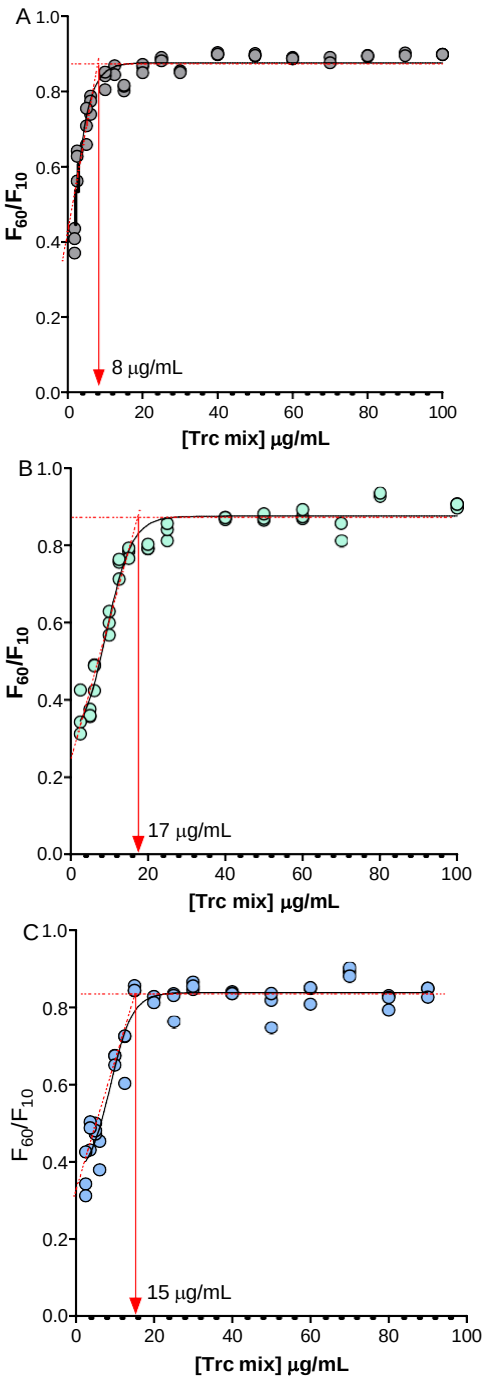

Figure 4.9. Monitoring the influence of formulation on aggregation concentration of Trc mix. **A.** Control, **B.** A4M and **C.** E4M. Fluorescence excitation and emission of Trc mix (100-1.25 µg/mL) were at 280 and 348 nm, respectively. Three repeats of each preparation are shown via scatter dotplots. Continual readings were taken for the first 60 minutes with F60/F10 the reading taken at 60minutes/reading taken at 10 minutes. A sigmoidal curve with a variable slope was fitted to each of the data sets (R2>0.99) and the intercept between the slope and the plateau was taken as the critical oligomerisation concentration.

A more detailed study was done in parallel on the oligomerisation of TpcC utilising fluorescence (Figure 4.10), circular dichroism, ion mobility mass spectrometry and scanning electron microscopy[15].

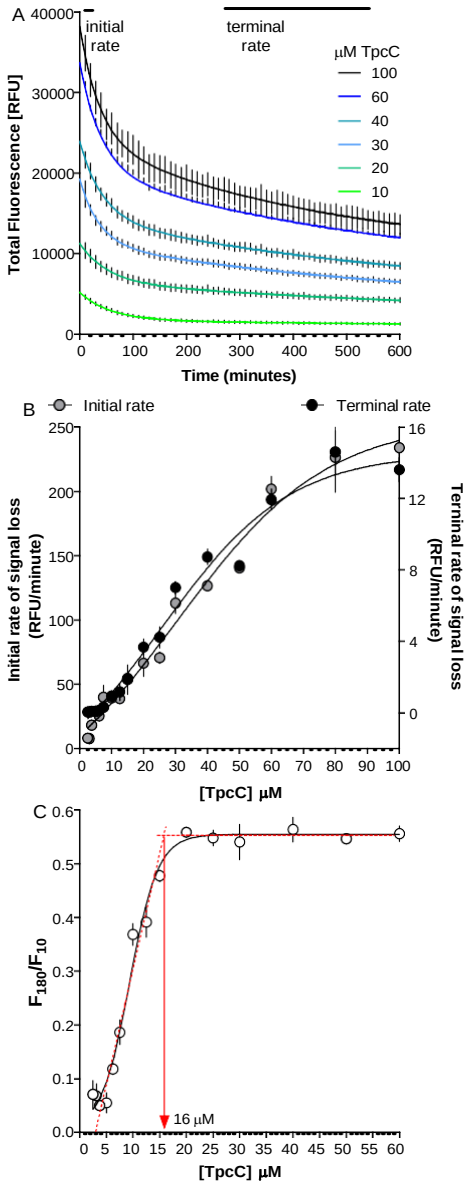

Figure 4.10. Monitoring the influence of concentration on the aggregation of TpcC. **A.** Decrease in total fluorescence of TpcC at different concentrations over time, **B.** Comparison of the initial and terminal rate of fluorescence decay over the TpcC concentration range **C.** Oligomerisation onset plot of TpcC. Continued readings were taken for the 600 minutes with F180/F10 the reading taken at 180 minutes/reading taken at 10 minutes. A sigmoidal curve with a variable slope was fitted to the data set (R^2>0.99) and the intercept between the slope and the plateau was taken as the critical oligomerisation concentration. Fluorescence excitation and emission of TpcC (100-3 µM) were at 280 and 348 nm, respectively. Data are the average of three determinations and SD.

The article on this study is has been accepted for publication in Biochimie [15] and we will only report in brief on the major findings concerning TpcC oligomerisation monitoring using fluorescence.

The Trp fluorescence investigations of TpcC (ranging from 3-100 µM) proved to be highly dependent on two factors namely, time and concentration. Due to the aromatic π-π stacking, there is a Trp fluorescence signal quenching for all different concentrations over 600 minutes (Figure 4.10A). The initial and the terminal rate of the Trp signal loss differs from one another but follows that same trend over the concentration range (Figure 4.10B). Similar to Trc mix, lower concentration of TpcC resulted in lower Trp fluorescence signal, while increased TpcC concentration resulted in higher Trp fluorescence signal, but it did not show a linear trend over the whole concentration range (Fig. 4.10C). The critical oligomerisation concentration in which the linear correlation between the TpcC concentration and Trp fluorescence signal was lost, was calculated to be 16 µM. (Figure 4.10 C). It is hypothesised that a higher concentration of TpcC (above 16 µM or 12 µg/mL) results in the formation and settling of the large aggregates/oligomers out of the solution, which leads to a decrease in the Trp fluorescence signal intensity. Furthermore, high oligomerisation concentration could explain cellulose derivatives formulation (A4M) had a limited effect on the TpcC activity against *C. albicans* reported in Chapter 3. Interestingly, in a parallel study done in our group, it was found that the oligomerisation concentration for the more hydrophobic TrcA 15 µM [16] or 12 µg/mL, also explaining the lack of influence of A4M and E4M.

Due to limited access to laboratory facilities in 2020 during COVID-19 lockdown restrictions, we were unable to complete the studies on E10M and K15M for Trc mix. However, it can be assumed that these two related cellulose polymers will also shift the critical oligomerisation concentration and this study will be complete with the formulation studies of the purified peptides and the fluorescence studies in a parallel project.

4.5 Conclusions

Trcs have a pronounced tendency to form oligomers/aggregates [1, 2, 3]. Trcs biological activity is proposed to be dependent on their oligomerisation, in particular the formation of amphipathic dimers that is hypothesised to be the active membrane interacting moieties [5]. Therefore, Trcs' loss of propensity to form dimers could result in loss of biological activity. However, Trcs oligomerisation is far from equilibrium and they form higher oligomers over a longer maturation time. Higher oligomers that are dependent on hydrophobic interactions are more stable [14] and will have a lower biological activity because of the limited solubility

and lower release of active dimers. Oligomerisation also results in more technical difficulties when handling the peptide, leading to variable results. By formulation of Trc with cellulose derivatives, we aimed to control the rate of the oligomerisation.

This study showed that the formation of Trc mix oligomers is highly dependent on three main factors, namely formulant, time and concentration. Higher concentrations of Trcs will form higher oligomers over prolonged maturation time [14]. By formulation of Trc mix with cellulose derivatives, we aimed to control the oligomerisation profile in three main ways, namely by choosing the optimal cellulose-derived formulant to limit unwanted oligomerisation, find the best ratio of peptide: formulant for stabilisation and finding an optimal maturation time.

It was found that formulations of Trc mix with various cellulose derivatives stabilise and curb the oligomer formation in solution, but that the viscosity of the formulant may play a role. As cellulose derivatives could result in the formation and stabilisation of smaller oligomers and they prevent the formation of large oligomers and rearrangement of these oligomers. Our cellulose formulations, therefore, resulted in lowering the fluorescence scattering of Trc mix, even after prolonged maturation. Furthermore, the total Trp fluorescence loss over 20 hours of maturation was lower for cellulose derivatives formulations of Trc mix when compared to the Trc mix control containing 1.5% ethanol. A higher concentration/ratio of cellulose derivative resulted in lower scattering, thus further stabilisation and less Trp fluorescence loss over 20 hours of maturation. One interesting aspect that came to the fore is that more stable 1:2 and 1:4 formulations did not lose activity against *C. albicans* as was found for the low viscosity formulants CHS, KLUE and KLUL. This indicated that the resultant solution conformation of the peptides was optimal to remain active. Furthermore, more viscous cellulose derivatives containing the methyl side chain, A4M, E4M, E10M and K15M had the better ability of stabilisation which corresponded with lower IC_{50}/MIC values reported in Chapter 3.

Cellulose derivatives changed the environment of the Trp residues leading to a change in fluorescence and therefore may have also changed the peptide conformation in solution. Although cellulose derivatives did not change the rate of the peptide oligomerisation (ΔRFU/minute over 12-60 minutes), they did influence the emission λ_{max} of formulated Trc mix at 50 and 6.25 µg/mL. A4M preparation of Trc mix at (50 and 6.25 µg/mL) had a lower λ_{max} compared to control and other cellulose derivatives possibly because it creates a more hydrophobic environment. Furthermore, all the formulations with 50 µg/mL Trc mix had higher λ_{max} values which could be due to the exposure of the Trp residue to polar side chains in the oligomer structure. The stacking of aromatic amino acid residues caused quenching,

combined with a blue shift in all the formulations from the expected λ_{max} of 350 nm of Trp, to between 336 nm and 342 nm.

It was observed that the cellulose derivatives decrease the critical oligomerisation concentration of Trc mix, possibly by direct interaction and chaotropic activity. The methyl side chains present within the cellulose derivatives structure can increase the hydrophobicity of the formulation resulting in lowering the oligomerisation of Trcs driven by hydrophobic clustering. Although higher concentration results in the formation of higher oligomers, upon addition of cellulose derivatives at a 1:4 peptide: formulant ratio, the critical oligomerisation concentration changed drastically from 8 µg/mL for Trc mix alone to 15 µg/mL and 17 µg/mL, in A4M and E4M formulations, respectively. The higher concentration of cellulose derivatives could stabilise the formulants, as the presence of more saccharide molecules were able to interact with more Trcs molecules and lower the water activity, thereby reducing the hydrophobic forces. Furthermore, more concentrated formulations were better stabilised over 20 hours of maturation and did not increase the data scattering that is linked to instability. The higher TpcC concentration that was found for the critical oligomerisation concentration of the purified TpcC could explain, the reason that A4M formulation had a limited effect on this peptide's activity (refer to Chapter 3). Conversely the more hydrophobic and more active peptide, TrcA showed minor activity loss in formulation with A4M and E4M (refer to Chapter 3). Therefore, it is hypothesised that there is an optimal oligomer size in the solution that is important for the biological activity of the peptide. Some of these oligomers may have been disrupted by the formulations. Another possibility for lower activity of formulated TrcA is that its target interaction groups were masked by interaction with the glucose moieties, as described by Juhl *et al*.[4]. TrcA is one of the most abundant peptides present the Trc mix that forms hetero-oligomers.

In conclusion, the cellulose derivatives successfully stabilised the Trc mix formulations resulting in lower Trp fluorescence signal loss. higher critical oligomerisation concentrations and more stable solution-phase oligomers that maintained biological activity. Therefore. it is concluded that cellulose derivatives prevent or slow down the formation of Trc mix oligomers over prolonged incubation time which consequently increase the biological activity of Trc mix against *Candida* species. However, much more development and optimisation are still needed in the formulation of the purified peptides to obtain optimal formulations.

4.6 References

1 Ruttenberg, M., King, T., and Craig, L. (1966) the chemistry of tyrocidine. VII. Studies on association behavior and implications regarding conformation. *Biochemistry* 5, 2857–2864.

2 Breslow, R., and Chipman, D. (1964) The use of tyrocidines for the study of conformation and aggregation behavior. *J. Am. Chem. Soc. 55*, 4195–4196.

3 Powers, J. P. S., and Hancock, R. E. W. (2003) The relationship between peptide structure and antibacterial activity. *Peptides 24*, 1681–1691.

4 Juhl, D., Van Rensburg, W., Bossis, X., Vosloo, JA., Rautenbach, M., and Bechinger. B. (2019) Tyrocidine A interactions with saccharides investigated by CD and NMR spectroscopies. *J. Pept. Sci*. *25*, 1-11

5 Munyuki, G., Jackson, G. E., Venter, G. A., Kövér, K. E., Szilágyi, L., Rautenbach, M., Spathelf, B. M., Bhattacharya, B., and Van Der Spoel, D. (2013) β-sheet structures and dimer models of the two major tyrocidines, antimicrobial peptides from *Bacillus aneurinolyticus*. *Biochemistry 52*, 7798–7806.

6 Lolla, P., Uptona, E., Nahouma, V., Economoua, C., Cocklina, S. (2012) The high resolution structure of tyrocidine A reveals an amphipathic dimer Patrick. *Biochem Biophys Acta 40*, 1301–1315.

7 Sheeham, D. (2000) Physical biochemistry: Principles and application. John Wiley and Sons, Ltd., Ireland, Cork 74-80

8 Lakowicz, J.R., (2006) Principles of fluorescence spectroscopy. Springer US. Boston. MA., 63-95 10.1007/978-0-387-46312-4

9 Bent. D. V., and Hayon. E., (1975) Excited state chemistry of aromatic amino acids and related peptides. II. Tyrosine. *J. Am. Chem*. *Soc. 97*. 2599–2606.

10 Chattopadhyay, A., and Raghuraman, H., Application of fluorescence spectroscopy to membrane protein structure and dynamics. *Curr. Sci. 87*. 175-180

11 Cheung, H.C., (1995) Resonance energy transfer. *Plenum Press, US, New York, 2,* 127-176.

12 Eftink, M.R. (1991) Fluorescence quenching, theory and applications. *Plenum Press, US, New York, 2,* 53-128

13 Vosloo, J. A. (2016) Optimised bacterial production and characterisation of natural antimicrobial peptides with potential application in agriculture. PhD Thesis, Department of Biochemistry, University of Stellenbosch. https://scholar.sun.ac.za/handle/10019.1/98411

14 Van Rensburg, W., (2019) The tyrocidines in the creation of antimicrobial cellulose and sterilising materials. PhD Thesis, Department of Biochemistry, University of Stellenbosch

15 Rautenbach, M., Kumar, V., Vosloo, J., Masoudi, Y., Wyk, R., Stander, M. (2021) Oligomerisation of tryptocidine C, a Trp-rich cyclodecapeptide from the antimicrobial tyrothricin complex, *Biochimie*, 181, 123-133

16 Personal communication, Rautenbach, M. and Battacharya, B., Department of Biochemistry, University of Stellenbosch

.

4.7 Supplementary data

Table S1 Summary of the Trp fluorescence in RFUs of different preparations/formulations of Trc mix after 1,4 and 20 hours of maturation.

		Fluorescence ± SD (n=12)		
Formulant	**Trc mix: formulant (*m/m*)**	**1 hour**	**4 hours**	**20 hours**
Control	-	5539 ± 4481	3347±1261	2345±1584
A4M	1:1	5844 ± 280.6	3347±1463	3839 ± 449.5
E4M	1:1	6087±865.1	4517±1351	4443 ± 454.1
E10M	1:1	5244±978.7	4822±1107	3511 ± 338.6
K15M	1:1	7130±903.2	3951±1211	5133 ± 325.9
A4M	1:2	8628±1340	5653±1260	8087 ± 369.5
E4M	1:2	8846±1122	7744±1212	8409 ± 347.6
E10M	1:2	9154±1029	8554±976.1	8361 ± 263.8
K15M	1:2	6413 ± 1729	8663±943.2	6291 ± 214.5
A4M	1:4	5910 ± 179.9	6249±577.6	5381±646.8
E4M	1:4	6850 ± 144.7	5488±453.5	6326±516.9
E10M	1:4	7120 ± 155.1	6632±455.6	6443±518.0
K15M	1:4	7335 ± 115.9	6633±362.1	6392±373.6

Table S2 Statistical comparison of Trp fluorescence between different Trc mix of fresh (1h) and matured (20h) preparations. Tabulated Trp fluorescence represents the mean 12 preparations with SD. Unpaired Student t-test was done on each of the analysed pairs.

	Fresh sample (1 hour)mean ± SD	Matured sample (20 hours)mean ± SD	P-value
Trc mix: cellulose derivatives 1 1 (*m/m*)			
A4M	5844±72.0	3839±1557	0.0010
E4M	6087 ± 249.7	4443±1573	0.0044
E10M	5244 ± 282.5	3511±1173	0.0007
K15M	7130 ± 260.7	5133±1129	<0.0001
Trc mix: cellulose derivatives 1 2 (*m/m*)			
A4M	8628 ± 386.8	8087±1280	ns
E4M	8846 ± 323.9	8409±1204	ns
E10M	9154 ± 297.0	8361±913.9	ns
K15M	6413 ± 499.1	6291±743.2	0.0093
Trc mix: cellulose derivatives 1 4 (*m/m*)			
A4M	5910±623.3	5381±646.8	ns
E4M	6850±501.1	6326±516.9	ns
E10M	7120±537.2	6443±518.0	ns
K15M	7335±401.6	6392±373.6	ns
Control	5539 ± 4481	2345±1584	0.0277

Table S3 Statistical comparison Trp fluorescence between different preparations at 1 4 and 20 hours of Trc mix. Tabulated Trp fluorescence represents the mean of 12 preparations with SD. One-way Anova with Bonferroni correlation test was done between each of the selected data sets groups.

			1 hour of maturation												
			1:4				1:2				1:1				
			K15M	E10M	E4M	A4M	K15M	E10M	E4M	A4M	K15M	E10M	E4M	A4M	Control
1 hour of maturation	1:4	K15M		ns	ns	ns	ns	ns	<0.05	ns	ns	ns	ns	0.001	ns
		E10M			ns	ns	ns	ns	<0.01	ns	ns	ns	ns	ns	ns
		E4M				ns	ns	ns	0.001	ns	ns	ns	ns	ns	ns
		A4M					ns	ns	0.001	0.001	ns	ns	ns	ns	ns
	1:2	K15M						ns	<0.01	<0.05	ns	ns	ns	ns	ns
		E10M							ns	ns	<0.05	ns	0.001	0.001	0.001
		E4M								ns	ns	ns	0.001	0.001	0.001
		A4M									ns	ns	<0.01	0.001	0.001
	1:1	K15M										ns	ns	ns	ns
		E10M											ns	ns	<0.05
		E4M												ns	ns
		A4M													ns
			4 hours of maturation												
			1:4				1:2				1:1				
			K15M	E10M	E4M	A4M	K15M	E10M	E4M	A4M	K15M	E10M	E4M	A4M	Control
4 hours of maturation	1:4	K15M		ns	ns	ns	ns	ns	ns	ns	ns	0.001	ns	<0.05	0.001
		E10M			ns	ns	ns	<0.05	<0.05	ns	ns	0.001	ns	<0.05	0.001
		E4M				ns	ns	<0.05	<0.05	ns	ns	0.001	ns	<0.05	0.001
		A4M					<0.05	0.001	0.001	ns	ns	ns	ns	ns	<0.05
	1:2	K15M						<0.01	<0.01	ns	ns	<0.01	ns	ns	0.001
		E10M							ns	ns	0.001	0.001	0.001	0.001	0.001
		E4M								ns	0.001	0.001	0.001	0.001	0.001
		A4M									<0.05	0.001	0.001	0.001	0.001
	1:1	K15M										ns	ns	ns	<0.01
		E10M											ns	ns	ns
		E4M												ns	ns
		A4M													ns
			20 hours of maturation												
			1:4				1:2				1:1				
			K15M	E10M	E4M	A4M	K15M	E10M	E4M	A4M	K15M	E10M	E4M	A4M	Control
20 hours of maturation	1:4	K15M		ns	ns	ns	ns	ns	ns	ns	ns	0.001	ns	<0.01	0.001
		E10M			ns	ns	ns	ns	ns	ns	ns	0.001	ns	0.001	0.001
		E4M				ns	ns	ns	<0.05	ns	ns	0.001	<0.05	<0.01	0.001
		A4M					ns	ns	0.001	0.001	ns	ns	0.001	ns	0.001
	1:2	K15M						ns	<0.05	ns	ns	0.001	ns	<0.01	0.001
		E10M							ns	ns	0.001	0.001	0.001	0.001	0.001
		E4M								ns	0.001	0.001	0.001	0.001	0.001
		A4M									0.001	0.001	0.001	0.001	0.001
	1:1	K15M										ns	ns	ns	0.001
		E10M											ns	ns	ns
		E4M												ns	<0.05
		A4M													ns

Table S4 Statistical comparison of Trp signal loss from 1 to 4 hours and 1 to 20 hours of maturation between different preparations of Trc mix. The values utilised were the mean 12 preparations with SD. One-way Anova with Bonferroni correlation test was done between each of the selected data sets groups.

			Signal loss from 1 to 20 hours of maturation												
			1:4				1:2				1:1				
			K15M	E10M	E4M	A4M	K15M	E10M	E4M	A4M	K15M	E10M	E4M	A4M	Control
Signal loss from 1 to 4 hours of maturation	1:4	K15M	ns	ns	ns	ns	ns	ns	ns	ns	ns	ns	ns	ns	<0.05
		E10M	ns	ns	ns	ns	ns	ns	ns	ns	ns	ns	ns	ns	<0.01
		E4M	ns	ns	ns	ns	ns	ns	ns	ns	ns	ns	ns	ns	0.001
		A4M	ns	ns	ns	ns	ns	ns	ns	ns	ns	ns	ns	ns	<0.01
	1:2	K15M	ns	ns	ns	ns	ns	ns	ns	ns	ns	ns	ns	ns	0.001
		E10M	ns	ns	ns	ns	ns	ns	ns	ns	ns	ns	ns	ns	<0.01
		E4M	ns	ns	ns	ns	ns	ns	ns	ns	ns	ns	ns	ns	<0.01
		A4M	ns	ns	ns	ns	ns	ns	ns	ns	ns	ns	ns	ns	<0.05
	1:1	K15M	ns	ns	ns	ns	ns	ns	ns	ns	ns	ns	ns	ns	ns
		E10M	ns	ns	ns	ns	ns	ns	ns	ns	ns	ns	ns	ns	ns
		E4M	ns	ns	ns	ns	ns	ns	ns	ns	ns	ns	ns	ns	ns
		A4M	ns	ns	ns	ns	ns	ns	ns	ns	ns	ns	ns	ns	ns
		Control	ns	ns	ns	ns	ns	ns	ns	ns	ns	ns	ns	ns	ns

			Signal loss from 1 to 4 hours of maturation												
			1:4				1:2				1:1				
			K15M	E10M	E4M	A4M	K15M	E10M	E4M	A4M	K15M	E10M	E4M	A4M	Control
Signal loss from 1 to 4 hours of maturation	1:4	K15M		ns	ns	ns	ns	ns	ns	ns	ns	ns	ns	0.001	ns
		E10M			ns	ns	ns	ns	ns	ns	ns	ns	ns	ns	ns
		E4M				ns	ns	ns	ns	ns	ns	ns	ns	ns	<0.05
		A4M					ns	ns	ns	??	ns	ns	ns	ns	<0.05
	1:2	K15M						ns	ns	ns	ns	ns	ns	ns	<0.01
		E10M							ns	ns	ns	ns	ns	ns	ns
		E4M								ns	ns	ns	ns	ns	<0.05
		A4M									ns	ns	ns	ns	ns
	1:1	K15M										ns	ns	ns	ns
		E10M											ns	ns	ns
		E4M												ns	ns
		A4M													ns

			Signal loss from 1 to 20 hours of maturation												
			1:4				1:2				1:1				
			K15M	E10M	E4M	A4M	K15M	E10M	E4M	A4M	K15M	E10M	E4M	A4M	Control
Signal loss from 1 to 20 hours of maturation	1:4	K15M		ns	ns	ns	ns	ns	ns	ns	ns	ns	ns	ns	ns
		E10M			ns	ns	ns	ns	ns	ns	ns	ns	ns	ns	<0.05
		E4M				ns	ns	ns	ns	ns	ns	ns		ns	<0.01
		A4M					ns	ns	ns		ns	ns	ns	ns	<0.01
	1:2	K15M						ns		ns	ns	ns	ns	ns	<0.05
		E10M							ns	ns	ns	ns	ns	ns	<0.01
		E4M								ns	ns	ns	ns	ns	<0.01
		A4M									ns	ns	ns	ns	<0.01
	1:1	K15M										ns	ns	ns	ns
		E10M											ns	ns	ns
		E4M												ns	ns
		A4M													ns

Chapter 5
Conclusions and future studies

5.1. Introduction

An increasing number of immunocompromised people have resulted in an increase in fungal infections. In addition, the limited number of available antifungal drugs has resulted in antifungal drug resistance [1, 2, 3]. Furthermore, the rapid development of resistance towards antifungal drugs and difficulties in new drug development has become a global problem [4]. The tyrocidines (Trcs) and the analogues, as small non-ribosomal antimicrobial peptides with proven anti-*Candida* activity [5] were chosen for this study. Trcs are interesting to study further as a potential novel generation of antifungal drugs. We tested the biological activity of Trcs against two of the most common human fungal pathogens namely *Candida albicans* and *C. glabrata.* As the relation of Trcs self-assembly structures and their activity was previously reported [6, 7], we decided to manipulate their oligomerisation via formulation. The formulants chosen for this study were cellulose derivatives containing methyl and ethyl side chains. The reason for this choice was the ability of Trcs to interact with the OH group of glucose which was previously reported [8]. We aimed to investigate the influence of the other side chains of cellulose derivatives on the Trc activity [9]. The self-assembly of the Trcs was monitored via fluorescence spectrometry as 4 out of 10 amino acid residues present within the Trc structure are good fluorophores. Furthermore, we attempted to stabilise the oligomerisation of Trcs, which could lead to loss of the biological activity, via formulation. Trcs oligomerisation profile is dynamic with a constant arrangement and rearrangement of the oligomers. Addition of cellulose derivatives to the Trcs aimed to curb the formation of the oligomers and stabilise the Trcs active moieties. Finally, we compared the anti-*Candida* activity of the Trcs their cellulose type formulations with two of the anti-Candida compounds available on the market namely, fluconazole and caspofungin [10, 11]. The environmental *C. albicans* strain studied in this project showed resistant toward both of these anti-fungal drugs.

5.2. Conclusions

5.2.1. Production and purification of single Trc analogues

The production and purification of five Trcs single analogues namely, TrcA, TrcB, TrcC, TpcB and TpcC was successfully achieved. All five analogues had a purity of higher than

90%. This aim was achieved through four main steps, namely, manipulated bacterial production of the tyrothricin complex using the soil bacterium *Br. parabrevis 8185,* organic extraction of the tyrothricin complex from the bacterial culture, removal of gramicidins (Grms) and non-peptide material and extraction of the Trcs and analogues. In the case of commercial tyrothricin, removal of Grms was the only necessary step. Linear Grms and non-peptide material as well as certain Trcs and analogues were removed at each step of the extraction and purification. As an example, although the DEE-acetone precipitation step resulted in the removal of all linear Grms from the non-supplemented crude extract of the tyrothricin complex, it caused major loss of TrcA during this step.

As part of this project focused on studying the biophysical behaviour of Trcs single analogue, high purity of each of the analogues was needed. RP-HPLC was utilised to isolate each of the Trcs single analogues with high purity. Isolation of Trcs single analogues with a purityof higher than 90% is a complicated task as Trcs have a great tendency of oligomerisation [12]. Trcs aggregation/oligomerisation results in peak broadening and inconsistent retention time, making RP-HPLC purification difficult. As an example, the retention time of Trc A_1/A, B_1/B, and C_1/C (from 6-hours matured commercial tyrothricin complex) was 2-3 minutes later than the fresh sample. By loading a lower concentration, as the peptide became purer onto the RP-HPLC system, and collecting all the HPLC fractions manually, these difficulties were averted. Furthermore, the purification of certain analogues was eased via supplementation of *Br. parabrevis* cultures via 20 mM Phe and 10 mM Trp. The amino acid supplementation with Phe and Trp of the culture successfully shifted the production towards TrcA and TpcC, respectively. Phe-supplementation proved to decrease the Grms production while Trp-supplementation increased Grms production, but also increased the production of the Trp containing peptides such as TrcC and TpcC. These results correlated with previous findings [13].

5.2.2. The biological activity of the Trcs

Anti-*Candida* activity of Trc mix and single Trc analogues

In general, Trcs showed promising activity against both *C. albicans* and *C. glabrata*. This is specifically very important, as the *C. albicans* strain studied in this project, proved to be resistant towards caspofungin and fluconazole while *C. glabrata* is inherently resistant towards fluconazole [14]. Furthermore, comparison of the anti-*Candida* activity of TrcA, Trc mix and TpcC with that of fluconazole and caspofungin, it was observed that exposure to the Trcs result in far less induction ofa metabolic stress response. This type of stress response of the *Candida* cells can ultimately lead to resistance as well as biofilm formation.

As eradication of biofilms is drastically more tedious than the eradication of planktonic cells, the fact that Trcs resulted in a lower level of the stress response and possible biofilm formation, is of importance. Furthermore, the stress response is the first step for the activation of signals which leads to expression of multidrug-resistant pumps to keep the anti-fungal compound out of the cells [15]. This means that there is a significantly smaller chance that *Candida* cells develop a resistance mechanism against Trcs due to rapid and multiple modes of action.

Another interesting point which came to the fore was the influence of Trc formulation maturation time on the anti-*Candida* activity. While maturation time enhanced the Trc mix activity toward *C. albicans,* it did not significantly influence the activity of either TrcA or TpcC. It must be noted that Trc mix contains a complex mixture of different analogues, mainly including Trc A_1/A, B_1/B, and C_1/C. It is possible, that longer incubation is needed to form stable hetero-oligomers that has high activity towards *Candida* cells. Alternatively, longer maturation (20 hours) of Trc mix may have resulted in heterooligomers that supported the release of more amphipathic dimers in the solution and therefore enhanced the activity. It is hypothesised that the highly active TrcA, which is one of the most hydrophobic Trcs, has a relatively stable oligomer and dimer population in solution, therefore longer maturation time was an ineffective factor in TrcA biological activity enhancement. TpcC on the other hand is a more polar peptide analogue but it has inherently lower activity against *C. albicans* and formulation or longer maturation also did not enhance the activity. Furthermore, parallel research showed that TpcC forms large oligomers/ aggregates [16]. Longer maturation time did not result in the rearrangement of the oligomers with the more release of active amphipathic dimers or oligomers.

Effect of cellulose derivatives on the anti-*Candida* activity of Trcs

Selected concentrations of Trc mix were formulated by seven different cellulose derivatives, these formulations differed from one another in viscosity and side chains. The formulation of Trc mix by high viscous cellulose derivatives significantly increased the anti-*Candida* activity of the peptide. Two out of 24 treated *Candida* cultures by 50 µg/mL Trc mix alone survived, while none survive when Trc mix was formulated. As expected, the survival of cultures increased as they were treated by lower concentrations of Trc mix such as 25 and 12.5 µg/mL. This difference in survival could be due to the presence of *Candida* persister cells [15]. We chose the formulants that were generally better to eradicate both populations of persister and normal *Candida* cells. The formulations in low viscous cellulose derivatives such as KLUE and KLUI, in addition to CHS did not enhance the Trc mix activity. The more

viscose formulants of Trc mix such as (A4m, E4M, E10M and K15) seemed to have a better anti- *Candida* activity. When Trc mix was formulated by an increased concentration of selected cellulose derivatives, it improved the stability while activity was maintained. For all the formulations, Trc mix formulated by E10M 1:4 (*m/m*) significantly had better anti-*Candida* activity compared to the control. Furthermore, when *C. glabrata* cultures were treated by different preparations of matured Trc mix, they showed good activity, but the activity of Trcs towards *C. albicans* was better compared to *C. glabrata.*

Although cellulose derivatives enhanced the anti-*Candida* activity of Trc mix they did not significantly influence the anti-*Candida* activity of the purified TrcA and TpcC. This ineffectiveness can be due to the stability of TrcA oligomers or inherit lower anti-*Candida* activity of the more polar and bulkier TpcC. Cellulose derivatives generally did not result in the rearrangement or stabilisation of TrcA or TpcC oligomers to enhance the anti-*Candida* activity.

5.2.3. Investigation of the stability of Trcs utilising fluorescence

In this study, it was aimed to both enhance the activity and solution stability of the Trcs via formulation. Overall, this aim was successfully achieved through the formulation of Trcs via cellulose derivatives. Stability of the drugs is an extremely important factor to consider in drug discovery and development. While the term drug stability refers to the extent in which a drug formulant retains its potency, physical and chemical characteristics during storage and use, in this study, the stability ofthe formulation referred to a wider definition.

Part of the creation of stable Trc formulant is to control the unwanted oligomerisation of Trcs. Trcs tend to oligomerise, especially at higher concentrations[12]. As Trcs oligomerisation is far from equilibrium, they form higher oligomers over a longer maturation time. The interaction of cellulose derivatives and Trc mix was observed to slow the formation of unwanted Trcs oligomers. The stability of these formulations was monitored via Trp fluorescence scattering. A formulation of Trc mix which showed less scatter over 20 hours of maturation time had better stability, while the aggregation/oligomerisation is supported by the lower total fluorescence or quenching at 20 hours versus 1 hour of maturation. It was found that the formulation of Trc mix by seven different cellulose derivatives successfully stabilised the Trc solution structures and oligomerisation in aqueous solution over 20 hours of maturation. This stability resulted in the lower scattering of Trp fluorescence signal and Trp fluorescence signal quenching over 20 hours of maturation. The cellulose derivatives formulant of Trc mixed differed in the side chain and viscosity, interestingly enough, the most stable formulations in terms of Trp fluorescence contained CHS and K15M, followed by

KLUE and KLUL. However, these low viscose formulants, KLUE, KLUL and CHS, did not enhance the Trc mix anti-*Candida* activity. It seems that highly stable oligomers may not have a high enough affinity to bind to the cell membrane of *Candida* cells. Another possibility is that the cellulose derivatives of low viscosity might mask the active groups in the peptide oligomers.

When Trc mix was formulated by the higher concentration of A4M, E4M, E10M and K15M, it was found that a higher concentration/ratio of cellulose derivative resulted in lower scattering and Trp fluorescence loss over 20 hours of maturation. However, 1:2 and 1:4 (*m/m*) of cellulose derivatives Trc mix showed better anti-*Candida* activity. This meant that unlike low viscous formulations of Trc mix, at the higher ratio of A4M, E4M, E10M and K15M, the resultant solution conformation of the peptides was optimal to remain active.

When the effect of time on the oligomerisation of Trcs mix was further investigated, it was found that there was a major Trp fluorescence loss was over the first six minutes of maturation for Trc mix in control solution and in A4M at 1:4 (*m/m*). This was an indication of rapid conformational rearrangement of Trc oligomers. However, once again when the peptide was formulated by a low viscous solution (in this case E4M), the large fluorescence loss did not occur indicating that Trc mix formulated in cellulose derivatives with low viscosity are more stable formulant compared to high viscosity cellulose derivatives.

When we measured the rate in which the oligomerisation took place, it was found that concentration is a major factor on the oligomerisation rate. Monitoring of Trp fluorescence over a broader concentration range of Trc mix and formulated Trc mix revealed that the formulants changed the critical concentration in which Trp environment changes, which would be related to the critical concentration of oligomerisation/aggregation. It was determined that the Trc mix critical concentration of oligomerisation was 8 µg/mL (~6 µM), while this concentration was higher for formulated Trc mix. The Trc mix formulations with A4M and E4M presented a critical concentration of oligomerisation as 17 µg/mL (~13 µM) and 15 µg/mL (~12 µM), respectively. The critical oligomerisation concentration can relate to the biological activity of the peptide. Trc mix in control solution has lower activity as the oligomerisation concertation is lower leading to unwanted oligomerisation, while formulated Trc mix has higher activity as the oligomerisation concertation is higher more active moieties are available at lower concentrations.

5.3. Future studies

This project was the first exploratory study on cellulose derivatives formulation of Trcs with anti-*Candida* activity and must be expanded to test more purified Trcs peptides and different formulations, such as lipid-type formylations. A previous study has shown that lipid-formulation significantly decreased the haemolytic activity of Trcs [17]. However, a preliminary study on the anti-*Candida* activity of Trc mix formulated cholesterol sulphate (CS), showed that this formulation of the Trc mix makes it inactive against *C. albicans*. This could be due to the similarity between cholesterol and ergosterol in the fungal membrane, with ergosterol possibly one of the targets of the Trcs. CS can compete for this interaction and lead to the loss of affinity towards binding the cell membrane. Besides human erythrocytes, it is recommended to test the toxicity of the formulations of Trcs against a vaginal cell line to assess the potential for topical application to combat vaginal candidiasis.

It would be beneficial to the fluorescence studies tracking the critical concentration of oligomerisation for more formulations and ratios, especially for the most promising formulant E10M, as well as K10M and the less viscous formulants KLUL and KLUE. This will clarify the influence of the formulants on the critical concentration of oligomerisation of the Trc peptides in relation to viscosity, stability, and activity. The fluorescence study on TpcC was only done in 20% acetonitrile in water and can be expanded to TpcC in 1.5% ethanol: water and formulated TpcC, to determine the oligomerisation concertation of TpcC when formulated by cellulose derivatives.

5.4. Last word

The environmental *Candida* strain was isolated from Eerste River in Stellenbosch. This river flows through the neighbourhood surrounding Stellenbosch in which people do not have access to clean piped water and as a result, they use the river water to cook, clean and to do other daily chores. A large number of people in these areas are immunocompromised suffering from diseases such as HIV and tuberculosis (TB). Many TB and HIV patients also suffer from recurring fungal infections. By using the river water, they are exposed to *Candida* contamination which can be deadly for the immunocompromised individuals. Furthermore, the lack of access of the residents of these areas to the medical health care is concerning.

Previous research has shown the ability of the Trcs to attach to the cellulose-based materials while remaining active against pathogenic bacteria [19]. This relates well to this study that shows the stabilisation of anti-*Candida* activity in the presence of cellulose derivatives.

Combining the previous research with the research in this study, cellulose type filters with Trcs could be used to treat the river water to eliminate *Candida* and other possible pathogenic bacteria and fungi. Trcs broad-spectrum activity and safety while consumed orally benefits the practicality of this proposal [20]. This study could therefore benefit compromised communities in the future, particularly because the production of the peptides is economical, and treatment of cellulose type filters would be relatively easy.

5.5. References

1 Xie, J.L., Polvi, E.J., Shekhar-Guturja, T., and Cowen, L.E. (2014) Elucidating drug resistance in human fungal pathogens, *Future Microbiol 9,* 523–42.

2 Chang, Y., Yu, S., Heitman, J., and Wellington, M. (2017) New facets of antifungal therapy, *Virulence 8*, 222–236

3 Ostrosky-Zeichner, L., Casadevall, A., Galgiani, J. N. Odds, F. C., and Rex, J. H. (2010) An insight into the antifungal pipeline: selected new molecules and beyond, *Nat. Rev. Drug Discov. 9,* 719–727.

4 Robbins, N., Wright, G. D., and Cowen L. E. (2016) Antifungal Drugs: The current armamentarium and development of new agents. *Microbiol Spectr. 4,* 1–20.

5 Troskie, A. M., Rautenbach, M., Delattin, N., Vosloo, J. A., Dathe, M., Cammue, B. P. A., and Thevissen, K. (2014) Synergistic activity of the tyrocidines, antimicrobial cyclodecapeptides from *Bacillus aneurinolyticus*, with amphotericin B and caspofungin against *Candida albicans* biofilms. *Antimicrob. Agents Chemother. 58,* 3697–3707.

6 Ruttenberg, M., King, T., and Craig, L. (1966) The chemistry of tyrocidine. VII. Studies on association behavior and implications regarding conformation. *Biochemistry 5,* 2857–2864.

7 Breslow, R., and Chipman, D. (1964) The use of tyrocidines for the study of conformation and aggregation behavior. *J. Am. Chem. Soc. 55,* 4195–4196.

8 Juhl, D., Van Rensburg, W., Bossis, X., Vosloo, JA., Rautenbach, M., and Bechinger. B. (2019) Tyrocidine A interactions with saccharides investigated by CD and NMR spectroscopies. J*. Pept. Sci. 25,* 5

9 Tang, X. J. Thibault, P., and Boyd R. K. (1992) Characterisation of the tyrocidine and gramicidin fractions of the tyrothricin complex from *Bacillus brevis* using liquid chromatography and mass spectrometry. *Int. J. Mass Spectrom. Ion Process. 122,* 153–179.

10 Brammer, K. W., and Farrow, P. R. (1990) Pharmacokinetics and tissue penetration of fluconazole in humans. *Rev Infect Dis 12*, S318–26.

11 Keating, G. M., and Figgitt D. P. (2003) Caspofungin. *Drugs 63,* 2235–2263.

12 Breslow, R., and Chipman, D. (1964) The use of tyrocidines for the study of conformation and aggregation behavior. *J. Am. Chem. Soc. 55,* 4195–4196.

13 Vosloo, J. A. (2016) Optimised bacterial production and characterisation of natural antimicrobial peptides with potential application in agriculture. PhD Thesis, Department of Biochemistry, University of Stellenbosch. https://scholar.sun.ac.za/handle/10019.1/98411

14 Miyazaki, T., Yamauchi, S., Inamine, T., Nagayoshi, Y., Saijo, T. K, I., Seki, M., Kakeya, H., Amamoto, Y., and Yanagihara, K. (2010) Roles of calcineurin and Crz1 in antifungal susceptibility and virulence of *Candida glabrata. Antimicrob. Agents Chemother. 54,* 1639–1643.

15 Lewis, K. (2008) Multidrug tolerance of biofilms and persister cells. *Curr Top Microbiol Immunol* 322,107-131

16 Rautenbach, M., Kumar, V., Vosloo, J., Masoudi, Y., Wyk, R., Stander, M. (2021) Oligomerisation of tryptocidine C, a Trp-rich cyclodecapeptide from the antimicrobial tyrothricin complex, *Biochimie,* 181, 123-133

17 Van Wyk, R. (2019) Development of cyclodecapeptides from the tyrothricin complex as anticancer peptides. MSc Thesis, Department of Biochemistry, University of Stellenbosch.

18 Rautenbach, M., Troskie, A. M., Vosloo, J. A. and Dathe, M. (2016), Antifungal membranolytic activity of the tyrocidines against filamentous plant fungi. *Biochimie 130*, 122-131

19 Van Rensburg, W. (2020) The tyrocidines in the creation of antimicrobial cellulose and sterilising materials. PhD Thesis, Department of Biochemistry, University of Stellenbosch.

20 Henderson, J. (1946) The status of tyrothricin as an antibiotic agent for topical application *J. Am. Pharm. Assoc. 35*, 141–147.